Titre: Title:	Dynamic Numerical Analysis of the Response of the Franklin Falls Dam to the 1982 Gaza (New Hampshire) Earthquake
Auteur: Author:	Angie Arbaiza Guzman
Date:	2017
Type:	Mémoire ou thèse / Dissertation or Thesis
Référence: Citation:	Arbaiza Guzman, A. (2017). Dynamic Numerical Analysis of the Response of the Franklin Falls Dam to the 1982 Gaza (New Hampshire) Earthquake [Mémoire de maîtrise, École Polytechnique de Montréal]. PolyPublie. https://publications.polymtl.ca/2915/

UNIVERSITÉ DE MONTRÉAL

DYNAMIC NUMERICAL ANALYSIS OF THE RESPONSE OF THE FRANKLIN FALLS DAM TO THE 1982 GAZA (NEW HAMPSHIRE) EARTHQUAKE

ANGIE ARBAIZA GUZMAN

DÉPARTEMENT DES GÉNIES CIVIL, GÉOLOGIQUE ET DES MINES

ÉCOLE POLYTECHNIQUE DE MONTRÉAL

MÉMOIRE PRÉSENTÉ EN VUE DE L'OBTENTION

DU DIPLÔME DE MAÎTRISE ÈS SCIENCES APPLIQUÉES

(GÉNIE CIVIL)

DÉCEMBRE 2017

UNIVERSITÉ DE MONTRÉAL

ÉCOLE POLYTECHNIQUE DE MONTRÉAL

Ce mémoire intitulé :

DYNAMIC NUMERICAL ANALYSIS OF THE RESPONSE OF THE FRANKLIN FALLS DAM TO THE 1982 GAZA (NEW HAMPSHIRE) EARTHQUAKE

présenté par : ARBAIZA GUZMAN, Angie

en vue de l'obtention du diplôme de : Maîtrise ès sciences appliquées

a été dûment acceptée par le jury d'examen constitué de :

M. SILVESTRI Vincenzo, Ph. D., Président

M. JAMES Michael, Ph. D., membre et directeur de recherche

M. DUHAIME François, Ph. D., membre

ACKNOWLEDGEMENTS

I would like to thank my supervisor, Prof. Michael James, for offering me the opportunity to pursue my Master's degree in such a challenging research field, for his constant guidance, support and patience. Without him, this thesis would not have been possible.

I also want to acknowledge the assistance provided by the New England District of the U.S. Army Corps of Engineers and Haley & Aldrich (Boston) who provided many of the references and the Gaza earthquake ground motion files. Special thanks to Natalie McCormack who took the time to show me the Franklin Falls Dam during a site visit and also answered to all my questions concerning its construction.

Thanks to the Natural Sciences and Engineering Research Council of Canada (NSERC) Discovery Grants Program for funding this research.

Last but not least, I would like to thank my family and friends for providing me with constant support and continuous encouragement throughout the years of study and throughout the research and the writing of this thesis.

RÉSUMÉ

Les effets néfastes des tremblements de terre sur les structures sont connus depuis des millénaires. Cependant, il a été récemment reconnu que les conditions régionales et locales influent de manière significative sur l'intensité et les caractéristiques du tremblement de terre, et donc sur l'ampleur et la structure des dommages (Seed et Idriss 1969). Par exemple, des différences importantes dans les caractéristiques sismiques de la côte ouest et de la côte est de l'Amérique du Nord sont attribuées aux différences dans les structures géologiques régionales. Les mouvements du sol sur la côte est sont caractérisés par des fréquences plus élevées et une atténuation moindre de l'énergie (p. ex. accélération du sol ou contenu énergétique) avec la distance de la source du tremblement de terre que sur la côte ouest (Tremblay et Atkinson 2001).

La côte ouest de l'Amérique du Nord est considérablement plus sismique que la côte est, ce qui a stimulé une grande concentration d'études sur les tremblements de terre de la côte ouest et une vaste base de données sur les mouvements sismiques de la côte ouest. De plus, l'activité sismique relativement faible de la côte est ainsi que l'historique limité des instruments et l'absence de failles en surface ont entraîné une incertitude dans l'évaluation des paramètres sismiques et des dangers sur la côte est (Acharya et al, 1982).

L'objectif principal de cette recherche est d'étudier le comportement d'un barrage en remblai sur la côte est de l'Amérique du Nord qui a été soumis à un tremblement de terre pour lequel des enregistrements du mouvement du sol ayant des accélérations importantes sont disponibles. Le barrage Franklin Falls, situé dans le centre-sud du New Hampshire (États-Unis), est l'un des seuls barrages sur la côte est de l'Amérique du Nord équipé d'accéléromètres et qui a été soumis à un tremblement de terre avec des accélérations significatives, le tremblement de terre Gaza de 1982 (New Hampshire).

Pour ce faire, une analyse préliminaire de déconvolution du mouvement du sol enregistré à la surface en aval du barrage a été réalisée. Des simulations supplémentaires ont ensuite été réalisées en utilisant PLAXIS 2D pour valider l'analyse préliminaire de déconvolution. L'objectif principal était d'évaluer si le mouvement du sol au roc calculé était en mesure de reproduire le même mouvement du sol mesuré sur la surface, pour finalement l'utiliser dans l'analyse numérique dynamique du barrage.

L'analyse numérique dynamique du barrage Franklin Falls a été réalisée à l'aide de PLAXIS 2D. L'objectif principal de l'analyse était d'évaluer la capacité de la modélisation 2D à simuler la réponse sismique des barrages aux mouvements du sol de la côte est à haute fréquence. De plus, l'applicabilité du modèle de Mohr-Coulomb et l'amortissement de Rayleigh a été évaluée pour ce type de structure et le niveau d'agitation induit.

Pour évaluer le comportement du barrage de Franklin Falls à une charge de tremblement de terre plus intense, une analyse complémentaire du barrage a été effectuée à l'aide du séisme de 1988 au Saguenay, Québec.

ABSTRACT

The damaging effects of earthquakes on structures have been known for millennia. However, it has been recently acknowledged that regional and local conditions significantly influence the intensity and characteristics of earthquake shaking and thus the magnitude and pattern of damage (Seed and Idriss 1969). For instance, important differences in earthquake characteristics in the west coast and east coast of North America are attributed to the differences in the regional geological structures. Due to relatively harder and more intact bedrock, ground motions on the east coast are characterized by higher frequencies and less attenuation of the energy (e.g. peak ground acceleration or energy content) with distance from the earthquake source than those on the west coast (Tremblay and Atkinson 2001).

The west coast of North America is significantly more seismically active than the east coast, which has provided an impetus for concentration of research on west coast earthquakes and a large database of ground motions and recorded dam seismic behavior for the west coast. Furthermore, the relatively low seismic activity of the east coast together with limited instrumentation history and lack of surface faulting have led to uncertainty in the assessment of seismic parameters and hazards on the east coast (Acharya et al. 1982).

The primary objective of this research is to study the behaviour of an embankment dam on the east coast of North America that has been subjected to an earthquake for which ground motion records of important acceleration are available. The Franklin Falls Dam, located in south-central New Hampshire, United States, is one of the few embankment dams in the east coast of North America equipped with accelerometers that has been subjected to significant earthquake accelerations, the 1982 Gaza (New Hampshire) earthquake.

To do so, a preliminary deconvolution analysis of the ground motion recorded at the surface downstream of the dam was performed. Additional simulations were then conducted using PLAXIS 2D to validate the preliminary deconvolution analysis. The main objective was to evaluate the ability of the calculated bedrock ground motion to match the measured ground motion on the surface, for use in dynamic numerical analysis of the dam.

The dynamic numerical analysis of the Franklin Falls Dam was performed using PLAXIS 2D. The main objective of the analysis was to evaluate the ability of 2D modelling to simulate the

seismic response of dams to high frequency, east coast ground motions. Furthermore, the applicability of the Mohr-Coulomb model and Rayleigh damping was evaluated for this type of structure and the level of shaking induced.

To evaluate the behaviour of the Franklin Falls Dam to a more intense earthquake loading, complementary analysis of the dam was conducted using the 1988 Saguenay earthquake (Quebec).

TABLE OF CONTENTS

LIST OF TABLES

LIST OF FIGURES

LIST OF SYMBOLS AND ABBREVIATIONS

a_{max}	maximum horizontal acceleration
a_h	horizontal pseudostatic acceleration
a_v	vertical pseudostatic acceleration
D_r	relative density
E	Young's modulus
e	void ratio
e_0	initial void ratio (-)
f	frequency of applied load
G	shear modulus
G_s	specific gravity
G_{max}	maximum shear modulus
I_h	Arias intensity in two orthogonal horizontal direction (m/s)
I_x	Arias intensity in x horizontal direction (m/s)
I_y	Arias intensity in y horizontal direction (m/s)
K	elastic bulk modulus (kPa)
k_{sat}	saturated hydraulic conductivity
k_h	horizontal coefficient of permeability
k_v	vertical coefficient of permeability
$(N_1)_{60}$	corrected number of blows in SPT test
M_w	moment magnitude
n	porosity
PGA	peak ground acceleration

p_a	atmospheric pressure, 100 kPa
S_u	undrained shear strength
SPT	standard penetration test
T_s	fundamental period of the sliding mass
V_s	shear wave velocity
γ_d	dry unit weight
ρ	density
ϕ'	drained friction angle
c'	cohesion
γ_w	unit weight of water
τ_c	shear stress
γ_c	shear strain
σ_1'	maximum effective principal stress
σ_2'	intermediate effective principal stress
σ_3'	minor effective principal stress
σ_v'	vertical effective stress
ξ_{max}	maximum damping ratio
ξ	damping ratio
Δu	excess pore water pressure
σ'	effective confining stress
σ_{v0}'	effective vertical stress
σ_{h0}'	effective horizontal stress
σ_n	normal stress
ψ	dilation angle
ν	Poisson's ratio

LIST OF APPENDICES

CHAPTER 1 INTRODUCTION

The damaging effects of earthquakes on structures has been known for millennia; written records of earthquakes date as far back as 3000 years (Kramer 1996). However, it has been recently acknowledged that regional and local conditions significantly influence the intensity and characteristics of earthquake shaking and thus the magnitude and pattern of damage (Seed and Idriss 1969). For example, Seed and Idriss (1969) found that deep deposits of soft soils tend to produce ground motions with long period characteristics, producing maximum effects on long period structures (i.e tall structures). One of the cases presented in this paper was the 1957 Mexico earthquake, where extensive damage was produced in multistory structures found on deep deposits of soft clay compared to low and stiff structures that were undamaged. It was also found that shallow deposits of stiff soils result in ground motions with short period characteristics, producing their largest effects on short period structures.

Moreover, important differences in earthquake characteristics in the west coast and east coast of North America are attributed to the differences in the regional geological structures. Due to relatively harder and more intact bedrock, ground motions on the east coast are characterized by high frequencies and less attenuation of the energy (e.g. peak ground acceleration or energy content) with distance from the earthquake source than those on the west coast (Tremblay and Atkinson 2001).

The west coast of North America is significantly more seismically active than the east coast, which has provided an impetus for concentration of research on west coast earthquakes and a large database of ground motions and recorded dam seismic behavior for the west coast. Furthermore, the low earthquake activity of the east coast together with short instrumentation history and lack of surface faulting have led to uncertainty in the assessment of seismic parameters and hazards on the east coast (Acharya et al. 1982).

Worldwide, about 70% of water retention dams are embankment (earthfill or rockfill) dams with the remaining consisting of concrete dams (Fell et al. 2005). This ratio is similar for the United States (USBR 2002) and Canada (CDA 2007). This is mainly due to the fact that embankment dams can be constructed on almost any type of foundation, whereas concrete dams require sound

rock foundations. Embankment dams are also more economical to construct than concrete dams since the majority of the construction materials can usually be obtained in the vicinity of the dam.

Seismic activity can cause damage to embankment dams, the primary means being:

- Slope instability due to the dynamic loads on the embankment;
- Liquefaction or cyclic mobility in the dam or the foundation leading to a loss of resistance and instability;
- Seismic densification or deformation resulting in a loss of free board, overtopping and failure.

The seismic performance (or stability) of embankment dams is typically evaluated as follows:

1. Development of a design earthquake loading using deterministic or probabilistic methods. In Canada, probabilistic methods are generally used and the design earthquake corresponds to a given recurrence interval (CDA 2007). Deterministic methods are used in California and the design earthquake loading is based on the maximum magnitudes associated with known faults, in the vicinity of the structure.

2. Analysis of the potential for excess pore water pressure generation, liquefaction or cyclic mobility and any associated strength loss.

3. Screening level analysis of stability using the pseudostatic method. In this method, the horizontal accelerations induced in the mass of a dam are simulated using a horizontal acceleration acting in the assumed direction of failure (upstream or downstream). Limit equilibrium, usually employing the method of slices, is then used to calculate a factor of safety with respect to a critical failure surface. The horizontal acceleration is calculated as a pseudostatic coefficient times the acceleration due to gravity at the base of the dam (Hynes-Griffin and Franklin 1984).

4. Permanent deformation analysis, which is an empirical method for estimating deformations in an earth dam subjected to seismic loading. This method is based on the probability that a deformation will be produced in the dam undergoing a given seismic load.

5. For critical structures or when the results of pseudostatic or permanent displacement analyses are not adequate, dynamic numerical analysis can be performed. Dynamic numerical analyses are employed to predict the seismic response of geotechnical systems, since they can give detailed indication of both the soil stress distribution and deformation (Visone et al. 2008). Although there are many examples of the dynamic numerical analysis of dams in the literature, there are few that simulate the response of an actual instrumented dam to an actual ground motion. This is problematic since the systems used to conduct dynamic numerical analysis (software, constitutive models, procedures) should be validated and verified as they represent the ultimate level of analysis for these critical structures.

The primary objective of this research is to study the behaviour of an embankment dam located on the east coast of North America that has been subjected to an east coast earthquake for which ground motion records of important acceleration are available. The Franklin Falls Dam, located in south-central New Hampshire, United States, is one of the few embankment dams in the east coast of North America equipped with accelerometers that has been subjected to significant accelerations, as a result of the 1982 Gaza (New Hampshire) earthquake.

Secondary objectives of this research include:

- Deconvolution analysis of the ground motion recorded at the surface downstream of the dam;
- Evaluation of the ability of 2D modelling to simulate seismic response of dams to high frequency east coast ground motions;
- Applicability of the Mohr-Coulomb model and Rayleigh damping to this structure given the level of shaking.
- Evaluation of the behaviour of the Franklin Falls Dam to a more intense earthquake: the 1988 Saguenay earthquake.

Chapter 2 presents a literature review of the Franklin Falls Dam (geology, seismicity, design, and construction), earthquake ground motions on the east coast of North America, evaluation of the dynamic response of embankment dams, and the response of the Franklin Falls Dam to the 1982 Gaza earthquake.

An overview of the research methodology is presented in Chapter 3.

Chapter 4 presents a scientific publication, S*imulation of the response of the Franklin Falls Dam to the 1982 Gaza (New Hampshire) earthquake*, submitted for publication in the *Soil Dynamics and Earthquake Engineering* journal.

Chapter 5 presents a complementary research consisting of dynamic numerical analysis of the response of the Franklin Falls Dam to the 1988 Saguenay (Quebec) earthquake.
A general discussion of the research, including the limitations and contributions of the research, is presented in Chapter 6.

Finally, conclusions and recommendations are presented in Chapter 7.

This thesis also contains a list of references and appendices that provide additional details and information on the research.

CHAPTER 2 LITERATURE REVIEW

This literature review presents the available information on the current state of the practice and research regarding several aspects associated with the objectives and scope of this research as described in Chapter 1. This chapter is composed of the following sections:

- Geological conditions of the Franklin Falls dam site including a description of the regional seismicity (Section 2.1);
- Design, construction and operation of the Franklin Falls dam, including a description of the existing subsurface conditions, materials and geotechnical properties (Section 2.2);
- General description of earthquake ground motions, together with their main characteristics and a description of east coast earthquake ground motions (Section 2.3);
- The response of the Franklin Falls dam to the 1982 Gaza earthquake (Section 2.4);
- Evaluation of the seismic response of dams including the pseudostatic method, permanent deformation analysis and numerical analyses (Section 2.5).

2.1 Geological conditions

2.1.1 Regional geology

New England is the northeastern region of the United States of America, consisting of the states of Maine, Vermont, New Hampshire, Massachusetts, Connecticut and Rhode Island. The bedrock of this region is characterized by highly folded and faulted sedimentary, metamorphic, and volcanic rocks of Paleozoic and Mesozoic age with discontinuous and isolated Precambrian age exposures of crystalline basement rock (Krinitzsky and Dunbar 1986). Figure 2-1 is a simplified geological map of the New England region.

The state of New Hampshire is characterized by highly folded metamorphosed sedimentary belts which establish a parallel series of north-northeast trending topographic ridges, separated by topographic valleys or synclinoriums (Krinitzsky and Dunbar 1986). The City of Franklin, which is located in south-central New Hampshire, is situated near the central portion of the Merrimack synclinorium, as shown in Figure 2-1.

The stratigraphy of the south-central New Hampshire area consists of a series of Ordovician, Silurian and Devonian stratified rocks (see Figure 2-1). Therefore, the area is mainly composed of granite, quartz monzonite, and granodiorite covered by a series of metamorphic volcanic rocks in the form of amphibolites, which in turn are overlain by a formation of marble, quartzite, and schist, and finally overlain by discontinuous quartzite (Krinitzsky and Dunbar 1986).

2.1.2 Local geology

The City of Franklin is located in the northern portion of the Appalachian Mountains, specifically in the White Mountains. Local geology is quite complex; the stratigraphy is the result of three major periods of mountain building and erosion as well as glaciation (Krinitzsky and Dunbar 1986). The glaciation resulted in thick accumulations of sediment (stratified sandy silt and silty sand with minor amounts of gravel and cobbles).

Faults mapped in New Hampshire, as well as the rest of New England, are illustrated in Figure 2-2. Observations along mapped faults in the state indicate that they are healed and possibly inactive for 90 million years or more (Boudette 1994). The fault lines illustrated in Figure 2-2 are normal faults, excluding the major Taconic thrusts (bold lines with teeth on hanging wall), and dominantly strike to the northeast (Hayman and Kidd 2002).

The closest faults to the Franklin Falls Dam site are located approximately 55 km to the northeast at Ossipee, 55 km to the southeast between Manchester and Portsmouth, and 40 km to the northwest near the Vermont border (Krinitzsky and Dunbar 1986). A general field reconnaissance of the Franklin Falls Dam site revealed possible faulting along the rock face forming the west abutment of the dam. This suspected faulting is approximately centered on a rock exposure located downstream from the crest of the spillway. The zone is approximately 23 m wide and contains two normal faults oriented at right angles to the rock face (Krinitzsky and Dunbar 1986).

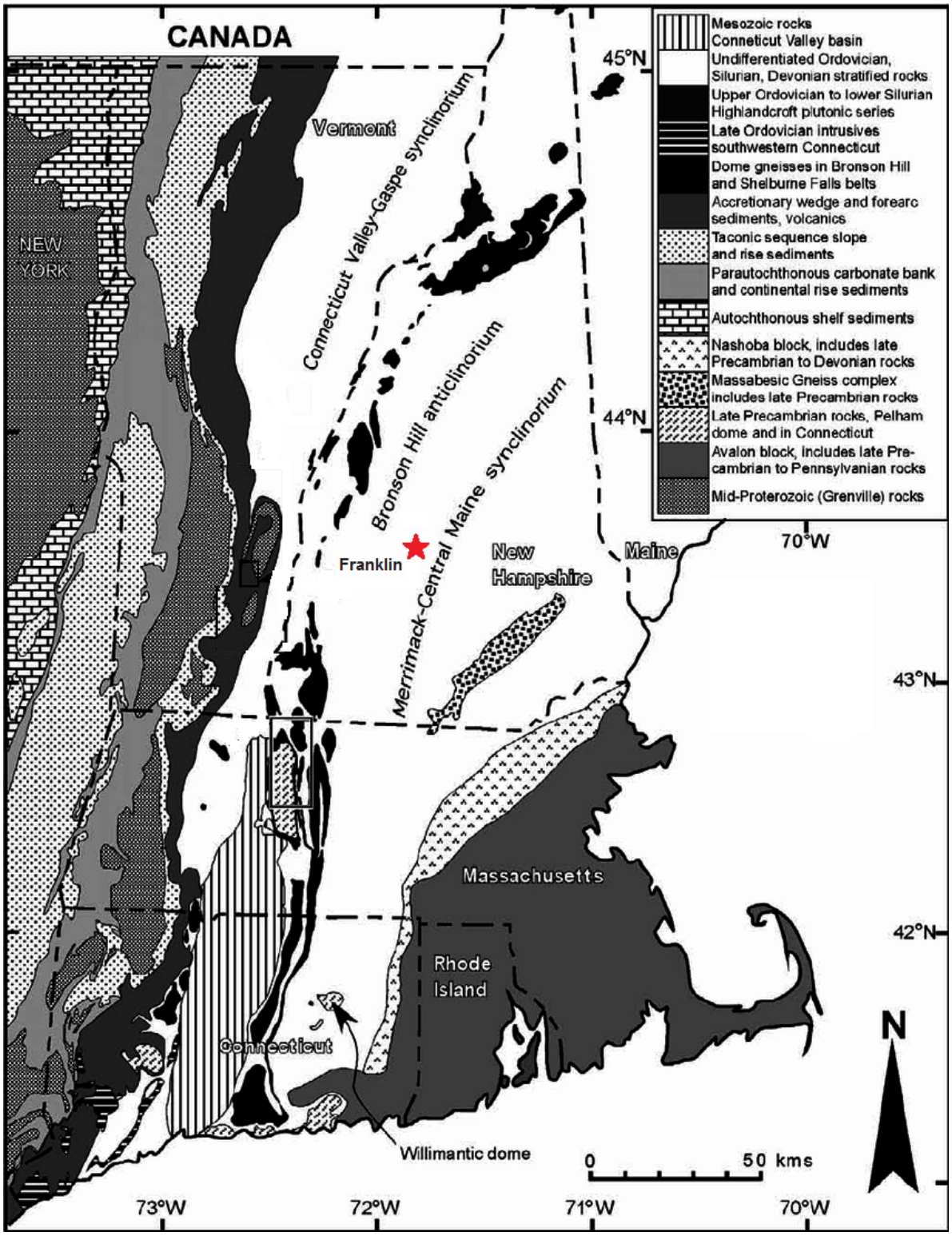

Figure 2-1: Simplified geological map of the New England region showing the location of the city of Franklin (Bell et al. 2004).

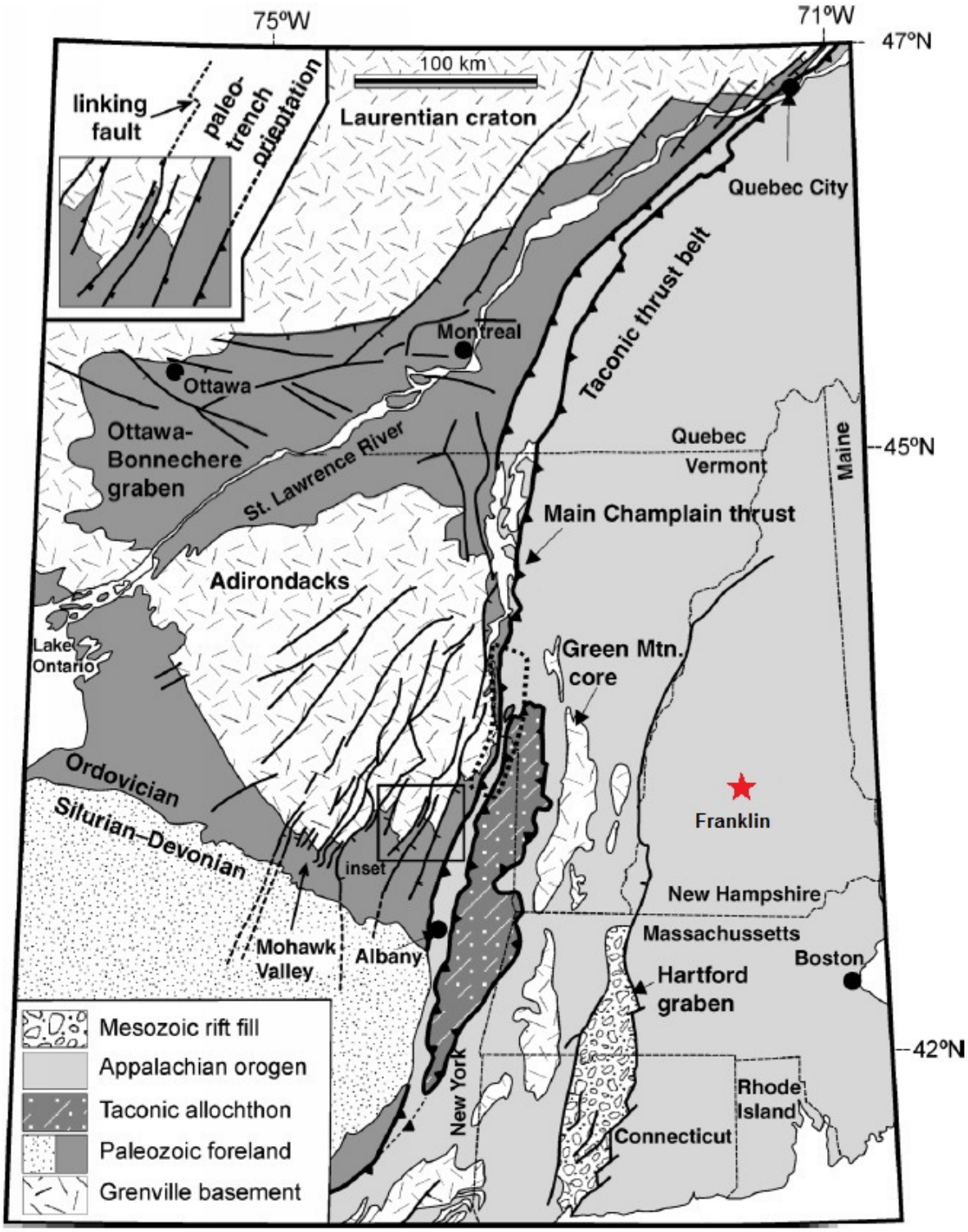

Figure 2-2: Map of New England illustrating faults and the relationship between geologic provinces (Hayman and Kidd 2002).

Lineaments are linear features associated with geological structures such as faults and can be extracted from satellite and aerial images. The known lineaments near the Franklin Falls Dam site are presented in Figure 2-3. The lineaments are generally oriented northeast and northwest, including a major mapped lineament running adjacent to the dam and parallel to the Pemigewasset River. According to Barosh (1985) this lineament belongs to a general zone of northwest trending lineaments forming the Winnipesaukee-Winooski lineament zone, extending from coastal New Hampshire and Maine through central New Hampshire and into central Vermont (Krinitzsky and Dunbar 1986).

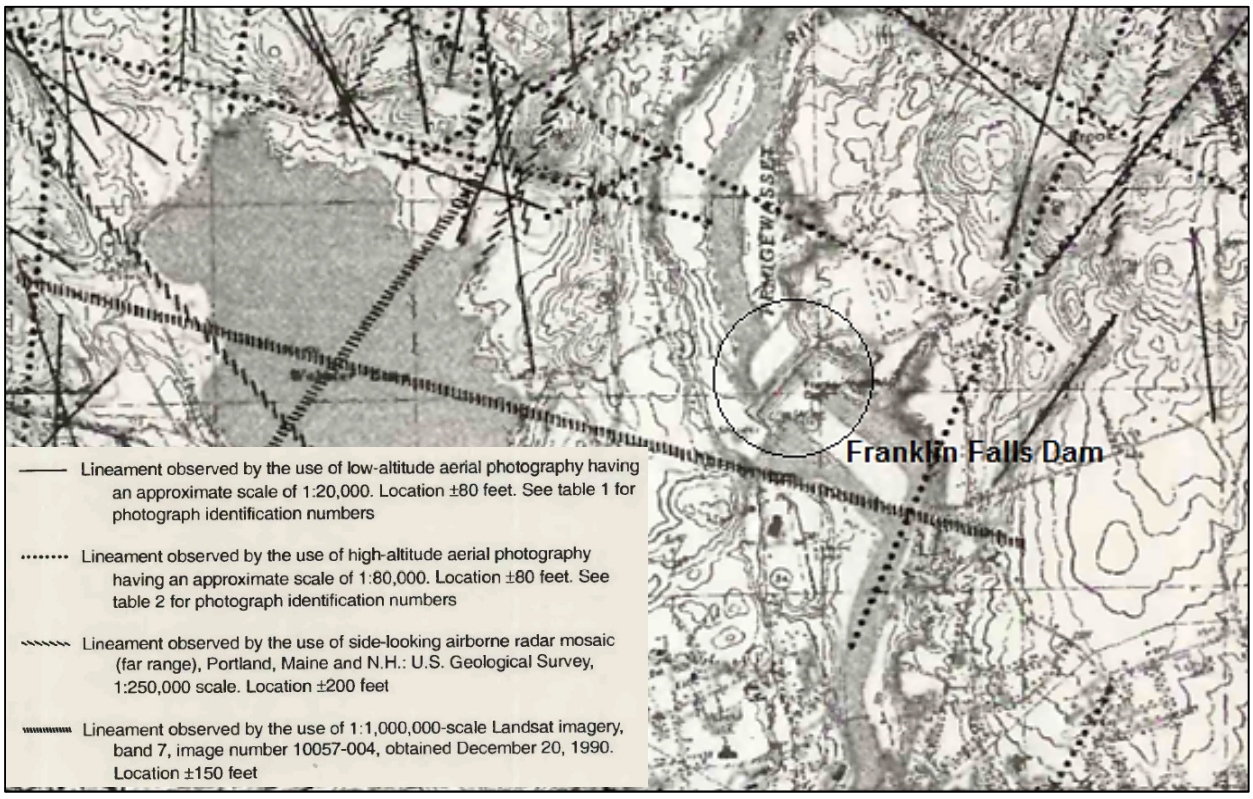

Figure 2-3: Lineament map of the Central New Hampshire bedrock aquifer assessment (Clark Jr et al. 1998).

2.1.3 Regional seismicity

No surface evidence of recent movement along existing faults or lineaments has been found in New Hampshire (Sanders et al. 1981). Therefore, the potential for severe earthquake ground motion at the Franklin Falls Dam site is extremely remote (Krinitzsky and Dunbar 1986).

In general, New Hampshire experiences low to moderate seismic activity, mostly concentrated along the eastern boundary and in the southern half of the state. Within the coastal zone, the south eastern area seismic activity is concentrated in the Ossipee area and along the Merrimack River (Krinitzsky and Dunbar 1986). The general seismic trend observed in central New Hampshire is believed to be part of the Boston-Ottawa seismic belt formed during the opening of the Atlantic Ocean (Krinitzsky and Dunbar 1986). Therefore, most of the seismic activity along the coast can be explained in terms of regional subsidence caused by crustal movements from a single stress field associated with continuing spreading of the Atlantic basin (Barosh 1981). This regional subsidence along the eastern coast, from Connecticut to Maine, varies between 1 and 4 mm per year according to Brown and Reilinger (1980).

Several probabilistic approaches have been proposed to predict an earthquake recurrence in the region (Chang 1983). Table 2-1 presents the proposed mean return periods for specific intensities for the entire New England area by Chiburis (1981). The intensity scale presented in Table 2-1 is the Modified Mercalli (MM), which rates earthquakes based on the damage produced in structures and landforms, as well as how they are felt by the population (USGS 1989). The corresponding surface wave magnitudes (M_s), which are based on the amplitude of Rayleigh waves that travel mainly along the upmost layers of the Earth, are also shown in Table 2-1.

Table 2-1: Proposed mean return period by Chiburis (1981)

MM intensity	M_s	Mean return time (years)
VI	4.6	0.6
	5.0	1.1
VII	5.2	1.5
	5.5	8.8
VIII	5.8	53
	6.0	175
IX	6.4	1 923
	6.5	3 500

2.2 Dam and site description

The Franklin Falls Dam was constructed between 1939 and 1943 on the Pemigewasset River, which joins with the Winnipesaukee River about 5 km downstream to form the Merrimack River. The dam derives its name from the town of Franklin Falls (south-central New Hampshire), where it is located (Krinitzsky and Dunbar 1986). The dam was constructed for flood control and is owned and operated by the New England District of the US Army Corps of Engineers (USACE).

The crest of the dam was constructed to an elevation of 126.8 m above sea level. The crest length of the dam is about 530 m and its maximum height is about 42 m above the stream bed. It is a zoned earth fill structure composed of an impervious core and pervious fills terraces. The appurtenant structures include a spillway located behind the west abutment founded on rock with a concrete 166-m-long weir, and two gate controlled outlet reinforced concrete conduits extending through the embankment and founded on bedrock (Brown 1941). An aerial photograph of Franklin Falls Dam is shown in Figure 2-4.

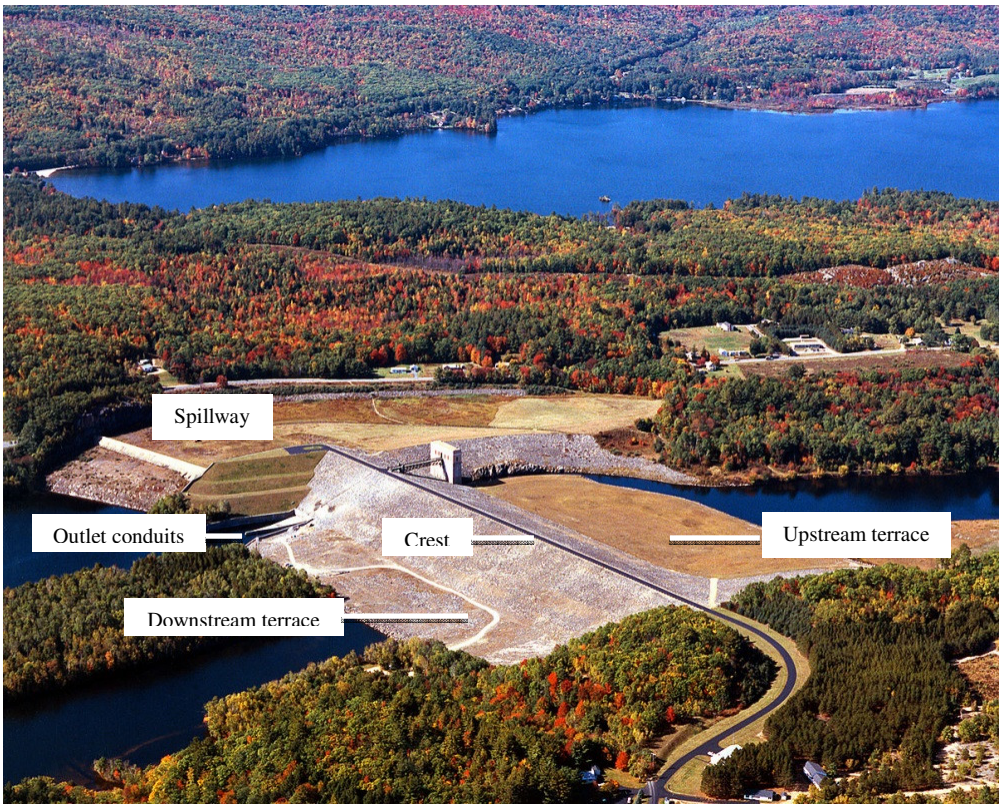

Figure 2-4: Aerial photograph of Franklin Falls Dam (USACE, 1999).

The Pemigewasset River flows across a narrow sandy flood-plain confined by high sand terraces lying on bedrock walls of a preglacial valley (Brown 1941). The river generally flows from north to south. However, locally (at the dam site) the river flows from northwest to southeast and the alignment of the dam is southwest-northeast.

2.2.1 Subsurface conditions

The foundation investigations for the Franklin Falls Dam involved explorations for the design of the concrete control structures and explorations for the embankment foundation. The investigations for the control structures were accomplished by driving 75-mm-diameter casing to bedrock and coring the rock. A total of 70 boreholes were completed. These boreholes extended for about 9 to 12 m deep with an average core recovery of 95%. The boreholes confirmed the nature of the rock being composed of hard granular schist containing numerous fractures in the upper weathered zones and scattered fractures throughout. The bedrock was judged to be suitable for supporting the planned structures, with only shallow cut-off grouting where the reduction of seepage and uplift pressures was an issue (Brown 1941). As shown in Figure 2-5, bedrock lies at considerable depth below the east abutment and under most of the dam, but outcrops along the west abutment, where it forms the foundation for the spillway and outlet structures (Brown 1941). The overburden was not sampled nor tested in these boreholes.

The embankment foundation investigations were extensive due to the variable nature of the glacial deposits found on the bottom of the valley. The investigations were conducted for about 1.5 years in conjunction with other field and laboratory work (Brown 1941). Based on this investigation, the composition of the overburden varies, both laterally and vertically, from silty, very fine sands to gravelly coarse sands. The upper material is composed of stratified, silty, fine sand underlain by medium to coarse sand. Below these stratified materials, unstratified deposits of compact, bouldery, and silty sand overlie bedrock (Chang 1987).

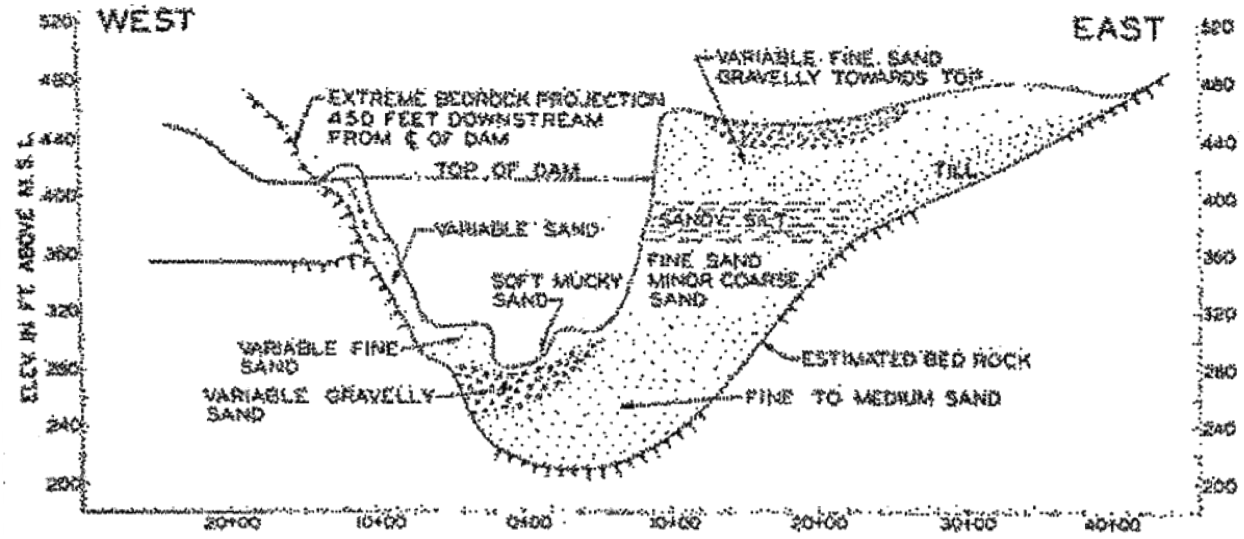

Figure 2-5: Geological profile, upstream from center line of the Franklin Falls Dam (Brown 1941).

The surface of the west abutment is inclined at about 1H:4.5V downwards towards the dam. The east abutment is a steep slope composed of overburden. There is a general horizontal continuity of three different zones of material: the lower zone from the base foundation (elevation 93 m to 113 m) composed of fine to medium sand with minor lenses of medium to coarse sand and of gravelly sand; the middle zone (elevation 113 m to 122 m) composed of stiff, sandy, medium to coarse silts with minor but persistent thin bands of fine to medium sand; the top zone varying from silty fine sands (above elevation 122 m) to gravelly medium to coarse sands in the upper 3 to 6 m (Chang 1987).

2.2.2 Design, construction and operation of the dam

2.2.2.1 Design

The Franklin Falls Dam was designed in the late 1930s by the USACE. The design team included Mr. F. Steward Brown, Chief of the Design Section of the U.S. Engineer Office as well as Prof. Arthur Casagrande of Harvard University and Mr. W.L. Shannon, as special consultants to the USACE (Brown 1941).

The design of the dam consisted in a zoned earth fill embankment with a core of compacted clayey till for seepage control. To limit the flow due to the permeability of the alluvial foundation, three alternatives were considered:

1. A blanket of low permeability soil extending from the core to the upstream cofferdam.
2. A sheet-pile cut-off wall extending from the bottom of the core to about mid-depth of the foundation soils.
3. Only the compacted core (USACE 1938; Brown 1940).

The Franklin Falls Dam was one of the first earth fill dams designed using modern methods of design and construction. In fact, many existing methods of design and construction were evaluated during the design and construction of the Franklin Falls Dam, including:

Permeability and seepage study – Two series of investigations totalling 24 boreholes were conducted within the footprint of the dam. Laboratory work on these samples included sieve analysis, permeability and shear tests. The first investigation (16 boreholes) disclosed the composition of the foundation in good detail but without adequate qualitative testing (Brown 1941).

Since the samples obtained from the first set of borings were not entirely satisfactory, the method of sampling was modified for the second set (USACE 1938). Samples from the second series of boreholes (8 boreholes) were relatively intact and were subjected to permeability testing at the Soil Mechanics Laboratory of the Harvard Graduate School of Engineering (Brown 1941).

A falling head device was used for all soil types except for coarse, uniform sand and gravel. The constant head device was used on coarse, uniform sand and gravel. Overall, good permeability values were obtained from the testing and permeability profiles were developped. In addition, seepage studies were conducted by Prof. Casagrande, including the study of the impervious upstream blanket of the dam, which was one of the different alternatives considered for the design of the dam to limit the flow and control seepage (Brown 1941).

Based on the findings of the study, the following assumptions were made with respect to seepage analysis (USACE 1938):

1. The foundation soils are anisotropic with a horizontal and vertical coefficient of permeability ratio (K_h/K_v) of 4;
2. The core and the upstream blanket are impervious;
3. The value of K_h for the dam (except the core) and the foundation soils above el. 85.3 m and below el. 79.2 m is $4.0x10^{-3}$ cm/s;
4. The value of K_h for the foundation soils between el. 85.3 m and 79.2 m is $4.0x10^{-2}$ cm/s.

The hydraulic regime of the impervious blanket was evaluated using flow nets, and is illustrated in Figure 2-6. The impervious blanket resulted in a total seepage loss of 12.5 $m^3/s/m$ and an average hydraulic gradient at the filter of 0.20.

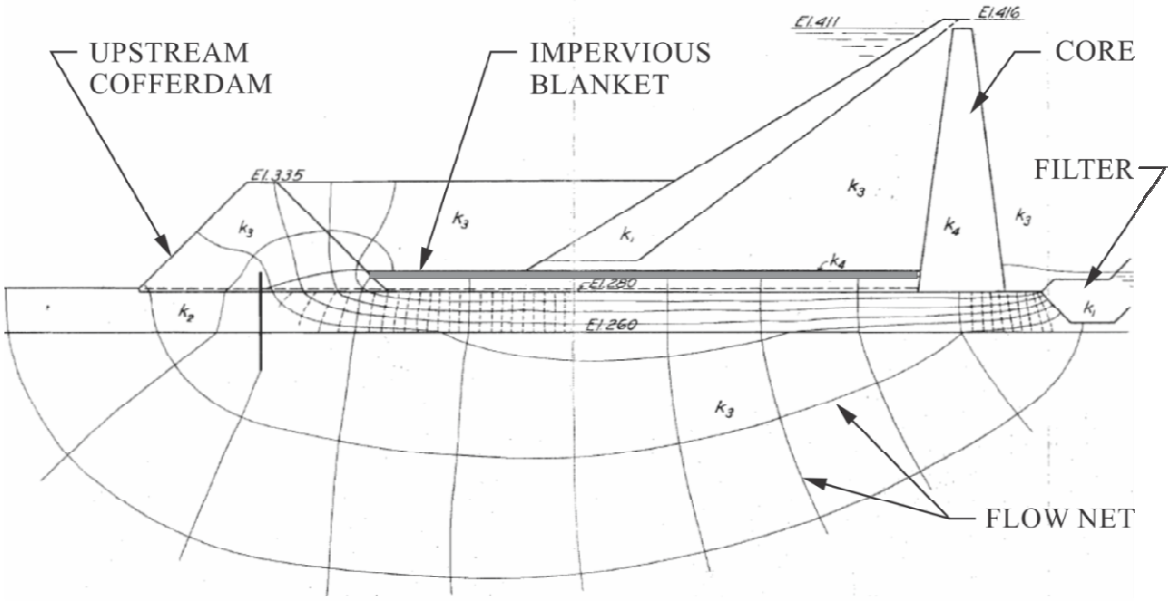

Figure 2-6: Flow net of the Franklin Falls dam with impervious blanket (USACE 1938).

Filter design – There was a concern with respect to the risk of internal erosion of the fine-grained foundation soils. Accordingly, the inclusion of a filter was considered. To verify the proposed grading of the filters of the drainage trench, laboratory studies were performed by Mr. G.E. Bertram at Harvard University (Brown 1941). Since the composition of this protective filter was primarily dependent upon the grain size distribution of the soil layers which are to be protected

from erosion, a large number of samples from the borings were subjected to grain size analysis. The grain size distributions wer obtained by sieve and hydrometer analyses (USACE 1938).

Ultimately, a two-layer filter of fine and coarse materials was selected. The gradations of the filters and the foundation materials are presented in Figure 2-7.

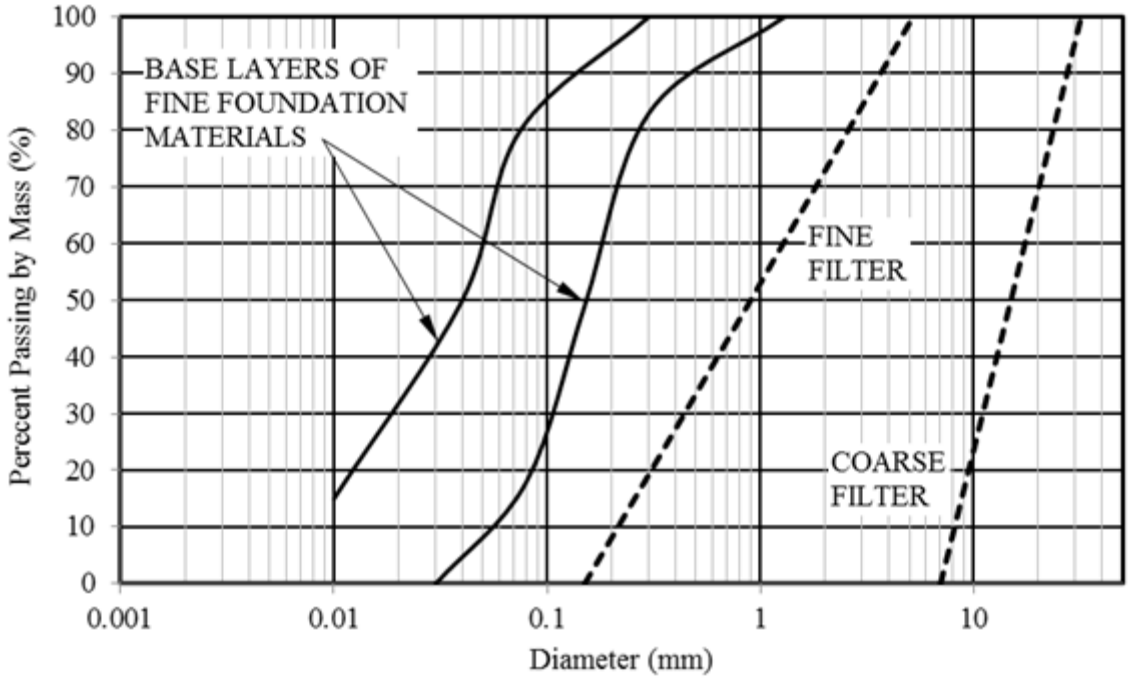

Figure 2-7: Grading of filter test materials (adapted from Brown, 1941)

Liquefaction prevention and triaxial testing – There was a concern that the loading of the dam would induce "static liquefaction" in the foundation soils. To establish the necessary degree of compaction of the sandy soils, a series of shearing tests were performed to determine the critical density of the soil. At first, two series of direct shear tests were conducted on soils from the Franklin Falls Dam site but resulted inconclusive with respect to volumetric behavior. A "simple" prototype triaxial compression testing apparatus had been developed by Prof. Casagrande at MIT in 1930. The Franklin Falls Dam project provided the impetus for the improvement of this device, such as the addition of a loading apparatus to allow stress or strain-controlled testing (USACE 1938). A diagram and a picture of the triaxial device are shown in Figure 2-8.

The triaxial testing results confirmed the existence of a critical density, dependent on the effective confining stress. The angle of internal friction of the soils was found to vary from 32° to 44° with decreasing void ratio. A minimum relative compaction of 80% was recommended for the embankment and foundation soils (USACE 1938). This degree was determined relative to laboratory maximum and minimum void ratio values.

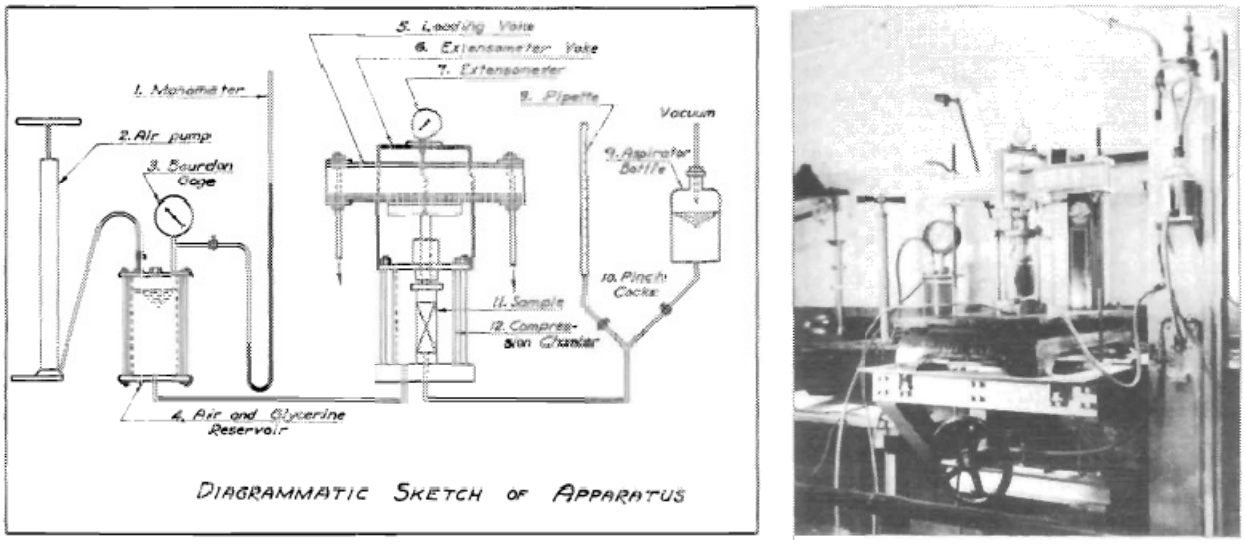

Figure 2-8: Diagram and picture of the first modern triaxial testing device (USACE 1938).

Compaction study – A series of field compaction tests of the pervious materials to be used to construct the dam was conducted to determine the feasibility of compacting the materials to the recommended minimum relative compaction of 80 % to prevent static liquefaction (USACE 1938).

Thirty-four compaction tests were conducted at the dam site with various types of tamping, vibrating and full-sized rolling equipment. These tests involved the construction of 34 low embankments to be compacted while varying the water content, number of passes and layer

thicknesses (1 to 5 m in depth) of the soil. Relatively undisturbed samples were taken from each embankment and sent to the U.S. Engineer Soils Laboratory (Boston District), Concord, New Hampshire, for determination of specific gravity, void ratio, degree of compaction, and water content. The efficacy of the various methods of compaction tested was determined by comparing the degrees of compaction attained (USACE 1938).

Ground modification study – To compact the loose, fine sand deposits of the foundation, a number of field experiments were conducted at the site consisting of the application of buried charges of explosives as a method of compaction for a large area of loose deposits. Charges were fabricated by binding and taping stick of dynamite around skeleton spools, which were jetted to the desired depths (about 5 m). An average increase of 30% resulted from the five blasts performed in the tests, the compaction effect extending to depths of 5 to 6 m.

Additional details of the design and construction can be found in James and Arbaiza (2015).

The final design of the dam consists of the embankment, an emergency spillway cut through the west abutment, and the low-level outlet works. The embankment zones, starting from the upstream side, are a dumped fill upstream berm; a rockfill upstream shell; transition zones of sand and gravel, selected pervious fill, and pervious fill, an impervious core, downstream transition zones of pervious fill, selected pervious fill; and a downstream rockfill shell and berm. An impervious blanket extends under the downstream portion of the dam extending about 180 m upstream from the core under the upstream dumped fill berm.

The crest width of the dam is of 11 m and the upstream and downstream slopes are of 3.25H:1V and 2.75H:1V respectively. As previously stated, the crest length of the dam is about 530 m and its maximum height is about 42 m above the stream bed. A typical cross-section of the dam is shown in Figure 2-9.

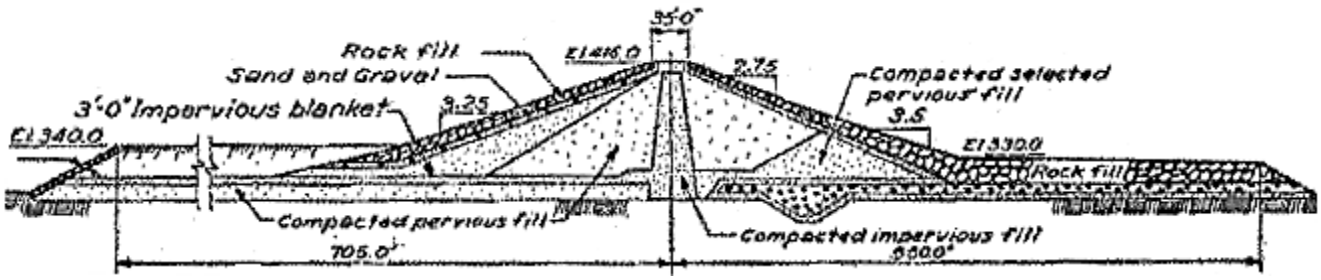

Figure 2-9: Typical cross-section of the dam (Brown 1941).

2.2.2.2 Construction

The construction of the Franklin Falls Dam began in November 1939 and was completed in October 1943 (USACE 1969). The embankment material was obtained from excavation for the spillway and outlet works and from selected borrow sites near the dam. The variable stratified sands found on the east terrace were used for the selected pervious fill, and the sand and gravel for the filters and concrete aggregates (Brown 1941). The impervious material for the core and the impervious blanket was taken from a borrow site about 6 km from the Franklin Falls Dam site. Rockfill for the shells was obtained from spillway and outlet excavations and was placed by dumping (USACE 1938).

Since the results of the ground modification study were favorable, the entire embankment foundation area was compacted with explosives prior to the construction of the dam. The subsidence of the compacted areas averaged from 60 to 75 cm, with an estimated reduction in void ratio from 0.95 to 0.80 (Brown 1941).

Following the compaction study, the pervious material of the dam was compacted by 30-cm-thick layers. Each layer was compacted at optimum water content using a rolling compactor, such as a tractor-drawn disc roller or a tractor-drawn small sheep's foot roller, by 6 passes and attaining a minimum degree of compaction of 80 % (USACE 1938).

Figure 2-10 and 2-11 are photographs taken in 1940 during the construction of the Franklin Falls Dam.

Figure 2-10: 1940 – Construction of Franklin Falls Dam, photograph taken looking downstream to stilling basin from west abutment, provided by Paul E. Cote and Pullen (2012).

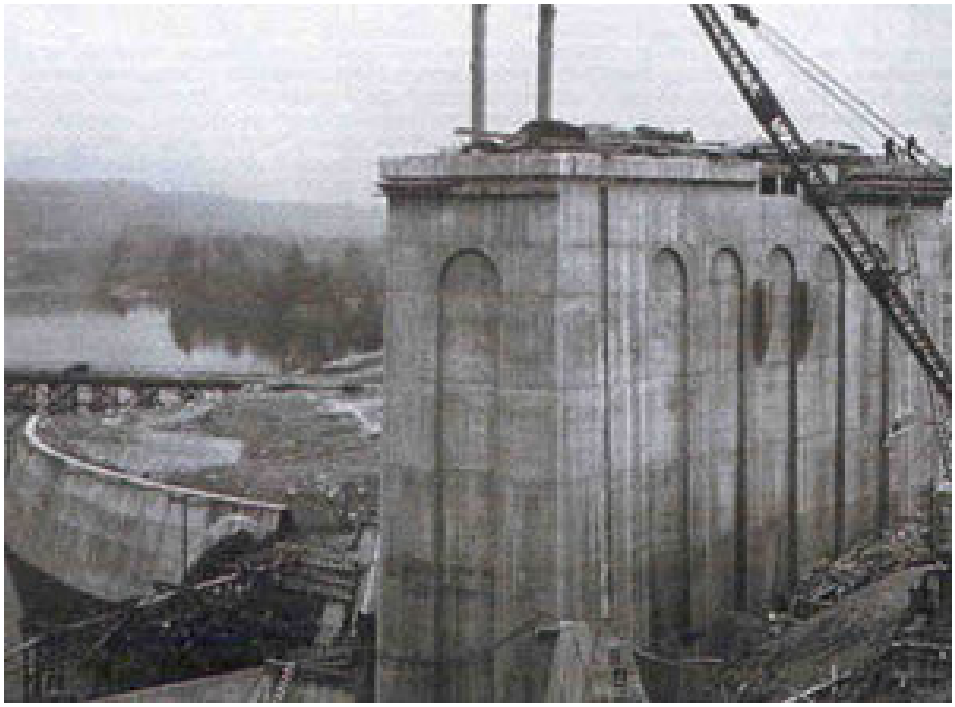

Figure 2-11: Construction of the gatehouse at the Franklin Falls Dam, provided by USACE (2016).

2.2.2.3 Operation

As mentioned, the Franklin Falls Dam was designed and constructed for flood control. During normal (nonflood) periods, the gates are maintained open to quickly develop a high rate of discharge during the early period of a flood, thus minimizing storage build-up. For minor increases in flow, the reservoir acts as a simple retarding basin, even with the gates fully open. During flood periods, Franklin Falls Dam is regulated as part of a reservoir system to provide protection to downstream communities. The upstream reservoir maximum pool elevation is of 125 m and the downstream water level is encountered near the surface of the valley at 96 m (USACE 1966).

Photographs of the dam taken on a site visit performed in November 2015 are shown in Figures 2-12 through 2-16.

Figure 2-12: Crest of the dam and downstream slope, looking north east, 2015.

Figure 2-13: Downstream slope, looking north from the west abutment, 2015.

Figure 2-14: Gate house and service bridge, looking north, 2015.

Figure 2-15: Outlet conduits downstream of the dam, looking south east, 2015.

Figure 2-16: Upstream terrace, looking north, 2015.

2.2.3 Materials and geotechnical properties

The majority of the geotechnical properties of the embankment materials were estimated from the laboratory testing associated with the foundation investigations performed by the USACE (1938). As stated in the previous section, the associated laboratory testing included gradation, shear, permeability, and density tests by the USACE's Concord laboratory and gradation, permeability, and density tests at Harvard University under the direction of Prof. Casagrande.

The permeability tests allowed the materials of the foundation to be classified into three groups:

- High permeability: Material composed of coarse sand, permeability coefficient > $1x10^{-2}$ cm/s;
- Intermediate permeability: Permeability coefficient between $1x10^{-2}$ to $2x10^{-3}$ cm/s;
- Low permeability: Material composed of fine sands, permeability coefficient < $2x10^{-3}$ cm/s.

Information about main embankment materials, such as the impervious core and compacted pervious fill (adjacent to the core), were obtained following the soils investigations conducted for the USACE in 1985 and 1987. Several borings were completed and selected samples from the borings were tested for grain size distribution and specific gravity (USACE, 1986; GEI, 1993).

Impervious core – The material for the impervious core is a well-graded till and was derived from a borrow site, about 6 km from the Franklin Falls Dam. The triaxial testing determined an angle of internal friction of 28° and a cohesion of 15 kPa.

Compacted pervious fill and dumped fill – Cohesionless material composed of uniform silty fine sand to well-graded gravelly sand, obtained from outlet structure excavations. Triaxial testing determined an effective angle of internal friction of 37°.

Selected pervious fill – Material containing less than 5% of fines, obtained from nearby borrow areas. Triaxial testing determined an effective angle of internal friction of 37°.

Overburden – As discussed, the foundation soils are composed of stratified sands, silts, and gravels that vary significantly with depth. Slope and foundation stabilities were estimated by the designers using an effective angle of internal friction of 37° (GEI 1993).

Table 2-2 summarizes the main geotechnical properties of the Franklin Falls Dam materials. As stated, the strength parameters were obtained by the triaxial shear tests performed by the USACE in 1938. These parameters, as well as the unit weight of the materials were used in the stability analyses performed by Geotechnical Engineers Inc. (GEI Consultants) in 1980. Although it is not certain if the unit weights were estimated by GEI Consultants, the values are comparable to those given in the literature (Holtz et al. 2011). These values are also comparable to those presented in the USACE's Sample Data & Gravel Correction Tables, from different samples obtained in the 1985 and 1987 soils investigations (USACE, 1986; GEI, 1993). In addition, laboratory test results from the USACE foundation investigation (1938) indicated specific gravity values for the foundation soils that varied between 2.50 and 2.82, which correspond to the unit weight values presented in Table 2-2.

Table 2-2: Main parameters of soils (USACE, 1938; GEI, 1993)

Material	γ, unsat (kN/m^3)	γ, sat (kN/m^3)	ϕ' (°)	c' (kPa)
Impervious core	21.8	22.2	28	15
Pervious fill	18.9	20.1	37	0
Rockfill	16.5	20.1	45	0
Sand and gravel	17.0	20.0	37	0
Dumped fill	17.3	18.9	37	0
Overburden	20.0	20.0	37	0

In 1980 and 1981, Goldberg-Zoino & Associates, Inc. evaluated the potential for liquefaction and cyclic mobility of the Franklin Falls Dam. Standard penetration testing, undisturbed sampling and a laboratory testing program of static and cyclic triaxial tests were performed on samples from three borings (GEI 1993).

To evaluate the potential for liquefaction, critical void ratios were determined with static triaxial tests and were compared with in situ void ratios. According to the results of the triaxial tests, the Franklin Falls Dam had negligible potential for liquefaction because the measured in situ void

ratios (average e = 0.72) were typically less than the lowest estimated critical void ratio (e = 0.74) (GEI 1993). The potential for cyclic mobility of the embankment soils, evaluated by using SPT data and cyclic triaxial testing, was also determined to be negligible because of the high density of the compacted embankment (GEI 1993).

2.3 Earthquake ground motions

2.3.1 General description of earthquake ground motions

Earthquakes are generated by sudden movement (or rupture) along a fault. A vast majority of significant earthquakes are generated by fault movement at tectonic boundaries. When an earthquake occurs, seismic waves radiate away from the zone of fault movement through bedrock and attenuate with distance due to dissipation and damping. Locally, seismic waves radiate upwards from bedrock through overburden, when present, and are modified by the response of the overburden and topographic effects before affecting structures such as dams (Kramer 1996).

2.3.2 Characteristics of ground motion records

Earthquake ground motions are generally measured using accelerometers that provide accelerations as a function of time in two horizontal directions (transverse and longitudinal) as well as in the vertical direction. From the time records of the acceleration, the velocities and displacements can be computed by integration (Newmark 1965).

Earthquake ground motion records (also known as accelerograms) are determined by the intensity (or energy) of the earthquake, which is related to the length of fault movement (or rupture), the type of fault movement, the source-to-site distance, regional bedrock characteristics, local subsurface conditions and topography. In other words, ground motion records reflect the influence of local conditions and can thus vary considerably with the characteristics of the overburden and topography. For instance, soft soils may amplify the accelerations and modify the frequency characteristics of the ground motion (Seed and Idriss, 1969).

Ground motions are characterized using different parameters, generally depending on the objective or application, such as:

Peak ground motion – The most common parameter to measure the amplitude of a particular ground motion is the peak ground motion (PGA), which is simply the largest absolute value of acceleration obtained from the accelelogram (Kramer 1996). The PGA is used to describe ground motions in a very general sense. However, the PGA provides no information on the frequency content or duration of the motion and may not be significant in determining the response of a dam (Newmark, 1965; Kramer, 1996).

Magnitude – The size of an earthquake can be evaluated by its magnitude, which could be characterized by the earthquake's energy or amplitude, or by the extent and size of distortion at the zone of rupture (Towhata 2008). The Richter local magnitude was the first widely-used method to measure the magnitude of an earthquake. However, it is not the most appropriate scale for description of earthquake intensity since it does not provide accurate estimates for large magnitude earthquakes and does not distinguish between different types of waves (Kramer 1996).

The moment magnitude, M_w, is based on the seismic moment released by an earthquake, which is a direct measure of the factors that produce rupture along a fault (Kramer 1996). The moment magnitude is applicable globally and is preferred due to its accuracy on determining the energy released by earthquakes of different intensities.

The body wave magnitude, m_b, is a worldwide magnitude scale based on the amplitude of the first few cycles of p-waves which are strongly influenced by the focal depth (Kramer 1996).

Spectral diagrams – The frequency content of a ground motion can be described by response spectra. Response spectra describes the maximum response of a single-degree-of-freedom system to a particular input motion as a function of frequency and damping ratio of the system (Kramer 1996). Spectral diagrams indicate the peak spectral acceleration, velocity or displacement associated with different frequencies (or periods) (Kramer 1996).

Fourier spectra – The frequency content of a ground motion can also be described by the Fourier amplitude spectrum. A Fourier amplitude spectrum shows how the amplitude of the motion is distributed with respect to frequency. A narrow spectrum implies that a motion is dominated by one frequency, whereas a broad spectrum indicate a ground motion with a variety of frequencies (Kramer 1996).

Predominant period (frequency) – The predominant period (or frequency), defined as the period of vibration corresponding to the maximum value of the Fourier amplitude spectrum, provides useful representation of the frequency content of a ground motion (Kramer 1996).

Duration of 'significant shaking' – The total duration of a ground motion is of importance in determining the response of a structure such as an embankment dam (Newmark 1965). For example, a motion of short duration may not produce enough load reversals to initiate in a structure, even if the amplitude of the motion is high (Kramer 1996). Duration can also be expressed in terms of equivalent cycles of shaking and is used in a wide range of applications including evaluation of liquefaction potential (Kramer 1996). The duration of significant shaking is evaluated beyond a particular threshold acceleration, which is typically above 0.05g.

Energy content (Arias intensity) – The Arias intensity measures the intensity of ground motion and represents the total energy per unit weight absorbed by an idealized set of oscillators (Kayen and Mitchell 1997). The Arias Intensity, illustrated in Equation (1), can be described as the integral of the square of the acceleration-time history and is defined by Arias (1970):

$$I_h = I_{xx} + I_{yy} = \frac{\pi}{2g}\int_0^t [a_x(t)^2]\,dt + \frac{\pi}{2g}\int_0^t [a_y(t)^2]\,dt \quad (1)$$

where I_{xx} and I_{yy} are horizontal orthogonal components of the Arias Intensity I_h in units of length per time, $a(t)$ is the acceleration-time history in units of g, and g is the acceleration of gravity (Kayen and Mitchell 1997).

2.3.3 East coast ground motions

The center and east coast of North America are seismically active, although to a much lesser degree than the west coast. The low level of earthquake activity in the east coast of North America together with short instrumentation history and lack of surface faulting leads to uncertain assessment of seismic hazards and seismicity parameters (Acharya et al. 1982). However, the New Madrid (1811-1812; Mw=7, 7.5, 7.7 and 7.7), Charleston (1886; Mw=7.3), Miramichi, (1982; Mw=5.1 and 5.7), Saguenay (1988; Mw=5.9) earthquakes are evidence of the potential for significant earthquakes in the center and in the east coast.

Due to relatively harder and more intact bedrock, earthquakes on the east coast exhibit less attenuation with distance from the source and ground motions are characterized by higher frequencies (Tremblay and Atkinson 2001).

It is noted that the use of the PGA as an index parameter of earthquake loading, could be overly conservative when applied to the east coast of North America. This is due to the fact that empirical correlations are largely based on western events. Therefore, eastern PGA values do not necessarily have the same implication for structural response (Atkinson and Boore 1990).

Three historic east coast earthquakes are presented, in chronological order, in the following subsections.

2.3.3.1 The 1982 Miramichi earthquake

On January 9, 1982, an earthquake with a body wave Magnitude (m_b) of 5.7 struck near Miramichi, New Brunswick (Wetmiller et al. 1984). This event, as well as the M_b 5.1 aftershock that struck 3 hours later was felt across the Maritime provinces, eastern Québec and the New England states, to distances of about 350 km from the epicenter (Cassidy et al. 2010). Since the immediate epicentral area was not populated, damage was very slight. Although there was no evidence of surface rupture, high-quality digital data and monitoring of the aftershocks indicated 25 mm of surface displacement identified as a secondary stress-induced movement along a pre-existing joint (Wetmiller et al. 1984)

Figure 2-17 presents the epicenter of the 1982 Miramichi earthquake and the Modified Mercalli (MM) intensity distribution of the main shock.

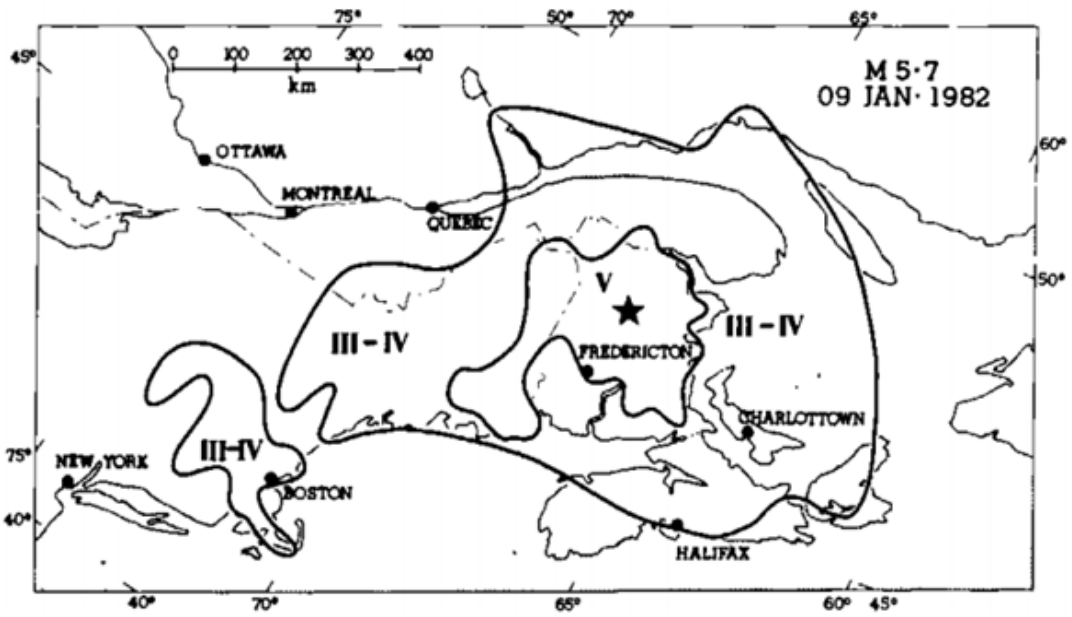

Figure 2-17: Epicenter of the 1982 Miramichi earthquale showing extent of Modified Mercalli intensity V and III (Basham and Adams 1984).

Most of the Miramichi ground motion records are characterized by high frequencies (approximately 40 Hz). Peak accelerations of these records are high but durations of significant ground motion (>0.05 g) were low. Figure 2-18 is a representative record of the ground motion from the Miramichi. The accelerogram was recorded on a rock site, at station Loggie Lodge located 6 km from the epicenter, and recorded a PGA of 0.58 g and a Nyquist frequency (highest frequency in the Fourier series) of 50 Hz (Bhan and Dunbar 1989).

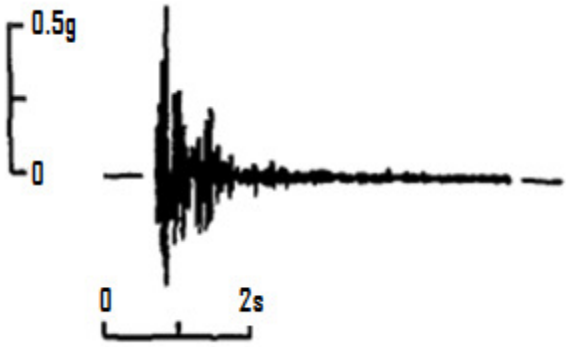

Figure 2-18: Acceleration of the 1982 Miramichi earthquake at station Loggie Lodge (Bhan and Dunbar 1989).

2.3.3.2 The 1982 Gaza Earthquake

At 19:42:42 EST on January 18, 1982, an earthquake of Richter magnitude 4.7 (m_b=4.4) occurred in south central New Hampshire (Chang 1983). The Weston Observatory and US Geological Survey estimated the focal depth to be between 4.5 and 8.0 km (Chang 1987). The Gaza earthquake was felt in most of New England, northern New York, and as far away as southern Quebec and northeastern Ontario (Chang 1983).

Thirty six accelerograms were recorded by accelerographs at five dams monitored by the New England division of the USACE, and by an instrument at a Veterans Administration Hospital (Manchester, NH) (Chang 1983). Figure 2-19 shows the recording stations and their distances from the epicenter.

The epicentral distance of the Franklin Falls Dam from this event was 8 km and significant ground movements were recorded in three accelerographs located at the crest, west abutment and downstream of the dam. No damage or deformation was observed on the dam following the event and only cosmetic damage to the gatehouse (a broken window) was reported (Chang 1983).

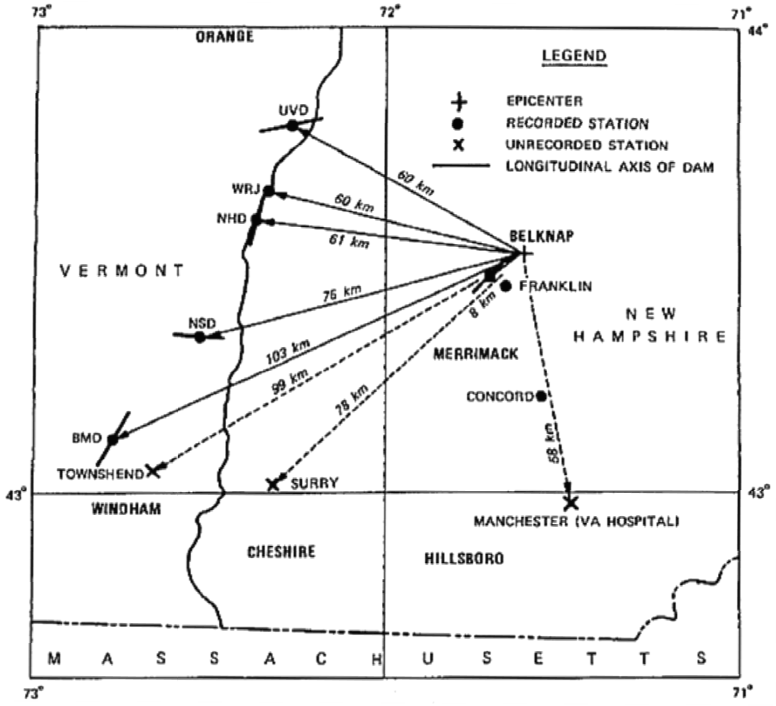

Figure 2-19: Epicenter of the 1982 Gaza Earthquake (Chang 1983).

The transverse component (perpendicular to the alignment of the dam) of the accelerograph located on the west abutment of the dam is shown in Figure 2-20. This device recorded a PGA of 0.55 g (predominant frequency of 14.5 Hz), which is the maximum acceleration recorded at the dam (Chang 1983). More information on the response of the dam is presented in Section 2.4.

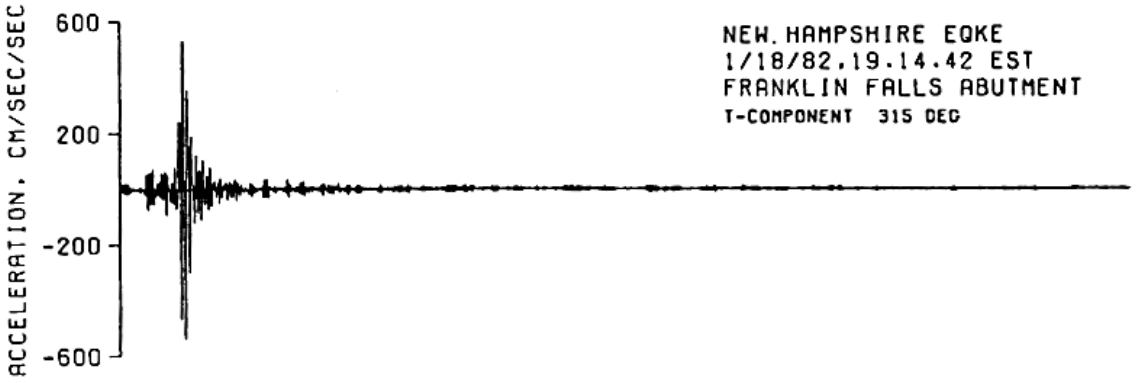

Figure 2-20: Transversal acceleration of the 1982 Gaza earthquake at the abutment of the Franklin Falls Dam (Chang 1983).

2.3.3.3 The 1988 Saguenay earthquake

On November 25, 1988, at 18:46 PM EST, an earthquake of m_b=5.9 occurred 40 km south of Chicoutimi, Quebec, Canada. The earthquake, with a focal depth of 25 km, was widely felt in eastern Canada and over a wide area of the northeastern United States (Somerville et al. 1990).

Damage in the populated epicentral area was modest, limited to cracked or fallen un-reinforced masonry walls. However, several landslides were attributed to the earthquake (Cassidy et al. 2010). Figure 2-21 shows the epicenter of the 1988 Saguenay earthquake and the Modified Mercalli (MM) intensity distribution of the main shock.

The earthquake was well recorded and provided an opportunity to obtain precise estimates of its source parameters (Somerville et al. 1990). The transverse ground motion record from station S16 (Figure 2-22), located 43 km from the epicenter, recorded a PGA of 0.13 g.

The Saguenay earthquake produced one of the largest set of strong motion recordings of any earthquake in the east coast (Somerville et al. 1990). Detailed analysis of seismic data from this

earthquake by a large number of researchers (e.g. Hough et al. 1989; Boore and Atkinson 1992; Boatwright and Choy 1992; Somerville et al. 1990) has provided valuable insight into the nature of moderate earthquakes in eastern North America (Cassidy et al. 2010).

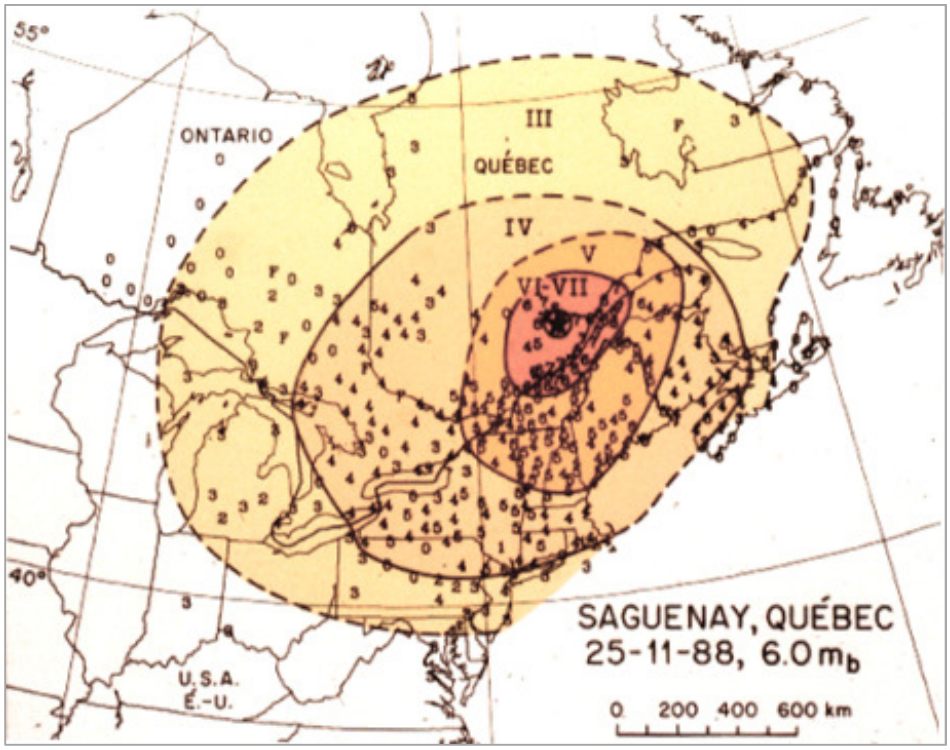

Figure 2-21: Epicenter from the 1988 Saguenay earthquake (Cajka and Drysdale 1996).

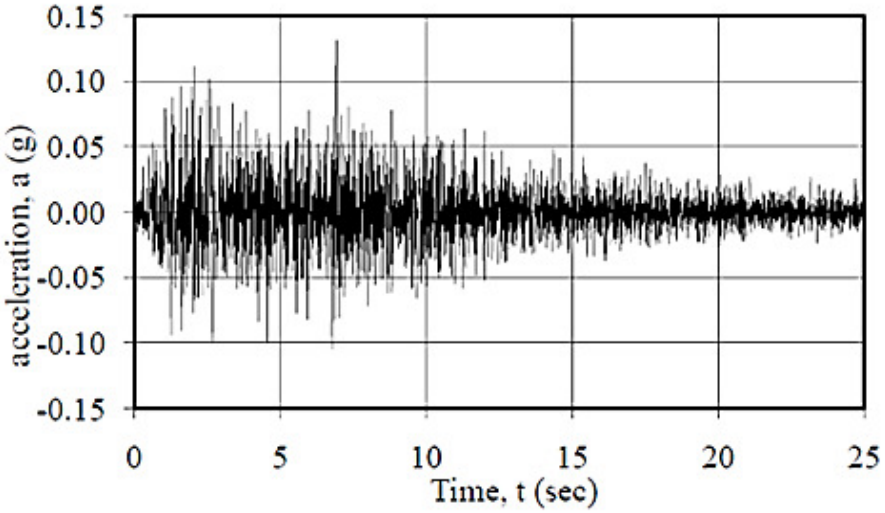

Figure 2-22: Ground motion of the 1988 Saguenay earthquake at station S16 (NRC, 2003).

2.4 The Response of the Franklin Falls Dam to the 1982 Gaza Earthquake

During the 1982 Gaza earthquake, accelerations were recorded on three accelerographs at the Franklin Falls Dam. The three accelerographs, shown in Figure 2-23 are located as follows (Chang 1987):

- Station A: west abutment, station 9+00, elevation 109.7 m;
- Station B: crest of the dam, station 17+00, elevation 126.8 m;
- Station C: level ground downstream of the dam, station 14+00, elevation 94.5 m.

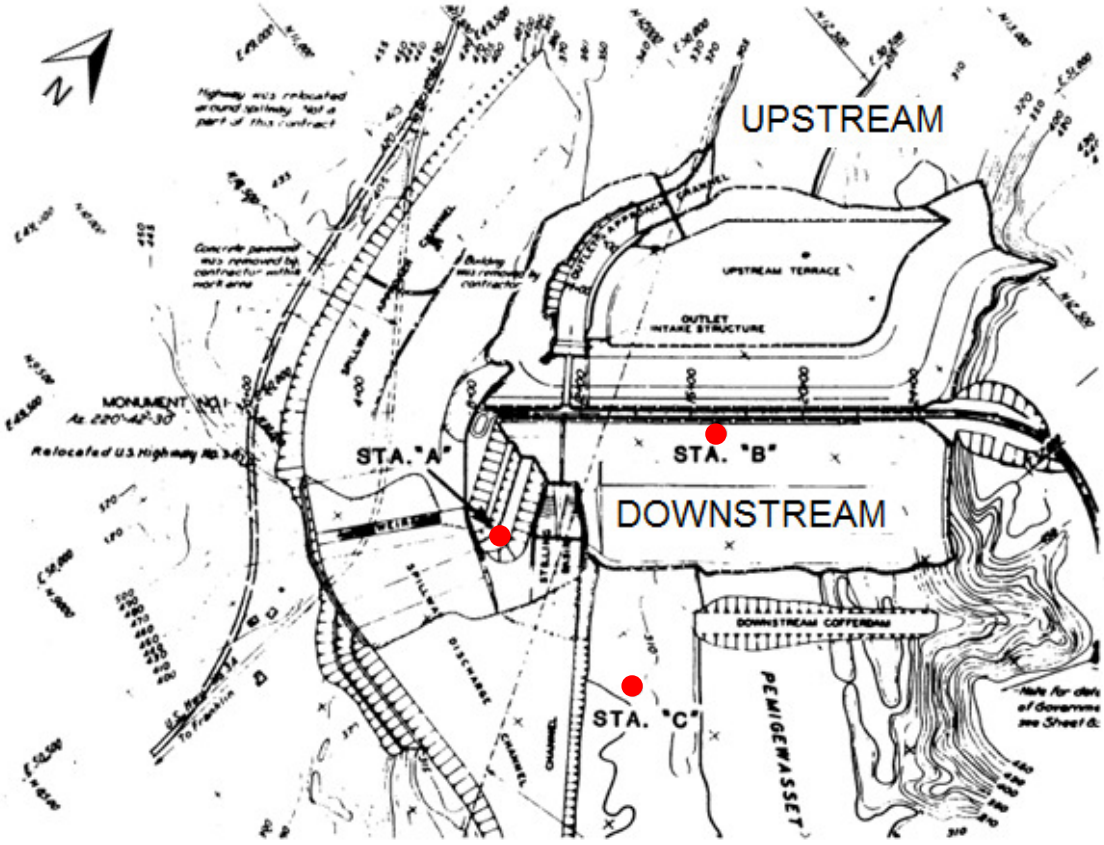

Figure 2-23: Plan view of the Franklin Falls Dam and location of accelerographs A, B and C (Chang 1987).

Each accelerograph consists of three components: longitudinal, transverse and vertical. The longitudinal and transverse components are oriented, respectively, parallel and perpendicular to the dam axis. Therefore, the transverse component is more important with respect to the seismic behavior of the structure since it acts in the direction of potential instability.

Chang (1983) analysed the strong motion data of the 1982 Gaza earthquake and corrected the 36 accelerograms, including the 9 accelerograms of the Franklin Falls Dam. In 1987, he analysed the spectral response of the dam and the natural periods of the dam and its foundation. Table 2-3 presents the main characteristics of the corrected ground motions.

Table 2-3: Main characteristics of the recorded ground motions from theGaza earthquake (James and Arbaiza 2015).

Location/ Direction	Peak ground acceleration PGA (g)	Arias Intensity I_a (m/s)	Predominant frequency f_p (Hz)	Mean frequency f_{MEAN} (Hz)
Crest				
Longitudinal	0.126	0.032	25.0	5.29
Transverse	0.313	0.079	16.7	7.41
Vertical	0.112	0.031	16.7	6.49
Abutment				
Longitudinal	0.285	0.089	12.5	13.89
Transverse	0.567	0.309	12.5	12.82
Vertical	0.175	0.025	25.0	7.14
Downstream				
Longitudinal	0.112	0.031	16.7	6.49
Transverse	0.260	0.082	12.5	8.93
Vertical	0.211	0.055	16.7	13.16

PGAs of 0.313 g, 0.567 g and 0.260 g were recorded in the transverse direction at the crest, the west abutment and downstream of the dam, respectively. The predominant frequency recorded (12 to 25 Hz) is higher than typical values of the west coast (4 to 6 Hz). Furthermore, the high PGA recorded in the transverse direction of 0.567 g at the west abutment indicate amplification of the ground motion due to topographic effects, which is typically seen along ridges and upper parts of slopes (Sigarán-Loría and Hack 2006).

Using the ground motion records, the Arias intensities were computed with SeismoSignal (version 5.1.2) by Seismosoft slr (2013), a software that processes strong-motion data. Arias intensity values of 0.313, 0.567 and 0.260 g were calculated by James and Arbaiza (2015) for the transverse components at the crest, the west abutment and downstream of the dam, respectively. As described in section 2.3.2, the Arias intensity is a measure of the energy content of a ground

motion per unit mass of soil and provides an indication of the potential for deformation or damage (Kayen and Mitchell 1997).

The measured transverse ground motions and spectral acceleration diagrams for 5% damping from the downstream and crest accelerographs are presented on Figure 2-24 and were also calculated with SeismoSignal. The ground motions are characterized by high frequencies typical of east coast events and the duration of significant shaking (>0.05g) is about 1 second. The spectral diagrams indicate strong responses for structures of relatively low periods, 0.1 to 0.2 s. At periods above 0.6 s, the spectral accelerations are close to zero.

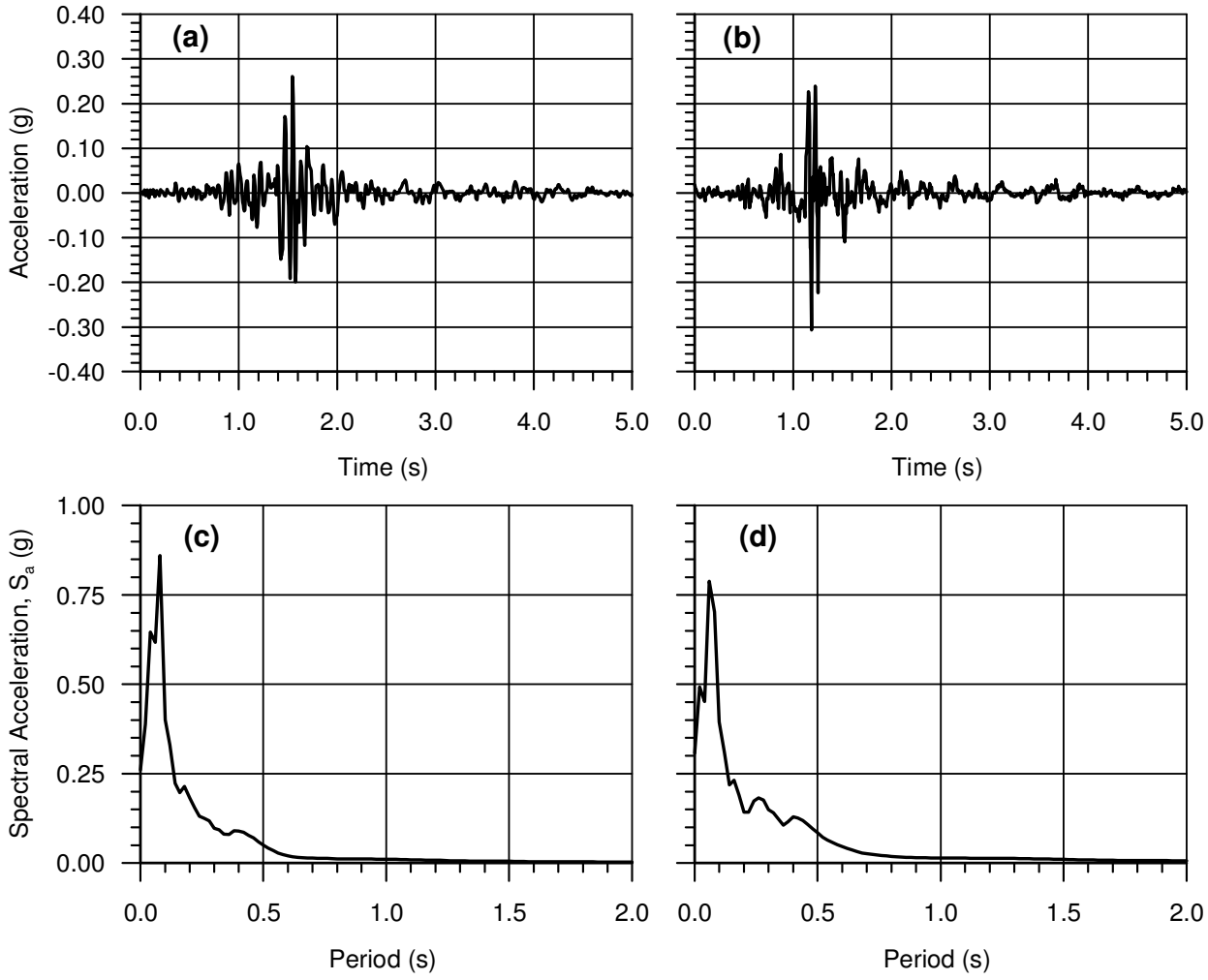

Figure 2-24: Measured transverse ground motions at the (a) downstream and (b) crest, and the corresponding spectral acceleration diagrams for 5% damping (c, d) (James and Arbaiza 2015).

2.5 Evaluation of the dynamic response of dams

The performance and stability of dams must be evaluated under all loading conditions that can reasonably be anticipated to occur during their life cycles. Due to the indeterminate life cycles of dams, these include seismic loads, even in regions of relatively moderate or low seismicity (CDA 2007). The CDA (2007) Dam Safety Guidelines recommend the following for the evaluation of the seismic performance of dams:

1. Determination of the Earthquake Design Ground Motion (EDGM), which is based on the consequences of failure of the dam and is expressed in terms of a recurrence interval. The recurrence interval varies from 500 years for dams where the consequences of failure are low to 10 000 years for dams where the consequences are extreme.
2. The parameters of the EDGM may be obtained from Earthquakes Canada and are based on a probabilistic approach and include composite contributions from several sources. These parameters include a PGA, a spectral acceleration at 5% damping, and a body wave magnitude.
3. The stability of the dam is evaluated using the pseudostatic (pseudo dynamic) method, as described in Hynes, Griffin and Franklin (1984). This is considered a screening level analysis due to the lack of precision of the method.
4. Permanent deformation analysis. This empirical method is based on the probability that a deformation will be produced in the dam undergoing a given seismic load.
5. If additional analysis is required, dynamic numerical analysis is undertaken.

These methods are discussed in more detail in the following sections.

2.5.1 The pseudostatic method

The pseudostatic method is the method most commonly employed to evaluate the seismic performance embankment dams. In this method, the horizontal accelerations induced in the mass of a dam by an earthquake are simulated using a static horizontal acceleration acting in the assumed direction of failure (upstream or downstream). Limit equilibrium, usually employing the method of slices, is then used to calculate a factor of safety with respect to a critical failure surface. The horizontal acceleration is calculated as a pseudostatic coefficient, times the acceleration due to gravity (Hynes-Griffin and Franklin 1984).

The pseudostatic coefficient is based on regional practice, government regulations and professional guidelines. The CDA (2007) recommends the method given in Hynes-Griffin & Franklin (1984). This method recommends a seismic coefficient equivalent to half the estimated PGA on bedrock (assuming that the dam is founded on bedrock) due to the design earthquake ground motion, with a minimum factor of safety of 1.0 and a 20% reduction in material strengths to account for strength loss during shaking.

The recommendations of Hynes-Griffin & Franklin (1984) are based on dynamic numerical modelling and assume that 1 m of deformation at the crest is acceptable. This method is limited to earthquakes with a maximum magnitude of 8.0 and to materials (embankment or foundation) not susceptible to liquefaction or subject to significant strength loss during shaking (Hynes-Griffin and Franklin 1984). Furthermore, the effect of the vertical component of the ground motion is not considered.

The pseudostatic method is known to be an inaccurate means of predicting dam performance. Seed and Idriss (1969) report several instances where dams with acceptable factors of safety evaluated using the pseudostatic method experienced failure during seismic loading. It should be noted that the earthquake magnitude, the duration of shaking, energy content and frequency are not considered by this method.

2.5.2 Permanent deformation analysis

Permanent deformation analysis is an empirical method for estimating deformations in an earth dam subjected to seismic loading. This method is based on the probability that a deformation will be produced in the dam undergoing a given seismic load. Newmark (1965) and Makdisi & Seed (1977, 1978, 1979) developed methods based on a correlation of the sliding of a block on an inclined plane and the movement of the mass on an assumed failure surface.

Bray and Travasarou (2007) proposed an updated approach to this method, which consists of applying a horizontal acceleration (pseudostatic coefficient) until obtaining a factor of safety of 1.0. The associated horizontal force is represented by k_y, the yield coefficient. In this approach, a predictive model is proposed to estimate seismic deviatoric displacements by computing the probability of zero displacement and the amount of the nonzero displacement.

This method considers the spectral acceleration of the ground motion, which is one of the most reliable parameters for the intensity of a ground motion. In addition, the initial fundamental period (T_s) capturing the dynamic response of the potential sliding mass is also considered (Bray and Travasarou 2007) and is defined as follows:

$$T_s = \frac{4H}{V_s} \tag{2}$$

where H is the average height of the sliding block and V_s the average shear wave velocity of the sliding mass. The shear wave velocity, V_s, can be estimated using equation 3, where G is the ratio of shear modulus and ρ the density of the soil.

$$V_s = \sqrt{\frac{G}{\rho}} \tag{3}$$

Similarly to the pseudostatic method, this approach can only be used when no liquefaction is expected to occur or when the materials are not susceptible to pore-water pressure development during seismic loading (Makdisi and Seed 1977). It should be noted that this method has been developed based on deformation of dams located on the west coast of North America.

2.5.3 Numerical analysis

The majority of the problems encountered in the area of geotechnical engineering can be studied using two dimensional numerical modelling based on the finite element (FE) or finite difference method. Dynamic FE analyses are favoured to evaluate the seismic response of a geotechnical system, since they can give detailed indication of both the soil stress distribution and deformation (Visone et al. 2008). To create a FE model, it is essential to select an appropriate model, divide the model into elements, extend equations of each element and determine the element's stiffness matrix, combine the element's matrix, and create a single matrix for the model (Akhlaghi and Nikkar 2014). The elements movement equation is given by equation (4), where $[M]$ is the whole mass matrix, $[C]$ the whole damping matrix, $[U]$ the model nods axial movement, and $\{R(t)\}$ the axial force of model points.

$$[M]\{\ddot{U}\} + [C]\{\dot{U}\} + [K]\{U\} = \{R(t)\} \tag{4}$$

Equation (4) can be solved by the Newmark method, which uses implicit time integration. The implicit method is one of the most current methods due to its reliable calculation process and accurate solution (Sluys 1992). The displacement and the velocity at the point in time $t + \Delta t$ are shown in equation (5) and (6), respectively.

$$U^{t+\Delta t} = U^t + \dot{U}^t \Delta t + \left(\left(\frac{1}{2} - \alpha\right)\ddot{U}^t + \alpha \ddot{U}^{t+\Delta t}\right)\Delta t^2 \tag{5}$$

$$\dot{U}^{t+\Delta t} = \dot{U}^t + \left((1-\beta)\ddot{U}^t + \beta \ddot{U}^{t+\Delta t}\right)\Delta t \tag{6}$$

The time step is represented by Δt. The coefficients α and β, not related to the Rayleigh damping coefficients, define the accuracy of the numerical integration and are subjected to the following conditions.

$$\beta \geq 0.5;\ \alpha \geq \frac{1}{4}\left(\frac{1}{2} + \beta\right)^2 \tag{7}$$

The damping matrix $[C]$ represents the material damping of the material caused by the viscous properties of the soil, friction and the development of irreversible strains. The damping matrix, illustrated in equation (8), is composed by a mass matrix $[M]$ and a stiffness matrix$[K]$.

$$[C] = \alpha[M] + \beta[K] \tag{8}$$

The Rayleigh coefficients, α and β determine the influence of mass and stiffness, respectively, in the damping of the system. Figure 2-25 illustrates the influence of the Rayleigh coefficients and the damping that is applied to the model, which is dependent on the frequency of the seismic charge transmitted to the soil.

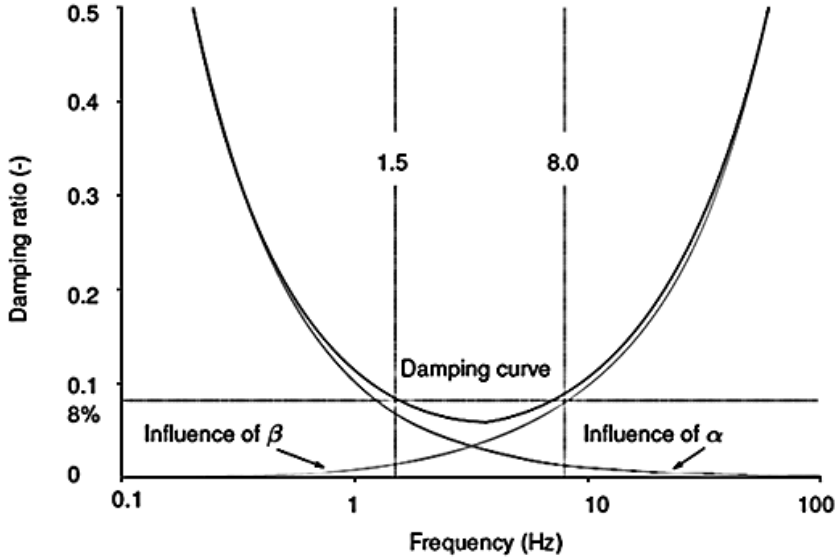

Figure 2-25: Example of Rayleigh damping parameter influence (Plaxis 2010).

From Figure 2-25 it can be seen that the higher the coefficient α, the more the lower frequencies are damped, and the higher β is, the more the higher frequencies are damped.

It should be noted that the dynamic analysis of a dam by means of FE can be complicated if the soil materials are subject to significant strength loss. A non-linear effective stress approach is therefore preferred in such conditions (Bull 1993).

2.5.3.1 Material models

Linear elastic model: The linear elastic model represents Hooke's law of isotropic linear elasticity, defined by Equation (9). This model considers that the soil only behaves in an isotropic linear manner, which could be suitable for low strain materials and as a first approximation for

the overall model. Stress states in this model are not limited and materials can show infinite strength.

$$\varepsilon = \frac{\sigma}{E} \tag{9}$$

The axial/normal strain, ε is at the same direction as the axial/normal stress, σ. The Young modulus, E, is the tensile modulus of the linear elastic soil. It should be noted that normal stresses produce volume changes and shear stresses produce distortion.

Mohr-Coulomb model: The Mohr-Coulomb model, well-known as linear elastic perfectly-plastic model, is also based on Hooke's law (for the linear elastic part) and on the Mohr-Coulomb failure criterion (for the perfectly plastic part). Figure 2-26 illustrates an example of the stress and strain relationship of soils. It could be noted that within the elastic region of the stress-strain diagram, stress is linearly proportional to strain. The perfectly plastic part is based on the Mohr-Coulomb failure criterion, which can be represented with equation (10) and Figure 2-27, which illustrates the failure envelope associated with the Mohr-Coulomb model (Labuz and Zang 2012).

$$\tau = c + \sigma \tan \phi \tag{10}$$

This equation can be represented as the straight line (Figure 2-27) inclined to the stress axis by the angle of internal friction, ϕ, c being the inherent shear strength of the material (also known as cohesion). At failure, the soil material passes from the elastic state to the plastic state.

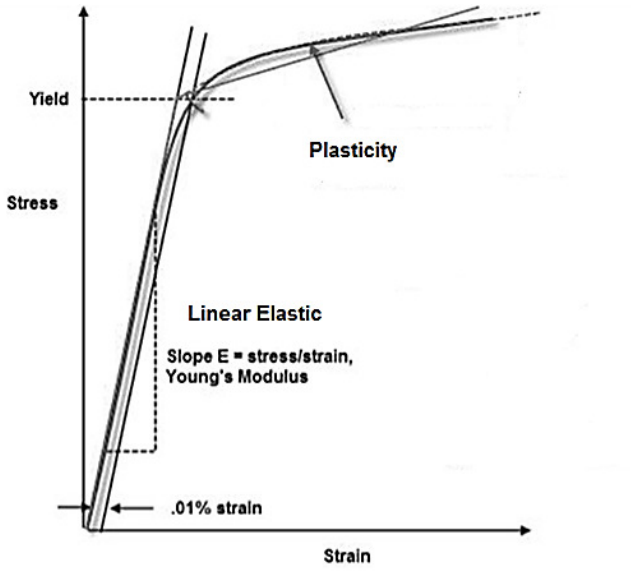

Figure 2-26: Stress-strain relationship of soils (Plaxis 2010).

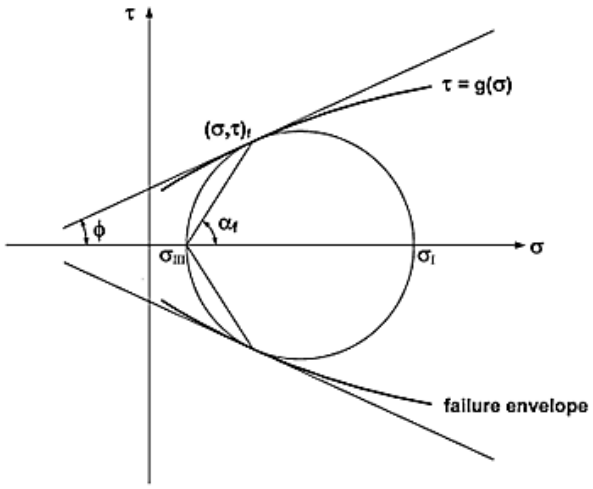

Figure 2-27: Mohr diagram and failure envelope (Plaxis 2010).

2.5.3.2 Case studies

This sections aims to present three cases of dynamic numerical analysis of earth fill dams.

Upper San Fernando Dam: Located northwest of Los Angeles and north of the Lower San Fernando dam, the Upper San Fernando Dam was built in 1922. The dam was about 24.4 meters high and was constructed on alluvial deposits overlying bedrock. The 1971 San Fernando

earthquake had a moment magnitude of 6.7 and an epicenter about 13 km from the dam site. The peak ground acceleration at the dam site was estimated to be about 0.6 g. After the earthquake, several longitudinal cracks were observed along the dam on the upstream slope. The maximum amount of horizontal displacements was about 2 m. It was suggested that soil liquefaction occurred due to increased water levels (Akhlahgi and Nikkar 2014).

Pseudostatic analyses using finite element and observed earthquake-induced deformations were evaluated by Akhlahgi and Nikkar (2014). Their findings indicated that the seismic coefficient increased with the increasing of the height of the dam. In addition, it was concluded that the constant seismic coefficient used in designing this dam was not realistic.

Santa Felicia Dam: Located in Ventura County, California, about 65 km northwest of Los Angeles, the Santa Felicia dam is an earth fill embankment built in 1954-55. The dam is about 83 m high above its lowest foundation and has an impervious core.

Nonlinear dynamic finite element analyses of this dam were performed by Prevost et al. (1985). The dam was subjected to two very different ground motions recorded during the 1971 San Fernando earthquake: a moderate motion of 35 seconds with a PGA of 0.22 g recorded at the dam site, and a strong motion of 15 seconds with a PGA of 1.2 g recorded near the epicenter of the earthquake at the Pacoima dam site. Comparisons between the results of 2D and 3D dynamic finite element were performed for the two motions, as well as comparisons between measured and computed earthquake responses of the dam.

Slight differences were found between the results of the 2D and 3D nonlinear analyses. Nonetheless, it was observed that, for the moderate motion, there was a good correlation between the crest acceleration time histories computed with the 2D and 3D nonlinear dam models. However, some differences were observed for the strong motion in crest acceleration time histories, induced stresses and strains in the dam material, and resulting permanent deformations (Prevost et al. 1985).

Kitayama Dam: Located in Japan, the Kitayama Dam was built in 1968 and is an earth dam about 25 meters high. The Kobe earthquake of January 17, 1995, in Japan caused slides on the upstream slope of the dam which was located about 33 kilometers northeast of the epicenter. The

minor damages did not compromise the safety of the dam. The recorded PGA at the Kobe University observation station, which is located on weathered rock and 24 km from the epicenter, was of 0.3 g.

Pseudostatic analyses using finite element were also evaluated by Akhlahgi and Nikkar (2014) for this dam. Their findings indicated that the seismic coefficient increased with the increasing of the height of the dam and that the constant seismic coefficient used in designing this dam was not realistic.

CHAPTER 3 APPROACH AND METHODOLOGY OF THE STUDY

The review of the literature revealed the following points:

1) The relatively low seismic activity and short instrumentation history of the east coast have led to uncertainty in the assessment of seismic parameters and hazards on the east coast.
2) The evaluation of the dynamic response of dams on the east coast is based on methods developed for dams on the west coast where earthquakes are characterized by significantly lower frequencies due to the regional geology.
3) The Franklin Falls Dam is one of the few earthfill dams on the east coast, equipped with accelerometers that has experienced significant accelerations.

Hence, a primary objective was to conduct dynamic numerical analysis of the response of the Franklin Falls Dam to the 1982 Gaza earthquake to see if existing practices in dynamic numerical analysis (e.g. software, material and damping models and methodologies) could simulate reasonably well the actual measured response of the dam.

To do so, it was necessary to conduct a deconvolution analysis of the ground motion recorded on level ground downstream of the dam. However, the subsurface conditions at this location were not known. A preliminary deconvolution analysis was conducted using the equivalent linear method. This analysis indicated the nature of subsurface conditions at the accelerometer (i.e. depth of overburden and shear wave velocity profile) and a ground motion on bedrock that generated a ground motion at the surface that was in very good agreement with the measured ground motion. The preliminary deconvolution analysis is reported in:

James and Arbaiza (2015). The Franklin Falls Dam: Design, Construction and Response to the 1982 Gaza (New Hampshire) Earthquake. In proceedings of the 2015 Annual Conference of the Canadian Dam Association, Mississauga, Ontario, 3-8 October, pp. 451-465.

The results of the preliminary deconvolution analysis were confirmed using PLAXIS (2D finite element analysis). This confirmed that the calculated ground motion on bedrock could be used to analyze the response of the dam to the Gaza event. The preliminary deconvolution analysis was also confirmed by St-Michel and James (2017) using FLAC (2D finite difference analysis).

The dynamic numerical analysis of the Franklin Falls Dam was conducted using PLAXIS 2D. The behavior of the dam material and the overburden were simulated using the Mohr-Coulomb model as implemented in PLAXIS. This is a conventional implementation of the Mohr-Coulomb model and allows for the inclusion of a dilatancy angle to simulate the volumetric response of the materials. Bedrock was simulated using the linear elastic model as implemented in PLAXIS. Damping due to shear strain development was simulated using Rayleigh damping. Given the relatively low level of shear strain expected (and found), the use of these material models and Rayleigh damping was deemed to be appropriate.

The dynamic numerical analysis was conducted in a parametric manner:

- Initial shear wave velocity profiles of the dam and of the foundation were estimated using empirical correlations based on the standard penetration test blow count. These profiles were varied in a rational manner until the calculated ground motion on the crest was in reasonable agreement with the measured ground motion.
- The degree of Rayleigh damping (ξ) and the associated parameters (α and β) were varied for correspondence with the average shear strain in the dam and agreement between the measured and calculated ground motions at the crest.
- The influence of the angle of dilatancy of the well-compacted materials of the dam was also evaluated.

In total, over 300 dynamic numerical simulations were conducted. Ultimately, it was found that the dynamic numerical analysis could simulate the response of the Franklin Falls Dam to the Gaza earthquake quite well.

The deconvolution analyses and the dynamic numerical analysis of the Franklin Falls Dam are presented in an article that has been submitted to the Journal of Soil Dynamics and Earthquake Engineering. This article is presented in Chapter 4 of this thesis.

Complementary research consisted of dynamic numerical analysis of the response of the Franklin Falls Dam to the 1988 Saguenay (Quebec) earthquake. This is presented in Chapter 5 of this thesis.

CHAPTER 4 ARTICLE 1: SIMULATION OF THE RESPONSE OF THE FRANKLIN FALLS DAM TO THE 1982 GAZA (NEW HAMPSHIRE) EARTHQUAKE

Arbaiza A. and James M. (2017) submitted to the Journal of Soil Mechanics and Earthquake Engineering (November, 29 2017).

Abstract:

The damaging effects of earthquakes on structures have been known for millennia. However, it has been recently acknowledged that regional and local conditions significantly influence the intensity and characteristics of earthquake shaking and thus the magnitude and pattern of damage (Seed and Idriss 1969). For instance, important differences in earthquake characteristics in the west coast and east coast of North America are attributed to the differences in the regional geological structures. Due to relatively harder and more intact bedrock, ground motions on the east coast are characterized by higher frequencies and less attenuation of the energy (e.g. peak ground acceleration or energy content) with distance from the earthquake source than those on the west coast (Tremblay and Atkinson 2001).

The Franklin Falls Dam, located in south-central New Hampshire, United States, is one of the few embankment dams in the east coast of North America equipped with accelerometers that has been subjected to significant earthquake loading: the 1982 Gaza (New Hampshire) earthquake. A dynamic numerical simulation of the Franklin Falls Dam to the 1982 Gaza earthquake was conducted and is presented here. The simulation was conducted using 2D plane strain finite element analysis and serves to validate applicability of this method for the simulation of the dynamic response of dams to high frequency ground motions. Furthermore, the applicability of the Mohr-Coulomb model and Rayleigh damping is evaluated for this type of structure and the corresponding level of shaking.

Nomenclature:

E	Young's modulus (MPa)

f	frequency (Hz)
G	shear modulus (MPa)
I_a	Arias intensity in two orthogonal horizontal direction (m/s)
I_x	Arias intensity in x horizontal direction (m/s)
I_y	Arias intensity in y horizontal direction (m/s)
$(N_1)_{60}$	corrected standard penetration test blow count (blows/30 cm)
M_w	moment magnitude
PGA	peak ground acceleration (g)
S_a	spectral acceleration (g)
SPT	standard penetration test
T_s	fundamental period of the sliding mass (s)
V_s	shear wave velocity (m/s)
γ_d	dry unit weight (kN/m^3)
ρ	total density (kg/m^3)
ϕ'	effective angle of internal friction (◦)
c'	cohesion (kPa)
γ_w	unit weight of water (9.81 m kN/m^3)
τ	shear stress (kPa)
γ_{xy}	shear strain (kPa)
σ_v'	vertical effective stress (kPa)
ξ	damping ratio
σ_{v0}'	initial effective vertical stress (kPa)
ψ	dilation angle (◦)
ν	Poisson's ratio

4.1 Introduction

The west coast of North America is significantly more seismically active than the east coast, which has provided an impetus for the concentration of research on west coast earthquakes and a large database of ground motions and recorded dam seismic behavior on the west coast. Furthermore, the low earthquake activity of the east coast together with limited history and lack of surface faulting have led to uncertainty in the assessment of seismic parameters and hazards on the east coast (Acharya et al. 1982).

Worldwide, about 70% of water retention dams are embankment dams (earth or rockfill) with the remaining consisting of concrete dams (Fell et al. 2005). This ratio is similar for the United States (USBR 2002) and Canada (CDA 2007). This is mainly due to the fact that embankment dams can be constructed on almost any type of foundation, whereas concrete dams require sound rock foundations. Embankment dams are also more economical to construct than concrete dams since the majority of the construction materials can usually be obtained in the vicinity of the dam at relatively low cost.

Slope instability, liquefaction or cyclic mobility, and seismic densification or deformation are some of the effects on embankment dams caused by seismic activity. The seismic performance (or stability) of embankment dams is normally evaluated as follows:

1. Development of a design earthquake loading using deterministic or probabilistic methods.
2. Analysis of the potential for excess pore water pressure generation, liquefaction or cyclic mobility and any associated strength loss.
3. Screening level analysis of stability using the pseudostatic method.
4. Permanent displacement analysis
5. For critical structures or when the results of pseudostatic analyses are not adequate or are questionable, dynamic numerical analysis can be conducted.

The primary objective of this paper is to study the behaviour of an embankment dam located on the east coast of North America that has been subjected to an east coast earthquake for which ground motion records of important acceleration are available. The Franklin Falls Dam, located in south-central New Hampshire, United States, is one of the few instrumented embankment

dams in the east coast of North America that has been subjected to significant earthquake loading: the 1982 Gaza (New Hampshire) earthquake.

4.2 The Franklin Falls Dam

The Franklin Falls Dam was constructed between 1939 and 1943 on the Pemigewasset River in South central New Hampshire (US). The dam derives its name from the town of Franklin Falls where it is located. It was constructed for flood control and is owned and operated by the New England District of the US Army Corps of Engineers (USACE).

The crest of the dam was constructed to an elevation of 126.8 m above mean sea level[1]. The crest length of the dam is about 530 m and its maximum height is about 42 m above the stream bed. It is a zoned earthfill structure with an impervious core and pervious fills terraces. The appurtenant structures include a spillway located behind the west abutment founded on rock with a concrete 166-m-long weir, and two gate-controlled outlet reinforced concrete conduits extending through the embankment and founded on bedrock (Brown 1941). An aerial photograph of Franklin Falls Dam is shown in Figure 4-1.

The Pemigewasset River flows across a narrow sandy flood-plain confined by high sand terraces lying on the rock slopes of a preglacial valley (Brown 1941). The river generally flows from north to south. However, locally (at the dam site) the river flows from northwest to southeast and the alignment of the dam is southwest-northeast.

[1] All elevations in this document are referred to mean sea level.

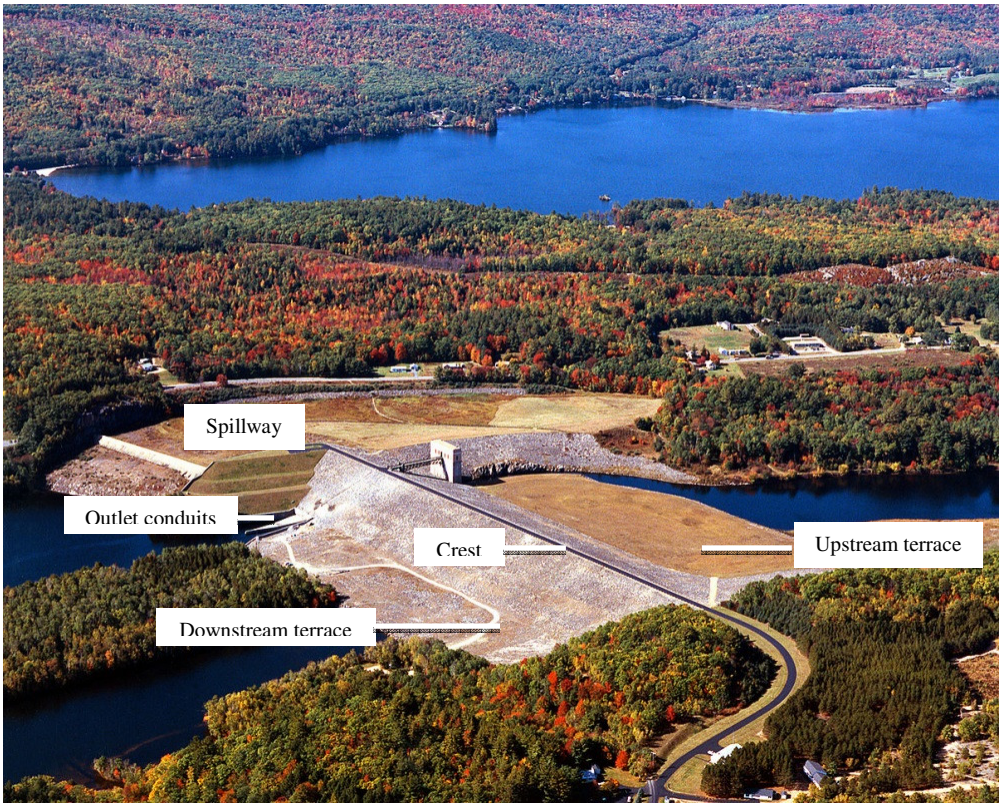

Figure 4-1: Aerial photograph of Franklin Falls Dam (provided by USACE, 1999).

4.2.1 Subsurface conditions

The foundation studies for the Franklin Falls Dam involved an investigation for the design of the concrete control structures and separate investigations for the embankment foundation. These investigations found that the bedrock is composed of hard granular schist containing numerous fractures in the upper weathered zones and scattered fractures throughout. As shown in Figure 4-2, bedrock lies at considerable depth below the east abutment and under most of the dam, but outcrops along the west abutment, where it forms the foundation for the spillway and outlet structures (Brown 1941).

The investigation of the embankment foundation required extensive investigations due to the variable nature of glacial deposits on the bottom of the valley. The investigations were conducted over a span of about 1.5 years and were conducted in conjunction with field and laboratory work (Brown 1941). Based on these investigations, the composition of the overburden varies, both laterally and vertically, from silty, very fine sands to gravelly coarse sands (Chang 1987).

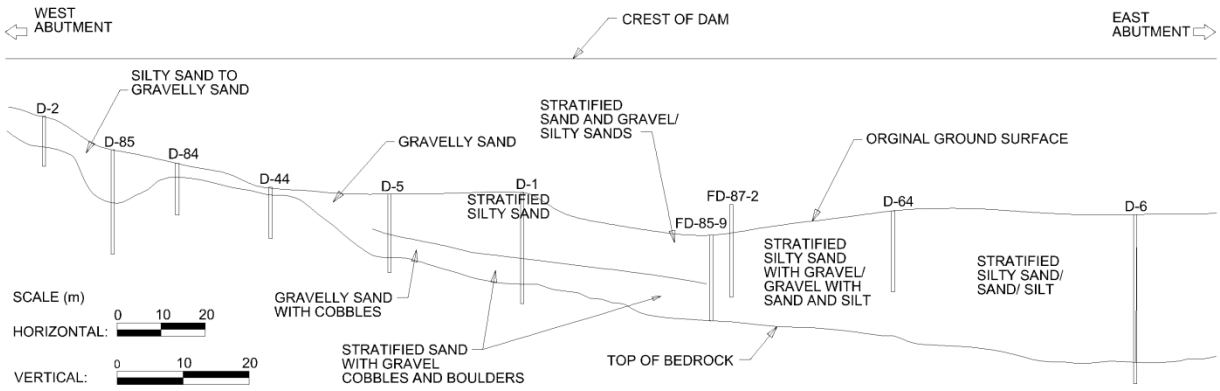

Figure 4-2: Longitudinal cross section of subsurface conditions (James and Arbaiza 2015).

The surface of the west abutment is inclined at about 1H:4.5V towards the dam. The east abutment is a steep overburden slope. There is a general horizontal continuity of three different zones of material: the lower zone from the base foundation (elevation 93 m to 113 m) composed of fine to medium sand with minor lenses of medium to coarse sand and of gravelly sand; the middle zone (elevation 113 m to 122 m) composed of stiff, sandy, medium to coarse silts with minor but persistent thin bands of fine to medium sand; the top zone varying from silty fine sands (above elevation 122 m) to gravelly medium to coarse sands in the upper 3 to 6 m (Chang 1987).

4.2.2 Design, construction and operation of the dam

The Franklin Falls Dam was designed in the late 1930s by the USACE. The design team included Mr. F. Steward Brown, Chief of the Design Section of the U.S. Engineer Office as well as Prof. Arthur Casagrande of Harvard University and Mr. W.L. Shannon, as special consultants to the USACE (Brown 1941).

The Franklin Falls Dam was one of the first earthfill dams designed using modern methods of design and construction. In fact, many existing methods of design and construction were evaluated during the design and construction of the Franklin Falls Dam, including permeability testing, filter design, static liquefaction analysis, and triaxial testing, compaction and ground modification study. Additional details of the design and construction can be found in James and Arbaiza (2015).

The final design of the dam consists of the embankment, an emergency spillway cut through the west abutment, and the low-level outlet works. The embankment zones, starting from the upstream side, are a dumped fill upstream terrace; a rockfill upstream shell; transition zones of sand and gravel, selected pervious fill, and pervious fill; an impervious core; downstream transition zones of pervious fill, selected pervious fill; and a downstream rockfill shell terrace. An impervious blanket extends under the downstream portion of the dam extending about 180 meters upstream from the core under the upstream dumped fill berm.

The crest width of the dam is of 11 m and the upstream and downstream slopes are of 3.25H:1V and 2.75H:1V respectively. As previously stated, the crest length of the dam is about 530 m and its maximum height is about 42 m above the stream bed. A typical cross-section of the dam is shown in Figure 4-3.

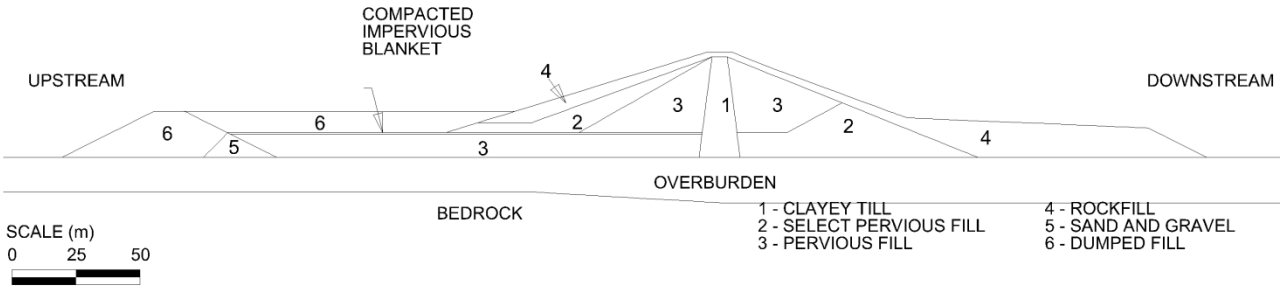

Figure 4-3: Typical cross section of Franklin Falls Dam (James and Arbaiza 2015).

The construction of the Franklin Falls Dam began in November 1939 and was completed in October 1943 (USACE 1969). The heterogeneous stratified sands found on the east terrace were used for the selected pervious fill, and the sand and gravel for the filters and concrete aggregates. The impervious material for the core and the impervious blanket was taken from a borrow site about 6 km from the site. Rockfill for the shells was obtained from spillway and outlet excavations and was placed by dumping (USACE 1938).

Overburden within the footprint of the dam was compacted with explosives prior to the construction of the dam. The subsidence of the compacted areas averaged from 60 to 75 cm, with an estimated reduction in void ratio that averaged from 0.95 to 0.80 (Brown 1941).

The pervious material of the dam was placed in 30-cm-thick layers, moisture conditioned to its optimal water content, and compacted by six passes of a rolling compactor such as a tractor-drawn disc roller or a tractor-drawn small-foot sheep foot roller. A minimum degree of compaction of 80 % was achieved (USACE 1938).

As mentioned, the Franklin Falls Dam was designed and constructed for flood control. During normal (nonflood) periods, the gates are maintained open to quickly develop a high rate of discharge during the early period of a flood, thus minimizing storage. For minor increases in flow, the reservoir acts as a simple retarding basin, even with the gates fully open. During flood periods, Franklin Falls Dam is regulated as part of a reservoir system to protect downstream communities. The upstream reservoir maximum pool elevation is of 125 m and the downstream water level is near the surface of the valley at elevation 96 m (USACE 1966).

4.2.3 Materials and geotechnical properties

The majority of the geotechnical properties of the embankment materials were estimated from the laboratory testing for the foundation investigations by the USACE in 1938. Information about the embankment materials, such as the impervious core and compacted pervious fill (adjacent to the core), were obtained from subsequent soil investigations conducted by the USACE in 1985 and 1987. These investigations included boreholes with standard penetration test sampling and conventional geotechnical laboratory testing (USACE, 1986; GEI, 1993).

Table 4-1 summarizes the main geotechnical properties of the Franklin Falls Dam materials. The strength parameters were obtained by the triaxial shear tests performed by the USACE in 1938. These parameters, as well as the unit weight of the materials were used in the stability analyses performed by Geotechnical Engineers Inc. (GEI Consultants) in 1980. The values are comparable to those given in the literature (Holtz et al. 2011). These values are also comparable to those presented in the USACE's Sample Data & Gravel Correction Tables, from different samples obtained in the 1985 and 1987 soils investigations (USACE, 1986; GEI, 1993). Laboratory test results from the USACE foundation investigation (1938) indicated specific gravity values for the foundation soils that varied between 2.50 and 2.82.

Table 4-1: Main parameters of soils (USACE, 1938; GEI, 1993)

Material	γ, unsat (kN/m3)	γ, sat (kN/m3)	ϕ' (˚)	c' (kPa)
Impervious core	21.8	22.2	28	15
Pervious fill	18.9	20.1	37	0
Rockfill	16.5	20.1	45	0
Sand and gravel	17.0	20.0	37	0
Dumped fill	17.3	18.9	37	0
Overburden	20.0	20.0	37	0

4.2.4 Instrumentation

The Franklin Falls Dam is equipped with three accelerographs, as shown in Figure 4-4, located as follows:

- Station A: west abutment, station 9+00, elevation 109.7 m;
- Station B: crest of the dam, station 17+00, elevation 126.8 m;
- Station C: level ground downstream of the dam, station 14+00, elevation 94.5 m.

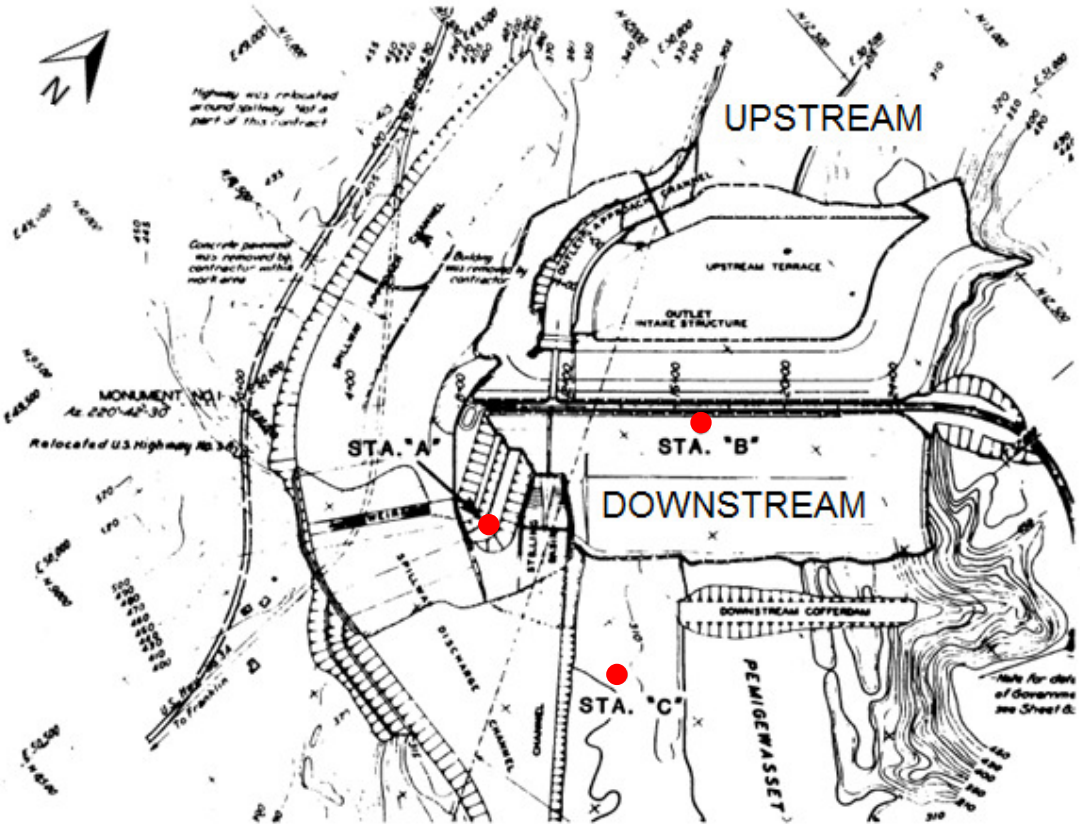

Figure 4-4: Plan view of the Franklin Falls Dam and location of accelerographs A, B and C (Chang 1987).

4.3 The 1982 Gaza earthquake and the response of the dam

At 19:42:42 EST on January 18, 1982, an earthquake of Richter magnitude 4.7 (m_b=4.4) occurred in south central New Hampshire (Chang 1983). The Weston Observatory and US Geological Survey estimated the focal depth to be between 4.5 and 8.0 km (Chang 1987). The Gaza earthquake was felt in most of New England, northern New York, and as far away as southern Quebec and northeastern Ontario (Chang 1983).

Thirty six accelerograms were recorded by accelerographs at five dams monitored by the New England division of the USACE, and by an instrument at a Veterans Administration Hospital (Manchester, NH) (Chang 1983).

The epicentral distance of the Franklin Falls Dam from this event was 8 km and significant ground movements were recorded in three accelerographs located at the crest, west abutment and downstream of the dam. No damage or deformation was observed on the dam following the event and only cosmetic damage to the gatehouse (a broken window) was reported (Chang 1983).

Each accelerograph measured the accelerations in three orthogonal components: longitudinal, transverse and vertical. The longitudinal and transverse components are oriented, respectively, parallel and perpendicular to the dam axis. Therefore, the transverse component is more important with respect to the seismic behavior of the structure since it acts in the direction of potential instability.

Chang (1983) analysed the strong motion data of the 1982 Gaza earthquake and corrected the 36 accelerograms to eliminate low frequency noise, including the 9 accelerograms of the Franklin Falls Dam. In 1987, Chang also analysed the spectral response of the dam and the natural periods of the dam (0.45 s) and its foundation (0.45 s). Table 4-2 presents the main characteristics of the corrected ground motions.

Table 4-2: Main characteristics of the recorded ground motions from the Gaza earthquake (James and Arbaiza 2015).

Location/ Direction	Peak ground acceleration PGA (g)	Arias Intensity I_a (m/s)	Predominant frequency f_p (Hz)	Mean frequency f_{MEAN} (Hz)
Crest				
Longitudinal	0.126	0.032	25.0	5.29
Transverse	0.313	0.079	16.7	7.41
Vertical	0.112	0.031	16.7	6.49
Abutment				
Longitudinal	0.285	0.089	12.5	13.89
Transverse	0.567	0.309	12.5	12.82
Vertical	0.175	0.025	25.0	7.14
Downstream				
Longitudinal	0.112	0.031	16.7	6.49
Transverse	0.260	0.082	12.5	8.93
Vertical	0.211	0.055	16.7	13.16

PGAs of 0.313 g, 0.567 g and 0.260 g were recorded in the transverse direction at the crest, the west abutment and downstream of the dam, respectively. Furthermore, the high PGA recorded in the transverse direction of 0.567 g at the west abutment indicate amplification of the ground motion due to topographic effects, which is typically seen along ridges and upper parts of slopes (Sigarán-Loría and Hack 2006).

The downstream accelerometer is located on level ground downstream of the dam. The distance from the toe of the downstream rockfill terrace to this instrument is approximately 150 m. Subsurface conditions at this location, specifically the depth to bedrock, are not known.

The Arias intensity is a measure of the energy content of a ground motion per unit mass of soil and provides an indication of the potential for deformation or damage (Kayen and Mitchell 1997). Using the ground motion records, the Arias intensities were computed with SeismoSignal (version 5.1.2) by Seismosoft (2013), a software that processes ground motion data. Arias intensity values of 0.079, 0.309 and 0.082 m/s were calculated for the transverse components at the crest, the west abutment and downstream of the dam, respectively.

The measured transverse ground motions and spectral acceleration diagrams for 5% damping from the downstream and crest accelerographs are presented on Figure 4-4 and were also

calculated with SeismoSignal. The ground motions are characterized by high frequencies typical of east coast events and the duration of significant shaking (>0.05g) is about 1 second. The spectral diagrams indicate strong responses for structures of relatively low periods, 0.1 to 0.2 s. At periods above 0.6 s, the spectral accelerations are close to zero.

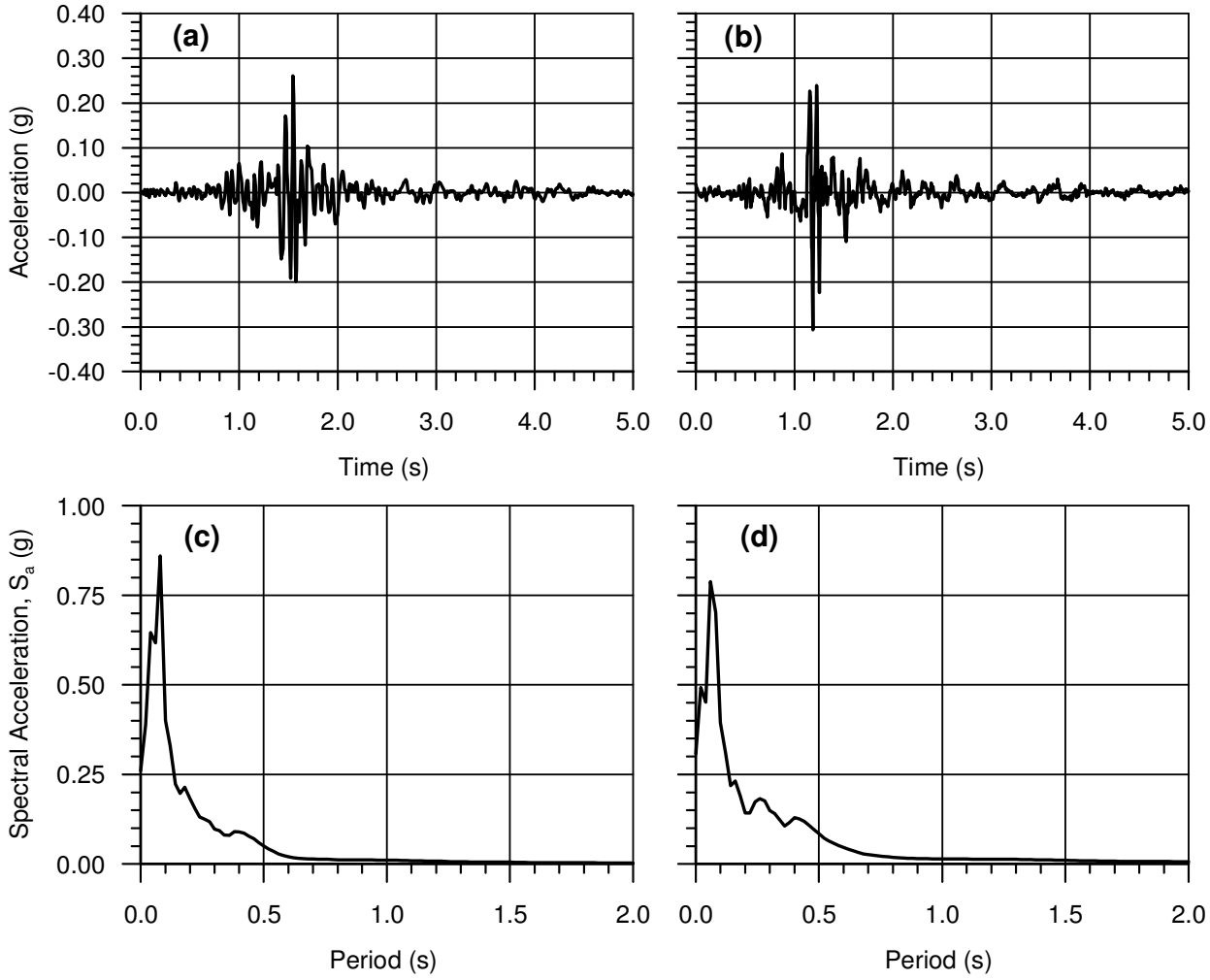

Figure 4-5: Measured transverse ground motions at the (a) downstream and (b) crest, and the corresponding spectral acceleration diagrams for 5% damping (c, d).

4.4 Preliminary deconvolution analysis

A preliminary deconvolution analysis of the downstream ground motion to estimate the ground motion on bedrock was conducted by James and Arbaiza (2015) and is summarized below.

The objective of this analysis was to develop an earthquake ground motion on bedrock at the downstream accelerograph capable of generating a ground motion at the surface, similar to the measured ground motion. The resulting ground motion on bedrock could then be used in the dynamic numerical analysis of the dam.

Two software programs were used in the deconvolution analysis: Strata (version alpha, revision 3999) by Kottke and Rathje (2009) and SeismoSignal (version 5.1.2) by Seismosoft slr (2013). Strata was used to conduct one-dimensional equivalent linear site response analyses and Seismosoft was used to analyze the ground motion records.

The first step of deconvolution analysis is to apply a measured surface ground motion to the top of the model based on known subsurface conditions. However, the subsurface conditions in the area of the downstream accelerograph were not known. To estimate the subsurface conditions in this area, three assumptions were made: (1) the subsurface conditions are similar to the conditions before ground modification (by explosives) and construction of the dam; (2) the densification effect of the rockfill terrace is at least equivalent to the densification effect of the ground modification; and (3) the overburden stress correction factor, C_N, can be used to back calculate what the corrected standard penetration test blow count, $(N_1)_{60}$, would have been before construction of the dam.

Shear wave velocity profiles for the overburden soil were determined using the correlations with the N_{60} values proposed by Wair et al. (2012) . Bedrock was modeled as elastic half-space with a shear wave velocity of 1524 m/s, according to a seismic refraction survey performed in 1986 (USACE 1986). The initially assumed subsurface conditions consisted of 20 m of sand overburden characterized by shear wave velocities that varied linearly from 100 m/s at the surface to 300 m/s at a depth of 20 m.

The resulting accelerations on bedrock were then recorded as the generated bedrock ground motion. The generated bedrock ground motion was then verified by applying it in the model to generate the surface ground motion and comparing the measured and generated surface ground motions. When the measured and calculated ground motions did not agree, the shear wave velocity profile and thickness of the overburden soil were adjusted in a rational manner and the

analysis was done again. The final subsurface conditions resulted of 12 m of sand overburden characterized by shear wave velocities that varied linearly from 125 m/s at the surface and 265 m/s at a depth of 12 m.

Figure 4-6 illustrates the transverse ground motion on bedrock generated by the deconvolution analysis. The generated ground motion on bedrock has a PGA of 0.157g and an Arias intensity of 0.025 m/s. As shown in Figure 4-7, the measured and calculated ground motion at the surface are in excellent agreement. This indicates that the estimated subsurface conditions at the downstream accelerometer and the calculated ground motion on bedrock are valid.

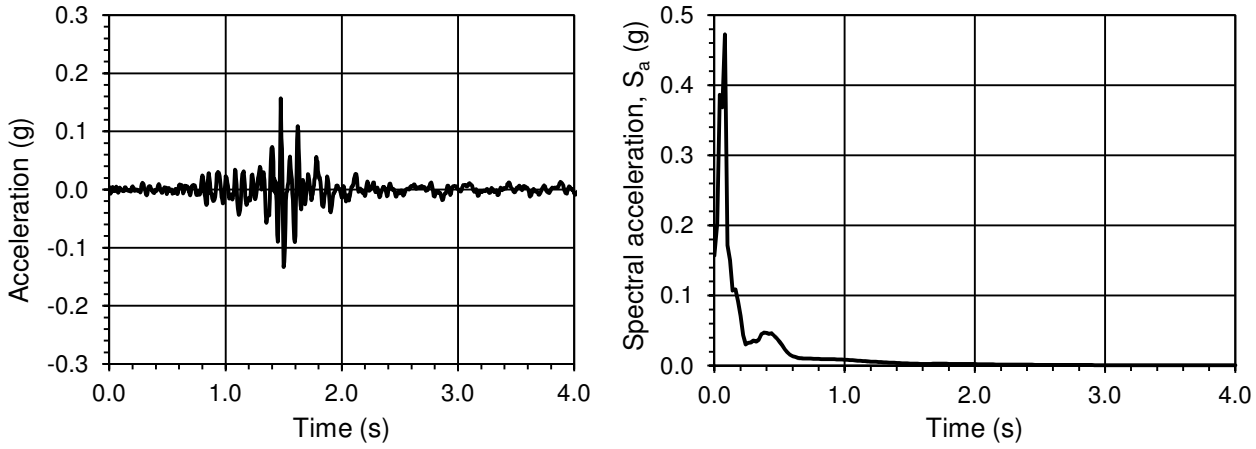

Figure 4-6: Calculated transverse ground motion on bedrock and spectral acceleration diagram for 5% damping at the downstream accelerograph (James and Arbaiza 2015).

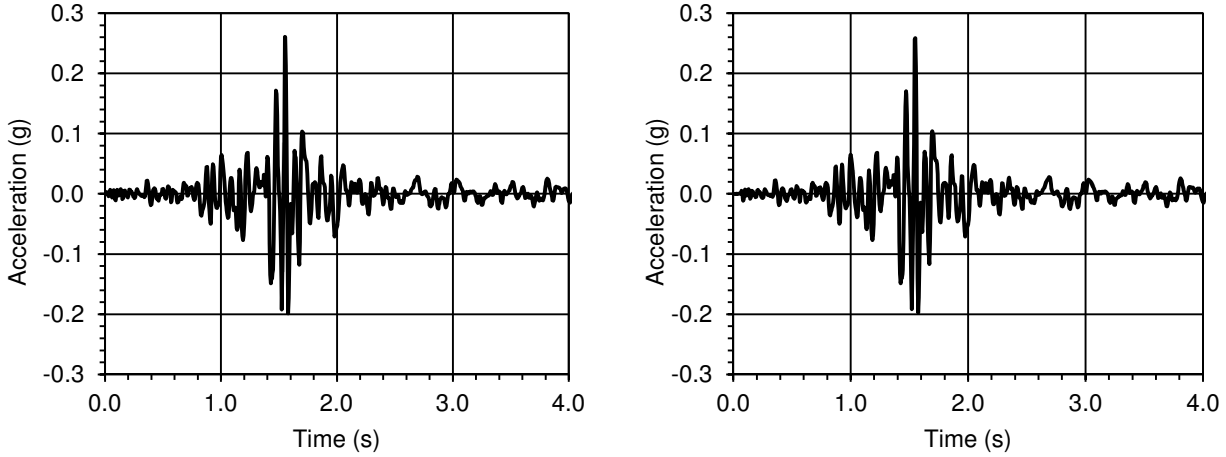

Figure 4-7: Measured (left) and calculated (right) transverse ground motion at the downstream accelerograph.

Additional details of the deconvolution analysis can be found in James and Arbaiza (2015).

4.5 Verification of the bedrock ground motion using PLAXIS 2D

Numerical modelling was conducted to validate the preliminary deconvolution analysis. The main objective was to evaluate the ability of the calculated bedrock ground motion to match the measured ground motion at the surface with finite element analysis.

The numerical modelling was conducted using PLAXIS 2D, which is a finite element (FE) package intended for the two dimensional analysis of deformation and stability in geotechnical engineering. The analyses consisted of two phases: a static phase to establish in-situ stresses, effective stresses and pore pressures before earthquake shaking, and a dynamic phase to simulate earthquake loading. The initial stress generation was obtained by the K_0 procedure in Plaxis which ensures full equilibrium to horizontal soil surfaces with soil layers parallel to the surface.

4.5.1 Subsurface conditions

The subsurface conditions used in the numerical analyses were those determined by the deconvolution analysis: 12 m of sand overburden characterized by shear wave velocities that varied linearly from 125 m/s at the surface and 265 m/s at a depth of 12 m. The phreatic surface was assumed to be at the ground surface.

4.5.2 Geometry and boundary conditions

The finite element mesh is presented in Figure 4-8 and it consists of a rectangular domain 200 m wide and 15 m high (12 m for the overburden and 3 m for the bedrock). The width allowed the lateral boundaries to be far enough minimizing the influence of the boundaries on the results, which were measured at the center of the model (Visone et al. 2008). The height of the elements respected equation (11) suggested by Kuhlemeyer and Lysmer (1973).

$$\Delta l \leq \frac{V_s}{10f} \tag{11}$$

Where V_s is the shear wave velocity of the elastic soil and f the maximum frequency associated with the maximum energy produced by the ground motion. With the lowest V_s of 125 m/s being at the top of the overburden and the predominant frequency of the ground motion of 12.5 Hz, the

maximum size of the elements is 1 m. The final finite model consists of 4 500 triangular elements at 15-nodes with a maximum element height of 1 m.

Boundary conditions were based on the calculation phase. For the first phase (static), boundary conditions consisted of vertical and horizontal fixity. For the second phase (dynamic), a free field condition was applied to the lateral boundaries (x_{min} and x_{max}) to simulate the propagation of the waves into the far field with minimum reflection of the boundary (Chouw et al. 2017). The ground motion was applied to the bottom of the model.

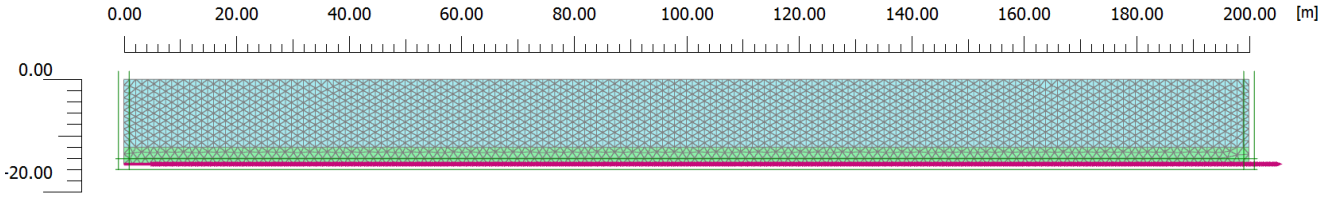

Figure 4-8: Finite element model of the downstream sector used in PLAXIS 2D

4.5.3 Material model and properties

The overburden soil and bedrock are modelled as linear elastic materials and their parameters are listed in Table 4-3. This model represents Hooke's law of isotropic linear elasticity, which is suitable for low strains and as a first approximation.

$$\varepsilon = \frac{\sigma}{E} \tag{12}$$

The model is applicable since it is assumed that the soil would not undergo any appreciable deformation due to the low intensity of the ground motion.

Table 4-3: Soil properties of the soil located under the downstream accelerograph.

Material	γ, sat (kN/m^3)	E' (MPa)	υ	G (MPa)	E_{oed} (kN/m^2)	V_s (m/s)	V_p (m/s)
Overburden	22	90-410	0.3	35-160	120-550	125-265	235-495
Bedrock	26	16 600	0.3	6 200	21 500	1 524	2 850

In PLAXIS, the material damping can be simulated with the Rayleigh formulation. To model the soil damping caused by the viscous properties of the soil, friction and the development of irreversible strains, Rayleigh damping was applied to the overburden. The Rayleigh damping matrix $[C]$ is composed by a mass matrix $[M]$ and a stiffness matrix$[K]$, and shown by equation (13).

$$[C] = \alpha[M] + \beta[K] \tag{13}$$

The Rayleigh coefficients, α and β determine the influence of mass and stiffness, respectively, to the damping. The influence of the Rayleigh coefficients and the damping that is applied to the model is dependent on the frequency of the seismic charge transmitted to the soil. It should be noted that lower frequencies are damped with increasing coefficient α, whereas higher frequencies are damped with increasing coefficient β. The parameters α and β are used in Plaxis to calculate a damping ratio, ξ.

The dynamic response of the overburden was assumed to be governed by the shear modulus reduction and damping curve of Darendeli & Stokoe (2001) for sand at a mean effective stress of 100 kPa. These curves are shown on Figure 4-9 and were used to estimate the damping ratio corresponding to a given shear strain.

The numerical analysis was conducted in an iterative manner. The Rayleigh damping coefficients, α and β, were varied until a solution in good agreement with the damping-shear strain curve of Figure 4-9 and between the measured and calculated ground motions at the surface was obtained.

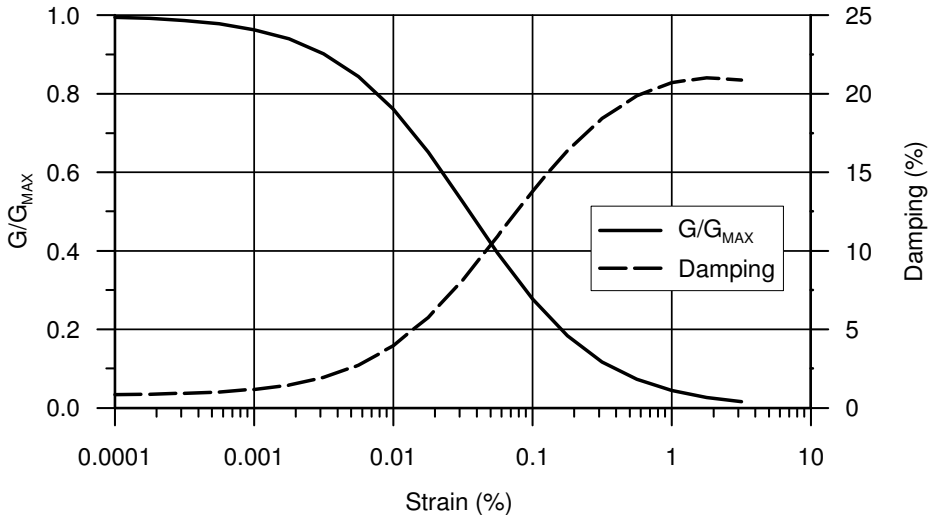

Figure 4-9: Shear damping ratios for sands at a mean effective stress of 100 kPa (Darendeli 2001).

4.5.4 Results of analysis

The results are shown in Figure 4-10 and summarized in Table 4-5. The generated PGA (0.206 g) is slightly lower than the measured value (0.260 g) whereas the Arias intensities are identical. The spectral parameters are somewhat lower at a period of 0.1 s and 0.5 s, and almost identical at a period 0.2 s.

As previously stated, the Arias intensity is a measure of the total energy of a ground motion, irrespective of frequency content and was therefore used as the most important parameter to determine the agreement of the generated ground motion to the measured ground motion at the downstream accelerograph. The spectral accelerations (at 0.1 s and 0.2 s) were also used to compare both ground motions since this parameter is a good indicator of the response of the dam to the frequency content of the ground motion. Since the PGA provides no information on the frequency content or duration of the motion, its value is of less importance when comparing the ground motions.

Table 4-4: Measured and generated ground motion at the downstream accelerograph using PLAXIS 2D.

Ground Motion Parameter	Measured value	Generated value
Peak Ground Acceleration, PGA (g)	0.260	0.206
Arias Intensity, I_a (m/s)	0.082	0.082
Spectral acceleration, Sa (T) (g)		
T=0.1 s	0.401	0.281
T=0.2 s	0.182	0.189
T=0.5 s	0.049	0.041

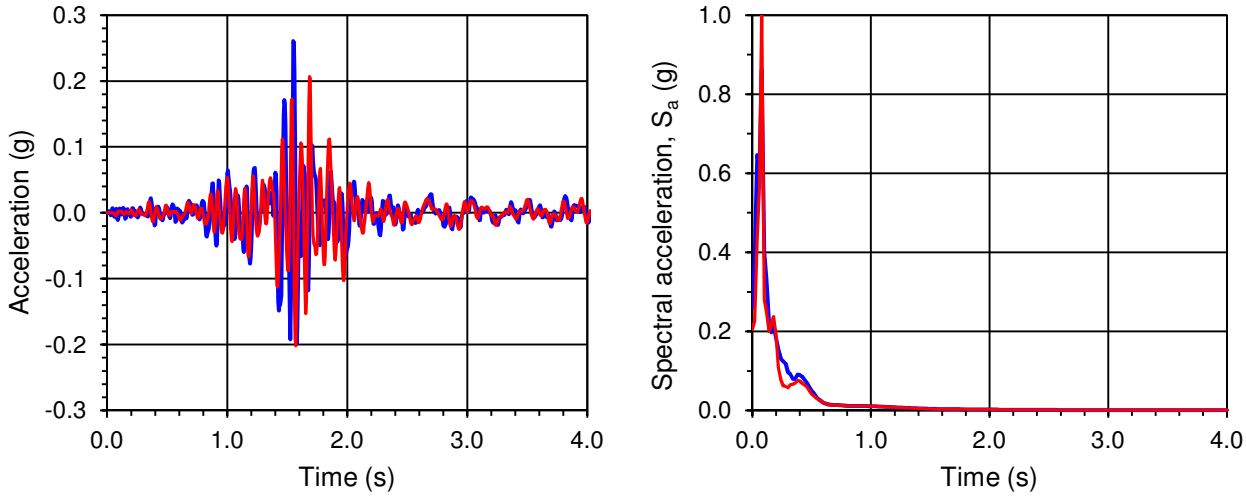

Figure 4-10: Measured transverse ground motion (blue) compared to generated transverse ground motion (red) and spectral acceleration diagram for 5% damping at the downstream accelerograph.

The results validate the subsurface conditions of the overburden soil at the location of the downstream accelerograph obtained by the preliminary deconvolution analysis. They also validate, in part, the ability of the model to simulate the response of the overburden to high frequency ground motions.

4.6 Verification of the bedrock ground motion using FLAC 2D

An additional validation of the ability of the calculated bedrock ground motion to match the measured ground motion on the surface was performed by St-Michel and James (2017). The analyses were conducted using FLAC 2D (Itasca 2016), a finite difference software program.

The subsurface conditions used in the numerical analyses were the same used for the preliminary deconvolution analysis. The boundary conditions for the dynamic phase consisted of a free field condition for the lateral boundaries to simulate the propagation of waves into the far field with minimum reflection at the boundary.

The overburden was modeled using the Mohr-Coulomb elastic-plastic model and the bedrock using the elastic model of FLAC. The properties of the overburden were a dry unit weight of 22 kN/m^3, an effective friction angle of 34°, and a Poisson's ratio of 0.35. Other parameters can be found in St-Michel and James (2017).

An analysis conducted using only Rayleigh damping resulting in 8.5% damping at a frequency of 12.5 Hz generated a surface ground motion in good agreement with the measured ground motion. Another analyses conducted with a combination of hysteretic damping and a 3.75% Rayleigh damping also generated a surface ground motion in good agreement with the measured ground motion and slightly better than the analyses conducted with only Rayleigh damping.

The main parameters of the measured and generated ground motion are presented in Table 4-5. From this table it could be seen that the Arias intensities are almost identical whereas the spectral accelerations at periods of less than 0.1 second are slightly lower than the measured ground motion. The measured and generated ground motion at the downstream accelerograph using the Rayleigh and hysteretic damping and the corresponding spectral acceleration at 5% damping are presented in Figure 4-11. From this figure it could be seen that the generated ground motions using Rayleigh and hysteretic damping are very similar to the motion measured at the downstream accelerograph.

Table 4-5: Measured and generated ground motion at the downstream accelerograph using FLAC 2D.

Parameter	Measured Value	Generated value using only Rayleigh damping	Generated value using Rayleigh and hysteretic damping
Peak Ground Acceleration, PGA (g)	0.260	0.203	0.197
Arias Intensity, I_a (m/s)	0.082	0.082	0.083
Spectral acceleration, Sa (T) (g)			
T=0.1 s	0.401	0.324	0.373
T=0.2 s	0.182	0.186	0.163
T=0.5 s	0.049	0.044	0.048

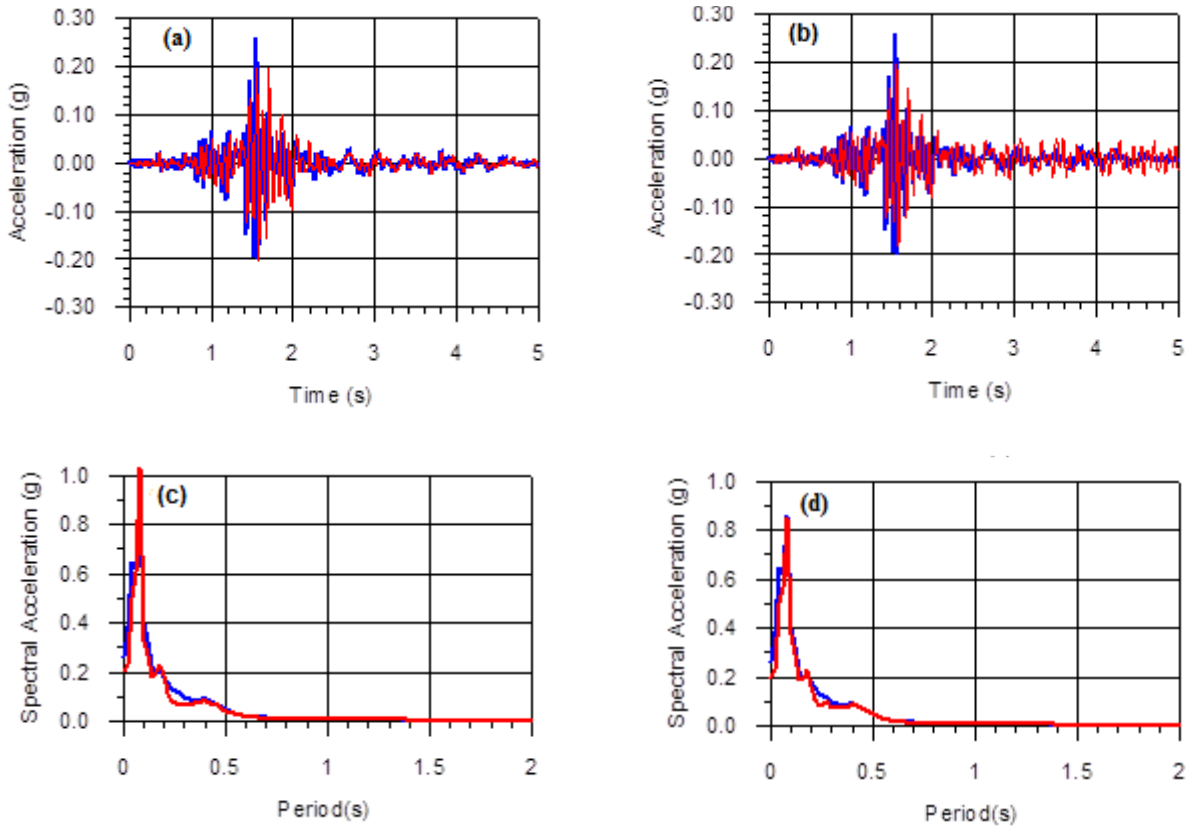

Figure 4-11: Measured transverse ground motions (blue) compared to generated ground motions (red) using (a) Rayleigh damping and (b) Hysteretic damping, and the corresponding spectral acceleration diagrams for 5% damping (c, d) (St-Michel and James 2017).

The results validate the subsurface conditions of the overburden soil at the location of the downstream accelerograph obtained by the deconvolution analysis. Additional details of the

deconvolution analysis verification of the bedrock ground motion using FLAC can be found in St-Michel and James (2017).

4.7 Dynamic numerical analysis of the dam

Numerical modelling of the Franklin Falls Dam was performed using PLAXIS 2D. The analyses consisted of two phases: a static phase to establish in-situ stresses, effective stresses and pore pressures before earthquake shaking, and a dynamic phase to simulate earthquake loading. The initial stress generation was obtained by a gravity loading to ensure stress equilibrium in the model.

4.7.1 Subsurface conditions

As mentioned, an extensive geotechnical exploration was conducted at the Franklin Falls Dam site to obtain soil samples and to characterize the area. For the purpose of this study, the subsurface conditions of the dam at station 18+00 were evaluated due to its proximity to the crest accelerograph which is located at station 17+00. The nearest borehole to the centerline is FD-85-9. Nearby, Borehole FD-87-2 is located upstream of the dam, and borehole FD-87-1 is located downstream of the dam. The closest boreholes located near the berms are FD-85-8 upstream and FD-85-4 downstream. All the mentioned boreholes were drilled between 1985 and 1987 after the construction of the dam. Figure 4-12 shows the cross section of the Franklin Falls Dam at station 18+00 and the mentioned boreholes. The stratigraphy of the boreholes is presented in Table 4-6.

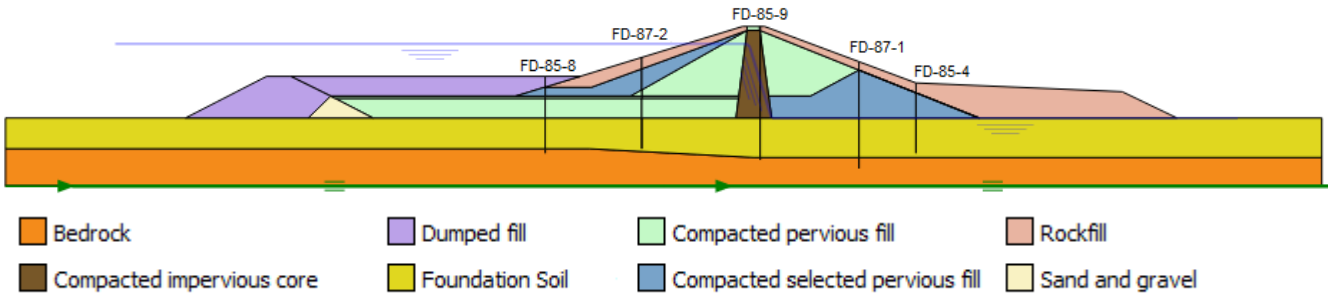

Figure 4-12: Cross section of the Franklin Falls Dam at station 18+00 used in PLAXIS.

Table 4-6: Stratigraphy encountered in boreholes located nearby station 18+00 of the Franklin Falls Dam.

Horizon	FD-85-9	FD-85-8	FD-85-4	FD-87-2	FD-87-1
Surface elevation (m)	127.6	105.1	100.2	115.8	111.7
Top of soil overburden elevation (m)	88.0	86.9	88.4	87.2	86.9
Thickness of soil overburden (m)	19.9	13.7	-	16.75	21.8
Elevation of top of bedrock (m)	68.1	73.2	-	75.0	65.1

4.7.2 Geometry and mesh conditions

The finite element is presented in Figure 4-13 and consists of a rectangular domain 600 m wide and 31 m high for the foundation soil (18 m) and bedrock (13 m). As mentioned in the previous section, the width allows the lateral boundaries to be far enough to minimize the influence of the boundaries on the results. The size of the elements was determined by equation (11) suggested by Kuhlemeyer and Lysmer (1973). Being the lowest V_s of 625 m/s at the upstream berm (dumped fill) and the predominant frequency of the ground motion of 16.7 Hz, the maximum allowable height of the elements is 3.7 m. The final finite model consists of a total of 6 730 triangular elements at 15-nodes with a maximum element height of 3.0 m.

For the static phase, boundary conditions consisted on vertical and horizontal fixity. For the dynamic phase, a free field condition was applied to the lateral boundaries to simulate the propagation of the waves into the far field with minimum reflection of the boundary (Chouw et al. 2017). The ground motion was applied to the bottom of the model (the bottom of bedrock).

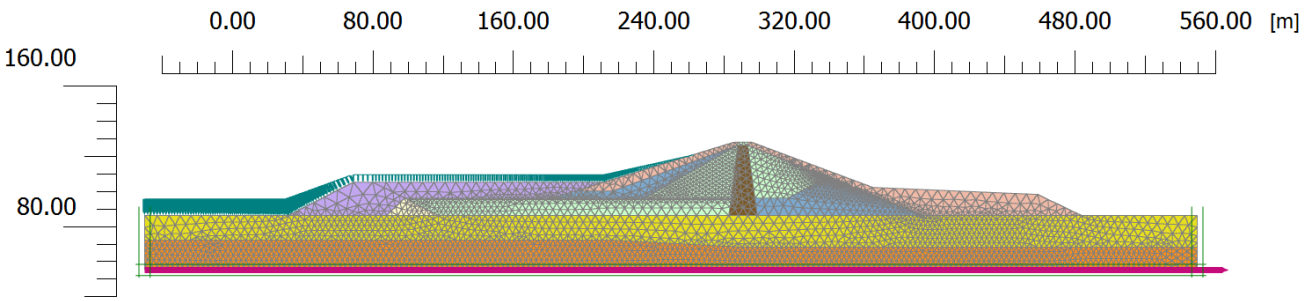

Figure 4-13: Finite element model of the Franklin Falls Dam used in PLAXIS 2D.

4.7.3 Material model and properties

The linear elastic model was used to simulate the bedrock. This model is suitable for very stiff materials and considers that the material behaves in an isotropic linear manner. Stress states in this model are not limited and materials can show infinite strength, which is acceptable here given the rigidity of the bedrock. The Mohr-Coulomb model was used for the foundation soil and dam materials. This linear elastic perfectly-plastic model, is also based on Hooke's law (for the linear elastic part) and on the Mohr-Coulomb failure criterion (for the perfectly plastic part).

The shear wave velocity profile at the overburden soil and some of the dam materials were determined and adjusted using the standard penetration tests that were performed in Boreholes FD-85-8, FD-85-9 and FD-85-4. Shear wave velocity values for the overburden were estimated using the correlations with the N_{60} values given in Wair et al. (2012), in equation (14).

$$V_s = a \cdot N_{60}^{b} \cdot \sigma'^{c}_{vo} \tag{14}$$

Where a, b and c are dimensionless constants equal to 30, 0.23 and 0.23 for sand. It should be noted that the correlations proposed by Wair et al. (2012) may be considered valid for N_{60} values of up to 100 blows per 30 cm.

The estimated shear wave velocity profiles are presented in Figure 4-14. As a first approximation, the Vs of the compacted impervious fill (core) was established at 575 m/s which corresponds to the maximum estimated value encountered in Borehole FD-85-9. To simplify the analyses, the Vs of the pervious fills were also assigned a constant value of 575 m/s with depth, which is

slightly superior to what was encountered in Boreholes FD-85-8 and FD-85-4. This value also corresponds to typical values of Vs for dense sands (Borcherdt, 1994). The Vs of the dumped fill, rockfill and foundation soil were taken from the literature due to the lack of data.

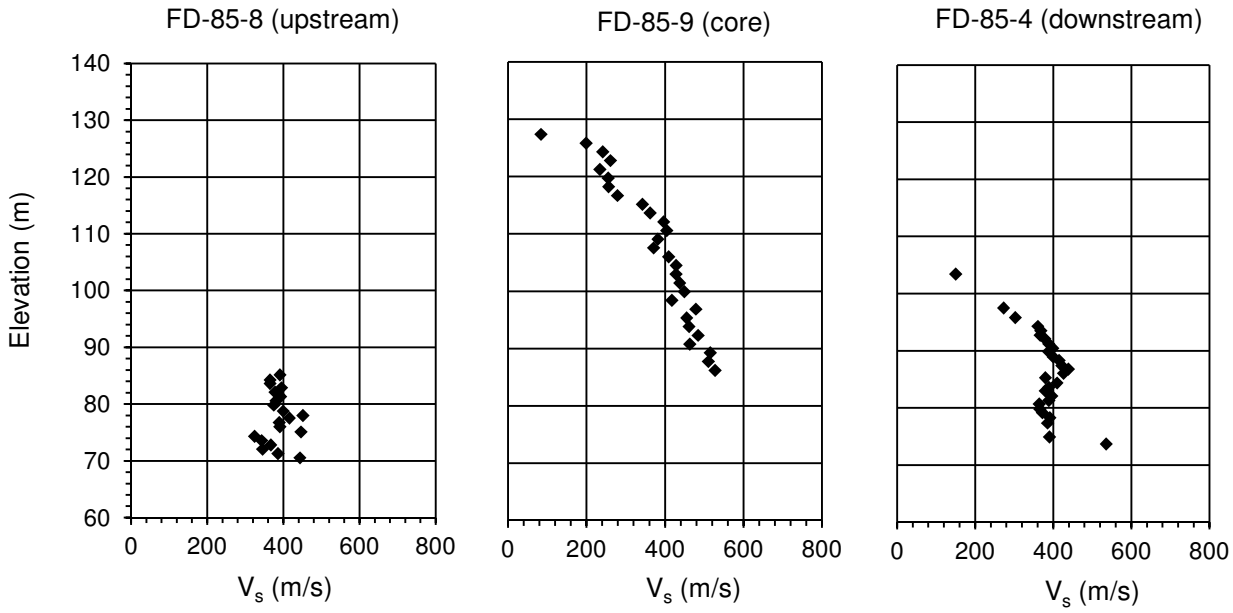

Figure 4-14: Estimated shear wave velocity profiles at Borehole FD-85-4, FD-85-9, and FD-85-4.

Table 4-7 presents the material properties of the Franklin Falls Dam materials used for the initial analysis. As previously stated, the soil strength properties (friction angle and cohesion) and the unit weights (unsaturated and saturated) were obtained by laboratory testing associated with the foundation investigations performed by the USACE in 1938 and following the soils investigations conducted for the USACE in 1985 and 1987.

Table 4-7: Material properties for the Franklin Falls Dam (initial analysis)

Material	γ, unsat (kN/m^3)	γ,sat (kN/m^3)	E' (MPa)	υ	V_s (m/s)	Phi (°)	C' (kPa)
Impervious core	20.0	21.5	1750	0.3	575	28	15
Selected pervious fill	18.9	20.1	1750	0.3	575	37	0
Pervious fill	18.9	20.1	1750	0.3	575	37	0
Rockfill	16.5	20.1	2845	0.3	625	45	0
Sand and gravel	17.0	20.0	1840	0.3	575	37	0
Dumped fill	17.3	18.9	1190	0.3	500	37	0
Foundation soil	20.0	21.5	2980	0.3	720	37	0
Bedrock	27.0	27.0	16600	0.3	1524	-	-

To simulate soil damping, friction and the development of irreversible strains, Rayleigh damping was applied to each material of the model. As previously stated, the influence of the Rayleigh coefficients and the damping that is applied to the model is dependent on the frequency of the seismic charge transmitted to the soil. The shear modulus reduction and damping curve of Darendeli & Stokoe (2001) shown on Figure 4-9 was used as a first approximation to model the dynamic response of the materials. These curves were used to estimate the damping ratio corresponding to a given average shear strain within the model. The damping ratio was modified in an iterative process until the model converges to the corresponding shear strain.

Firstly, the target frequencies were calibrated using the procedure proposed by Hudson et al. (1994) and Hashash and Park (2002) which suggests that the first target frequency, f_1, is the first natural frequency of the soil deposit, while the second target frequency, f_2, is the closest odd integer larger than the ratio f_p/f_1, where f_p is the predominant frequency of the ground motion.

The first natural frequency of the soil deposit is characterized by the V_s and the thickness H of the soil deposit and is described in Equation (15).

$$f_1 = \frac{V_s}{4H} \tag{15}$$

The target frequencies f_1 and f_2, and the damping ratio ξ are varied in an iterative process until obtaining a ground motion at the crest in reasonable agreement with the measured ground motion at the crest. The Rayleigh parameters α and β were automatically determined by the program.

4.7.4 Model simulations

To compare the recorded and calculated ground motions at the crest several parameters were used, including the PGA, the Arias intensity I_a and the spectral accelerations Sa (T=0.1 s), Sa (T=0.2 s) and Sa (T=0.5 s). A degree of importance was attributed to each parameter (low = 1, medium = 3, and high = 10).

In the same manner as the deconvolution analysis, a low degree of importance was assigned to the PGA. The Arias intensity was assigned high importance whereas the values of Sa (T=0.1 s) and Sa (T=0.2 s) were considered of medium importance. The value of Sa (T=0.5 s) was considered of low importance. For each run, delta was calculated according to the following formulation.

$$\Delta = \sum_{i=1}^{5} \frac{ABS(P_m - P_g)}{P_m} \cdot C_i \tag{16}$$

Where P_m and P_g are the parameters of the measured and generated ground motion at the crest of the dam respectively. The coefficient of the parameter C_i represents the ratio of importance attributed to a parameter. The sum of deltas for each run was then compared, aiming to obtain a value close to zero since it indicates that the PGA, I_a and Sa values of the two motions are identical. To obtain a value close to zero, the Rayleigh damping, the target frequencies, the shear wave velocities, the dilatancy angle, and other parameters were adjusted rationally.

4.7.5 Results of analysis

More than 300 numerical analyses were performed for this study. The material properties and shear wave velocities were adjusted in an iterative process to minimize the differences between the measured and calculated ground motions at the crest. Figure 4-15 shows the delta values Δ of the main trial runs. Each run was evaluated using the delta values, until obtaining relatively good agreement of the ground motions at the crest.

Rayleigh damping values of 2%, 5% and 7.5% were compared in this study. Furthermore, the shear wave velocities indicated in Table 4-7 were used and were increased or decreased by a factor of 0.75, 1.0, 1.25 and 1.5. As shown in Figure 4-15 (a), the best fit (a Δ of 0.6) corresponded to a Vs factor of 0.75 for all the materials in conjunction with a damping ratio of 7.5%. The Rayleigh damping parameters α and β were then varied using a damping ratio of 7.5% and a 0.75 Vs factor for all the materials. From Figure 4-15 (b), it could be concluded that different combinations of α and β resulted in Δ values of 0.2 to 0.8. For example, an α of 3.5 and a β of 1.25×10^{-3} resulted in a Δ value of 0.2, whereas an α of 3.4 and a β of 1.5×10^{-3} resulted in a Δ value of 0.8.

The Vs profile of the foundation soil was then varied for a 7.5% damping ratio and 0.75 Vs for the embankment materials. Figure 4-15 (c) shows that the best fit (Δ of 0.15) results in a Vs profile that varies from 500 (top of the foundation soil) to 600 m/s (bottom of the foundation soil). Finally, the influence of the dilatancy angle of the materials was also taken into consideration and is illustrated in Figure 4-15 (d) using a 7.5% damping ratio (with α of 1.5 and β of 3×10^{-3}) and 0.75 Vs for the embankment materials and a Vs profile from 500 to 600 m/s for the foundation soil. This final analysis indicated that a constant dilatancy angle of 5° resulted in better agreement with the measured ground motion at the crest accelerograph (Δ of 0.12).

The final simulations gave good results and it was concluded that the site characteristics derived from the optimization process were feasible. The best fit resulted in a delta value of 0.1 (sum of the coefficients for each parameter), indicating identical Arias intensity values and very similar spectral accelerations for T=0.1 s, 0.2 s and 0.5 s as indicated in Table 4-8. This resulted in a Rayleigh damping value of 7.5% and a factor of 0.75 for the shear wave velocities.

Figure 4-16 shows the transverse ground motion estimated with PLAXIS at the crest of the dam. This figure also illustrates how the estimated spectral acceleration is almost identical to the recorded ground motion. It is noted, however, that there is a significant difference in the time of the more intense shaking of the measured and calculated ground motions. This difference may be partially due to the differences in the arrival time and moment of triggering of the accelerometers at the crest and downstream. However, it is probably due, in part, to the limited ability of

numerical modelling to simulate the complex interactions of earthquake ground motions and geotechnical systems.

Figure 4-17 shows the calculated horizontal and vertical deformation of the Franklin Falls Dam due to earthquake shaking, which are negligible (less than 1 cm). As noted, no damage or deformation was observed on the actual dam as a result of the Gaza event.

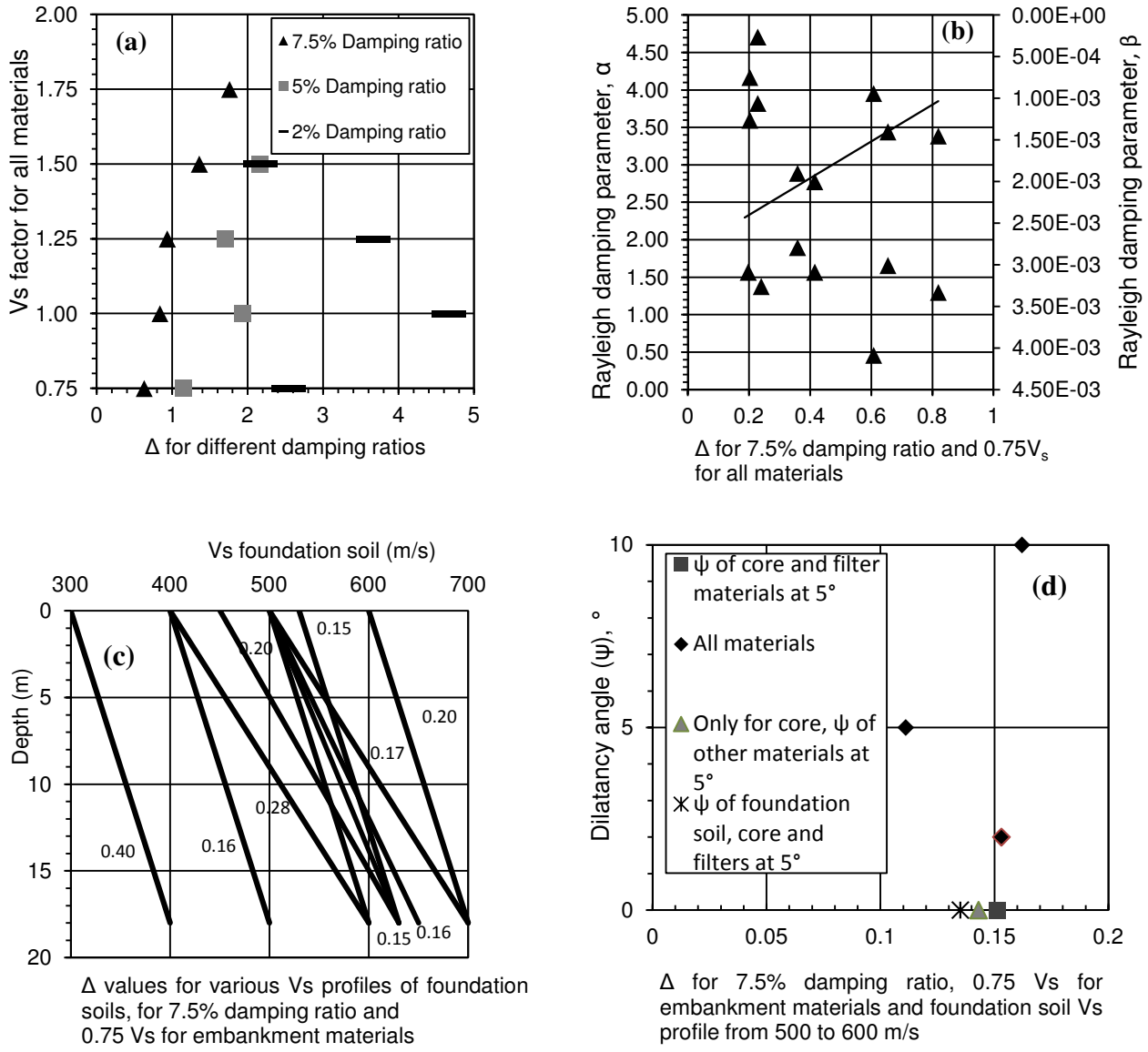

Figure 4-15: Model simulations (a) varying the Vs factors and damping ratio for all the materials, (b) varying the Rayleigh damping parameters α and β for 7.5% damping ratio and 0.75 Vs for all materials, (c) varying the Vs profile of the foundation soil for 7.5% damping ratio and 0.75 Vs for the embankment materials, and (d) varying the dilatancy angle of the materials for 7.5% damping ratio and 0.75 Vs for the embankment materials and a Vs profile from 500 to 600 m/s for the foundation soil.

Table 4-8: Measured and generated ground motion at the crest accelerograph using PLAXIS 2D.

Ground Motion Parameter	Generated value First iteration	Generated value Last iteration	Measured value
Peak Ground Acceleration, PGA (g)	0.118	0.187	0.313
Arias Intensity, I_a (m/s)	0.056	0.082	0.082
Spectral acceleration, Sa (T) (g)			
T=0.1 s	0.174	0.242	0.402
T=0.2 s	0.295	0.149	0.145
T=0.5 s	0.186	0.081	0.087

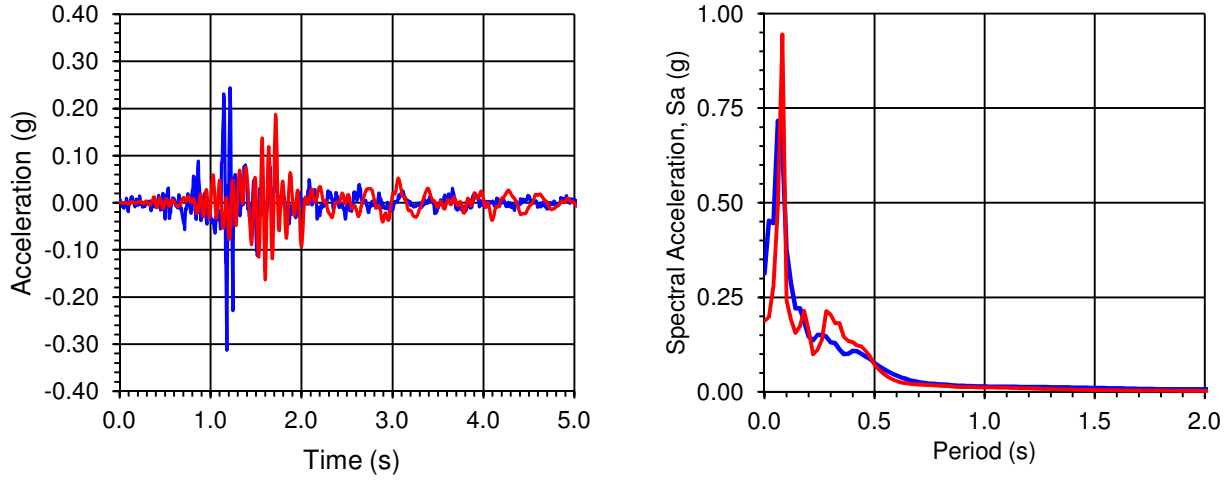

Figure 4-16: Recorded (blue) and estimated (red) transverse ground motions at the crest, and the corresponding spectral acceleration diagrams for 5% damping.

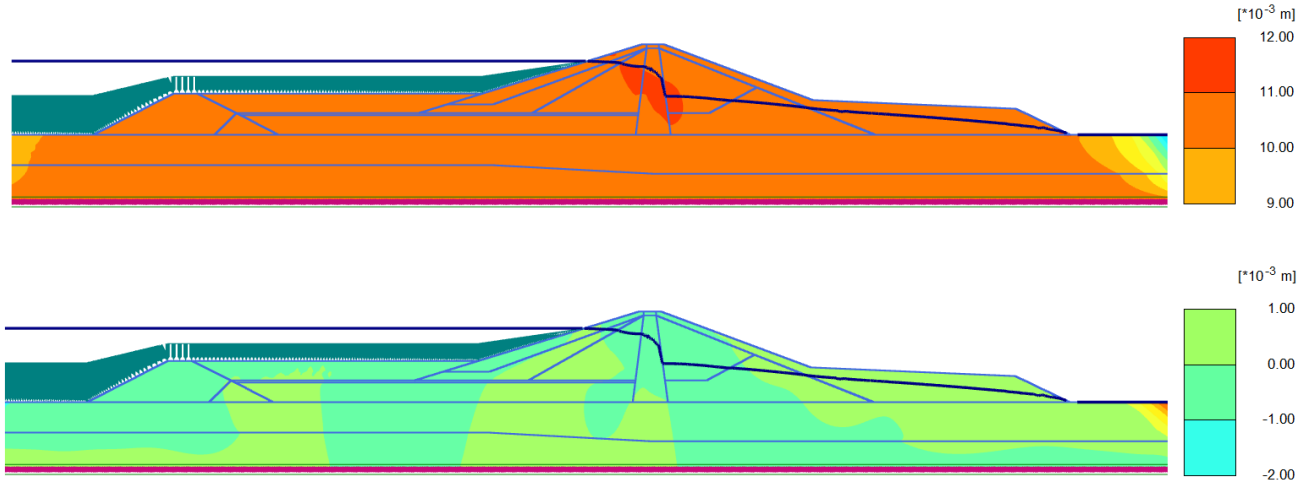

Figure 4-17: Horizontal (top) and vertical (bottom) deformations of the Franklin Falls Dam.

4.8 Discussion and conclusion

In the present study, the deconvolution analysis of the downstream ground motion at the Franklin Falls Dam generated by the 1982 Gaza earthquake was verified using dynamic numerical modeling with PLAXIS 2D. The generated ground motion was in good agreement with the measured ground motion. Dynamic numerical analysis of the Franklin Falls Dam was then performed with PLAXIS, indicating very good agreement with the recorded ground motion at the crest of the dam.

Based on the analyses presented in this study the following conclusions can be made.

i) The estimated shear wave velocities with the standard penetration tests were fairly accurate since the results converged to a Vs factor of 0.75, which represents Vs values of 430 m/s for the impervious and pervious fills.
ii) A damping ratio of 7.5% for all the materials resulted in good agreement with the measured ground motion at the crest, which is in accordance with the relatively low intensity of the ground motion. This corresponds to an average shear strain of about 0.1% in the model (see Figure 4-8).
iii) A decreased damping parameter α and an increased damping parameter β results in better accordance with the measured ground motion. This results in a minor influence of the mass and a higher influence of the stiffness in the model.
iv) The shear wave velocity of the foundation soil resulted in a profile that increased with depth, rather than a constant value, which validates the consolidation and the decrease of void ratio of the soil with depth.
v) A dilatancy angle of 5 degrees for all the materials resulted in better results compared to low (0 to 2 degrees) and high (10 degrees) dilatancy. Since the majority of the materials that compose the Franklin Falls dam are well-compacted granular materials, the 5 degrees dilatancy angle is in accordance to typical values for dense granular soils.

It should be noted that the use of the PGA as an important parameter of earthquake response is misleading and could be overly conservative when applied to the east coast, since the majority of recorded data is based on west coast earthquakes. Hence, eastern PGA values do not necessarily relate to structural response due to the higher frequency content. Since the Arias intensity indicates the potential for deformation irrespective of the frequency content, it should be used as an important parameter of earthquake response.

While seismic safety issues continue to receive increasing attention, a major shortcoming in the practice of seismic engineering design is the lack of real earthquake rock records in the east coast of North America, which have resulted in the use of synthetically generated records. For this reason, the ground motion of the Franklin Falls Dam from the Gaza earthquake is of great importance and can be added to the database of east coast ground motions for the analysis of other dams in similar seismic environments. Furthermore, this analysis can be used to verify and calibrate the pseudo-static and permanent displacement methods with respect to east coast ground motions.

CHAPTER 5 COMPLEMENTARY RESULTS

To evaluate the response of the Franklin Falls Dam to a more intense earthquake loading, complimentary analysis of the dam was conducted using the 1988 Saguenay earthquake (presented in section 2.3.3). As mentioned, the Saguenay earthquake produced one of the largest set of strong motion recordings of any earthquake on the east coast (Somerville et al. 1990). Detailed analysis of seismic data from this earthquake by a large number of researchers (e.g. Hough et al. 1989; Boore and Atkinson 1992; Boatwright and Choy 1992; Somerville et al. 1990) has provided valuable insight into the nature of moderate earthquakes in eastern North America (Cassidy et al. 2010).

The transverse ground motion record from station S16 (Figure 5-1a) located 43 km from the epicenter was used as the input signal for the numerical analysis. This ground motion is characterized by a PGA of 0.13g and a duration of 25 seconds. The duration of significant shaking (>0.05g) is approximately 10 seconds. The ground motion was evaluated using SeismoSignal. It has an Arias intensity of 0.18 m/s, a predominant frequency of 25 Hz and a mean frequency of 8 Hz. Figure 5-1b presents the spectral acceleration of the ground motion at 5% damping. As can be observed, this ground motion is expected to have significant effect on structures of low natural periods (or high natural frequencies). The main characteristics of the S16 transverse ground motion (S16T) are summarized in Table 5-1.

The dynamic numerical modelling of the dam was conducted using PLAXIS 2D. The analyses consisted of two phases: a static phase to establish in-situ stresses, effective stresses and pore pressures before earthquake shaking, and a dynamic phase to simulate earthquake loading. The initial stress generation was obtained by a gravity loading to ensure stress equilibrium in the model. The subsurface conditions, geometry, mesh conditions, material model and properties are the same as described in section 4.7. The Rayleigh damping parameters determined for the analysis of the Gaza earthquake were used for this analysis due to the materials of the dam being well-compacted and the intensity of earthquake loading. Also, shear strains were not expected to be significantly higher, and both ground motions are characterized by relatively high frequencies.

The Saguenay S16T ground motion was applied to the bottom of the model (bedrock) to simulate the occurrence of an earthquake.

The elements used for the evaluation of the response of the dam were the parameters of the calculated ground motion at the crest and the magnitudes and patterns of horizontal and vertical displacements within the dam at the end of shaking.

The ground motion measured at the crest of the dam as a result of the Saguenay S16 (transverse) ground motion is plotted in Figure 5-1c and the corresponding spectral acceleration at the crest for 5% damping is plotted in Figure 5-1d. The ground motion at the crest has a PGA of 0.207g and an Arias intensity of 0.495 m/s. It is characterized by high frequencies, with a predominant frequency of 2.6 Hz and a mean frequency of 3.4 Hz. The amplification factors between bedrock and the crest are 1.59 and 2.74 for the PGA and Arias intensity, respectively. These amplification values are well within what is expected at the crest of a dam composed of well-compacted materials (Seed and Idriss 1969). The spectral acceleration at the crest (Figure 5-1d) has a peak value of about 1g at a period of 0.4 seconds. The peak spectral acceleration of the input motion (Figure 5-1b) was about 0.3g at a period of approximately 0.04 seconds. Given that the predominant frequency of the dam in the transverse direction is 2.6 Hz (a period of 0.4 seconds), the response of the dam resulted in an expected increase in the fundamental period of the ground motion as it passed upwards though the dam.

Table 5-1 presents the main characteristics of the generated ground motion at the crest of the dam alongside those of the input ground motion (S16). The amplification and change in frequency content of the ground motion as a result of the dynamic response of the dam are evident.

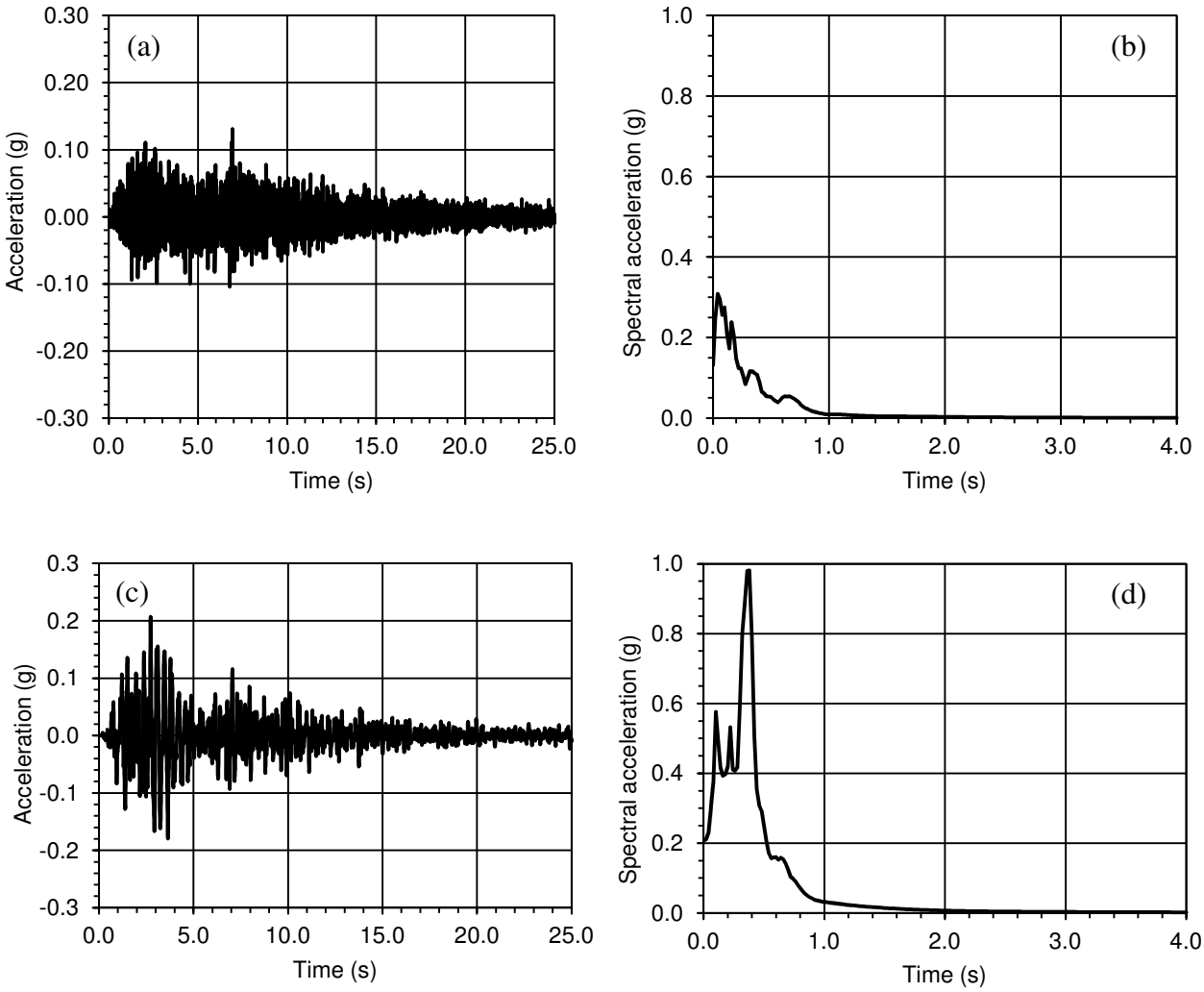

Figure 5-1: Ground motion (a) and spectral acceleration diagram (b) for 5% damping of Saguenay ground motion S16 (Transverse); Calculated ground motion (c) and special acceleration diagram for 5% damping (d) at crest of dam.

Figure 5-2 shows the horizontal (a) and vertical (b) deformations of the Franklin Falls Dam in response to the Saguenay earthquake. Though still relatively minor (less than 2 cm), they are about twice of those induced by the Gaza event. Nonetheless, the low level of deformation (and shear strain) confirms the use of the Mohr-Coulomb model and Rayleigh damping for this analysis.

Table 5-1: Main parameters of the Saguenay S16T ground motion and the ground motion at the crest of the dam.

Ground Motion Parameter	1988 Saguenay earthquake, m_b=5.9	Crest of Dam
Peak Ground Acceleration, PGA (g)	0.131	0.207
Arias Intensity, I_a (m/s)	0.177	0.495
Maximum spectral acceleration for 5% damping (g)	0.309	0.981
Period of maximum spectral acceleration for 5% damping (s)	0.040	0.380
Predominant frequency, f_P (Hz)	25.0	2.6
Mean frequency, f_M (Hz)	8.0	3.4

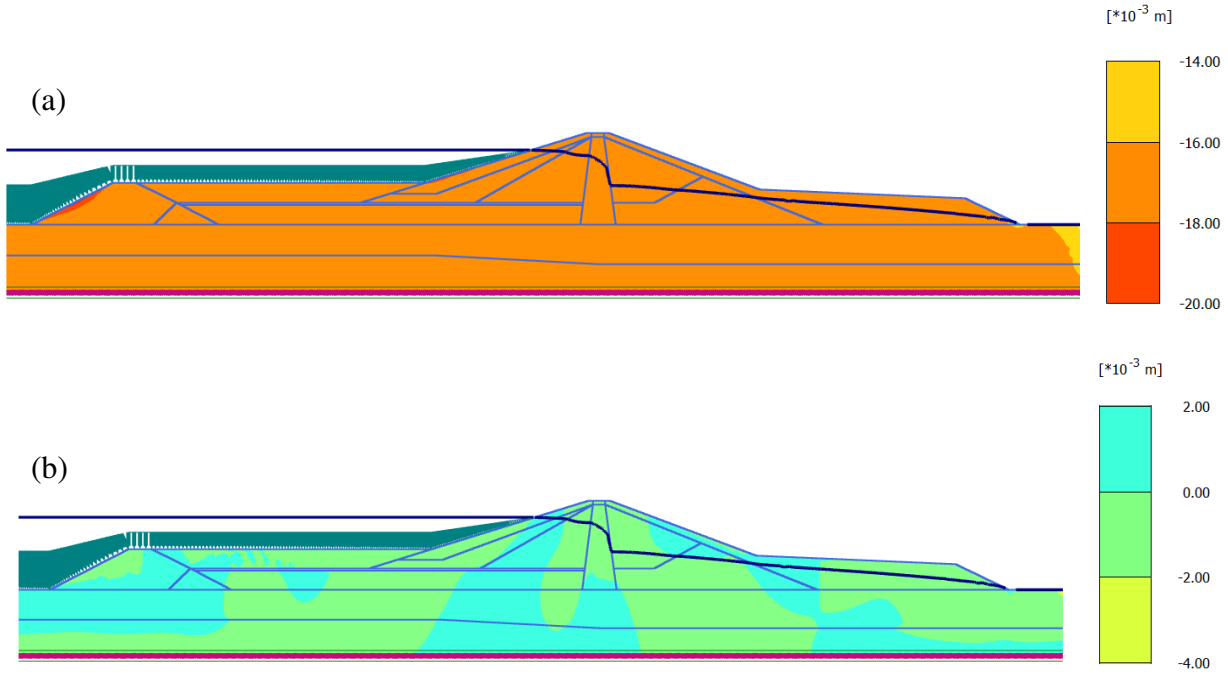

Figure 5-2: Horizontal (a) and vertical (b) deformations of the Franklin Falls Dam subjected to the 1988 Saguenay earthquake (record S16).

CHAPTER 6 GENERAL DISCUSSION

The primary objective of this research was to study the behaviour of an embankment dam on the east coast of North America that has been subjected to an east coast earthquake for which ground motion records of important acceleration are available. The Franklin Falls Dam, located in south-central New Hampshire, United States, is one of the few embankment dams in the east coast of North America equipped with accelerometers that has been subjected to significant earthquake loading: the 1982 Gaza (New Hampshire) earthquake.

To do so, it was necessary to conduct a deconvolution analysis of the ground motion recorded on level ground downstream of the dam. This preliminary deconvolution analysis was conducted by James and Arbaiza (2015) and resulted in a ground motion on bedrock that could then be used in the dynamic numerical analysis of the dam. The preliminary deconvolution analysis concluded that:

- The subsurface conditions are similar to the conditions before ground modification (by explosives) and construction of the dam.
- The densification effect of the rockfill terrace is at least equivalent to the densification effect of the ground modification.
- The correlations with the N_{60} values proposed by Wair et al. (2012) to determine shear wave velocity profiles are valid.
- The overburden stress correction factor, CN, can be used to back calculate what the corrected standard penetration test blow count, $(N1)_{60}$, would have been before construction of the dam.

Following the preliminary deconvolution analysis of the downstream ground motion at the Franklin Falls Dam generated by the 1982 Gaza earthquake, a verification was performed using dynamic numerical modeling with PLAXIS 2D. The generated ground motion was found to be in good agreement with the measured ground motion. The results validated the subsurface conditions of the overburden soil at the location of the downstream accelerograph obtained by the preliminary deconvolution analysis. They also validated, in part, the ability of the model to simulate the response of the overburden to high frequency ground motions.

Dynamic numerical analysis of the Franklin Falls Dam was performed with PLAXIS 2D. Based on the analyses presented in this study the following conclusions can be made.

- The correlations with the N_{60} values proposed by Wair et al. (2012) to determine shear wave velocity profiles are valid.
- The shear wave velocities estimated from the standard penetration tests were fairly accurate since the results converged at a Vs factor of 0.75, which represents Vs values of 430 m/s for the impervious and pervious fills.
- A damping ratio of 7.5% for all the materials resulted in good agreement with the measured ground motion at the crest, which is in accordance with the high frequencies of the ground motion.
- A decreased Rayleigh damping parameter α and an increased Rayleigh damping parameter β results in better accordance with the measured ground motion. This indicates a minor influence of the mass and a higher influence of the stiffness in the model.
- Parametric analyses of the shear wave velocity of the foundation soil resulted in a profile that increased with depth, rather than a constant value, which validates the consolidation and the decrease of void ratio of the soil with depth.
- A dilatancy angle of 5^o for all the materials resulted in better results compared to low (0 to 2^o) and high (10^o) dilatancy. Since the majority of the materials that compose the Franklin Falls dam are well-compacted granular materials, the 5^o dilatancy angle is in accordance to typical values for granular soils.
- The significant difference in the time of the more intense shaking of the measured and calculated ground motions may be partially due to the differences in the arrival time and moment of triggering of the accelerometers at the crest and downstream. However, it is probably due, in part, to the limited ability of numerical modelling to simulate the complex interactions of earthquake ground motions and geotechnical systems.
- The Mohr-Coulomb model to simulate the behavior of the dam material and the overburden, as well as Rayleigh damping to simulate damping due to shear strain development was deemed to be appropriate given the relatively low level of shear strain expected and found.

Lastly, a complementary analysis of the dam was conducted using the 1988 Saguenay earthquake. The objective was to evaluate the behaviour of the Franklin Falls Dam to a more intense earthquake loading. This ground motion was expected to have significant effect on structures of low natural periods (or high natural frequencies). The main findings of this complimentary study were:

- Significant amplification factors were found between the bedrock and the crest. These amplification values are well within what is expected at the crest of a dam composed of well-compacted materials (Seed and Idriss 1969).
- The response of the dam resulted in an expected increase in the fundamental period of the ground motion as it passed upwards though the dam.
- Though the deformations were relatively minor (less than 2 cm), they were about twice of those induced by the Gaza event.
- The low level of deformation (and shear strain) confirms the use of the Mohr-Coulomb model and Rayleigh damping for the analysis.

It should be noted that the use of the PGA as an important parameter of earthquake response is misleading and could be overly conservative when applied to the east coast, since the majority of recorded data is based on west coast earthquakes. Hence, eastern PGA values do not necessarily relate to structural response. Since the Arias intensity indicates the potential for deformation irrespective of the frequency content, it should be used as an important parameter of earthquake response.

Several methods to anticipate the seismic performance of embankment dams have been developed based on observations of the seismic behavior of dams on the west coast and verified and calibrated based on numerical modeling that used west coast ground motions. Furthermore, a major shortcoming in the practice of seismic engineering design is the lack of real earthquake rock records in the east coast of North America, which have resulted in the use of synthetically generated records. For this reason, the ground motion of the Franklin Falls Dam from the Gaza earthquake is of great importance and can be added to the database of east coast ground motions for the analysis of other dams in similar seismic environments. Furthermore, this analysis can be used to verify and calibrate the pseudo-static and permanent displacement methods with respect to east coast ground motions.

CHAPTER 7 CONCLUSION AND RECOMMENDATIONS

The relatively low seismic activity and short instrumentation history of the east coast have led to uncertainty in the assessment of seismic parameters and hazards on the east coast. Furthermore, the evaluation of the dynamic response of dams on the east coast is based on methods developed for dams on the west coast where earthquakes are characterized by significantly lower frequencies due to the regional geology. The main objective of this research was to study the behaviour of an embankment dam on the east coast of North America that has been subjected to an earthquake for which ground motion records of important acceleration are available.

As mentioned, The Franklin Falls Dam, is one of the few embankment dams in the east coast of North America equipped with accelerometers that has been subjected to significant earthquake loading, the 1982 Gaza (New Hampshire) earthquake.

To do so, a preliminary deconvolution analysis of the ground motion recorded at the surface downstream of the dam was performed. Additional simulations were then conducted using PLAXIS 2D to validate the preliminary deconvolution analysis. Finally, a dynamic numerical analysis of the Franklin Falls Dam was performed using PLAXIS 2D. A complimentary analysis of the dam was then conducted using the 1988 Saguenay earthquake (Quebec) to evaluate the behaviour of the Franklin Falls Dam to a more intense earthquake loading.

Following the results of these studies, the following recommendations are proposed:

- Two-dimensional dynamic numerical analysis of the Franklin Falls dam using the finite difference method (FEM).
- Three-dimensional dynamic numerical analysis of the Franklin Falls Dam.
- Evaluate the response of the dam to a west coast ground motion.
- Verify and calibrate the pseudo-static and permanent displacement methods with respect to east coast ground motions.

REFERENCES

Acharya, H., et al. (1982). "Seismic hazard in northeastern United States." Soil Dynamics and Earthquake Engineering Conference, Southampton, England **1**(1): 979-996.

Akhlaghi, T. and A. Nikkar (2014). Evaluation of the pseudostatic analyses of earth dams using FE simulation and observed earthquake-induced deformations: case studies of upper San Fernando and Kitayama dams. T. S. W. Journal. **2014**.

Atkinson, G. M. and D. M. Boore (1990). Recent trends in ground motion and spectral response relations for North America. Earthquake Spectra. **6:** 15-35.

Barosh, P. (1985). "Earthquake controls and zonation in New York." US. Geological Survey Open-File Report **85**(836): 54-75.

Barosh, P. J. (1981). "Cause of seismicity in the eastern United States: A preliminary appraisal." Earthquakes and earthquake engineering: the eastern United States **1**: 297-417.

Basham, P. W. and J. Adams (1984). The Miramichi, New Brunswick earthquakes: near-surface thrust faulting in the northern Appalachians. Geoscience Canada. **11**.

Bell, T., et al. (2004). "Partitioning of deformation along an orogen and its effects on porphyroblast growth during orogenesis." Journal of Structural Geology **26**(5): 825-845.

Bhan, S. and S. Dunbar (1989). The effect of high-frequency ground motion on the Maple-X10 reactor, Atomic Energy Control Board Canada.

Boudette, E. L. (1994). "Radon in New Hampshire: New Hampshire Department of Environmental Services Environmental Fact Sheet WD-WSEB-2-3."

Bray, J. D. and T. Travasarou (2007). "Simplified procedure for estimating earthquake-induced deviatoric slope displacements." Journal of Geotechnical and Geoenvironmental Engineering **133**(4): 381-392.

Brown, F. S. (1941). Foundation investigations for Franklin falls dam. B. S. o. C. Engineers. Boston, MA, United States. **28:** 126-143.

Brown, L. D. and R. E. Reilinger (1980). "Releveling data in North America: Implications for vertical motions of plate interiors." Dynamics of Plate Interiors: 131-144.

Bull, J. W. (1993). Soil-Structure Interaction: Numerical Analysis and Modelling, Taylor & Francis.

Cajka, M. and J. Drysdale (1996). Intensity report of the November 25, 1988 Saguenay, Quebec, earthquake, Natural Resources Canada.

Cassidy, J., et al. (2010). Canada's earthquakes:'The good, the bad, and the ugly'. Geoscience Canada. **37**.

CDA (2007). Dam Safety Guidelines. Canadian Dam Association.

Chang, F. K. (1983). Analysis of strong-motion data from the New Hampshire earthquake of 18 January 1982, Army Engineer Waterways Experiment Station, Vicksburg, MS (USA). Geotechnical Lab.

Chang, F. K. (1987). Response Spectral Analysis of Franklin Falls Dam, New Hampshire, US Army Corps of Engineers, Waterways Experiment Station, Geotechnical Laboratory.

Chiburis, E. (1981). Seismicity, recurrence rates, and regionalization of the northeastern United States and adjacent southeastern Canada, The Commission.

Chouw, N., et al. (2017). Seismic Performance of Soil-Foundation-Structure Systems: Selected Papers from the International Workshop on Seismic Performance of Soil-Foundation-Structure Systems, Auckland, New Zealand, 21-22 November 2016, CRC Press.

Clark Jr, S. F., et al. (1998). Lineament map of Area 6 of the New Hampshire bedrock aquifer assessment, central New Hampshire. Open-File Report.

Darendeli, M. B. (2001). Development of a new family of normalized modulus reduction and material damping curves.

Fell, R., et al. (2005). Geotechnical engineering of dams, CRC Press.

GEI (1993). Foundation soils investigations review and assessment of seismically induces pore pressure Franklin Falls Dam. N. E. D. U.S. Department of the Army, Corps of Engineers. Winchester, MA.

Hashash, Y. M. and D. Park (2002). "Viscous damping formulation and high frequency motion propagation in non-linear site response analysis." Soil Dynamics and Earthquake Engineering **22**(7): 611-624.

Hayman, N. W. and W. Kidd (2002). "Reactivation of prethrusting, synconvergence normal faults as ramps within the Ordovician Champlain-Taconic thrust system." Geological Society of America Bulletin **114**(4): 476-489.

Holtz, R. D., et al. (2011). An Introduction to Geotechnical Engineering, Pearson.

Hudson, M., et al. (1994). "QUAD4M User's manual." A computer program to evaluate the seismic response of soil structures using finite element procedures and incorporating a compliant base.

Hynes-Griffin, M. E. and A. G. Franklin (1984). Rationalizing the Seismic Coefficient Method, DTIC Document.

Itasca (2016). FLAC (Fast Lagrangian Analysis of Continua). I. C. G. Inc. Minneapolis, Minnesota.

James, M. and A. Arbaiza (2015). The Franklin Falls Dam: Design, Construction and Response to the 1982 Gaza (New Hampshire) Earthquake. Canadian Dam Association. Mississauga, Ontario.

Kayen, R. E. and J. K. Mitchell (1997). "Assessment of liquefaction potential during earthquakes by Arias intensity." Journal of Geotechnical and Geoenvironmental Engineering **123**(12): 1162-1174.

Kayen, R. E. and J. K. Mitchell (1997). Assessment of liquefaction potential during earthquakes by Arias intensity. J. o. G. a. G. Engineering. **123:** 1162-1174.

Kottke, A. R. and E. M. Rathje (2009). "Technical manual for Strata."

Kramer, S. L. (1996). Geotechnical Earthquake Engineering, Pearson.

Krinitzsky, E. and J. Dunbar (1986). Technical report No. GL-86-16: Geological-Seismological Evaluation of Earthquake Hazards at Franklin Falls Damsite, New Hampshire, Department of the Army.

Kuhlemeyer, R. L. and J. Lysmer (1973). "Finite element method accuracy for wave propagation problems." Journal of Soil Mechanics & Foundations Div **99**(Tech Rpt).

Labuz, J. F. and A. Zang (2012). Mohr–Coulomb failure criterion. The ISRM Suggested Methods for Rock Characterization, Testing and Monitoring: 2007-2014, Springer**:** 227-231.

Makdisi, F. and H. B. Seed (1979). "Simplified procedure for evaluating embankment response." Journal of Geotechnical and Geoenvironmental Engineering **105**(ASCE 15055).

Makdisi, F. I. and H. B. Seed (1977). A simplified procedure for estimating earthquake-induced deformations in dams and embankments, Earthquake Engineering Research Center, College of Engineering, University of California.

Makdisi, F. I. and H. B. Seed (1978). "Simplified procedure for estimating dam and embankment earthquake-induced deformations." Journal of Geotechnical and Geoenvironmental Engineering **104**(Proceeding).

Newmark, N. M. (1965). "Effects of earthquakes on dams and embankments." Geotechnique **15**(2): 139-160.

Paul E. Cote, N. S. and T. Pullen (2012). Franklin Falls – The Toughest Trenchless Crossing in New Hampshire. Nashville, TN, North American Society for Trenchless Technology.

Plaxis (2010). Plaxis 2010 reference manual, Plaxis, Delft, Netherlands.

Prevost, J. H., et al. (1985). "Nonlinear dynamic analyses of an earth dam." Journal of Geotechnical Engineering **111**(7): 882-897.

Sanders, C., et al. (1981). Low-Sun-Angle Aerial Reconnaissance of Faults and Lineaments in Southern New England. IN" PROC. EARTHQUAKES & EARTHQUAKE ENG.: THE EASTERN U. S.".

Seed, H. B. and I. M. Idriss (1969). "Influence of soil conditions on ground motions during earthquakes." Journal of the Soil Mechanics and Foundations Division **95**(1): 99-138.

Sigarán-Loría, C. and R. Hack (2006). Two-dimensional assessment of topographical site effects on earthquake ground response. M. Proceedings of 4th international FLAC symposium on numerical modeling in geodynamics**:** 29-31.

Sluys, L. J. (1992). Wave propagation, localisation and dispersion in softening solids, TU Delft, Delft University of Technology.

Somerville, P. G., et al. (1990). The 25 November 1988 Saguenay, Quebec, earthquake: Source parameters and the attenuation of strong ground motion. Bulletin of the Seismological Society of America. **80:** 1118-1143.

St-Michel, J. and M. James (2017). Deconvolution analysis of the 1982 Gaza (New Hampshire) earthquake. Geo Ottawa 2017. Canadian Geotechnical Society. Ottawa.

Towhata, I. (2008). Geotechnical Earthquake Engineering, Springer Berlin Heidelberg.

Tremblay, R. and G. M. Atkinson (2001). "Comparative study of the inelastic seismic demand of eastern and western Canadian sites." Earthquake Spectra **17**(2): 333-358.

USACE (1938). Foundation study for Franklin Falls Dam. Boston, MA.

USACE (1966). Master Plan for reservoir development of the Franklin Falls reservoir. Waltham, MA, US Army Corps of Engineers.

USACE (1969). Report of the Chief of Engineers U.S. Army, U.S. Government Printing Office.

USACE (1986). "Subsurface Investigation of Franklin Falls Dam." US Army Corps of Engineers, New England.

USACE (2016). "Franklin Falls Dam." Retrieved January, 2017.

USBR (2002). 100 Years of embankment dam design and construction in the US Bureau of Reclamation. U.S. Department of the Interior, Bureau of Reclamation. Nevada, Las Vegas**:** 67.

USGS (1989). The Severity of an Earthquake, General Interest Publications of the U.S. Geological Survey.

Visone, C., et al. (2008). Remarks on site response analysis by using Plaxis dynamic module. P. P. Bulletin**:** 14-18.

Wair, B. R., et al. (2012). "Guidelines for estimation of shear wave velocity profiles." PEER report **8**: 95.

Wetmiller, R., et al. (1984). "Aftershock sequences of the 1982 Miramichi, New Brunswick, earthquakes." Bulletin of the Seismological Society of America **74**(2): 621-653.

APPENDIX A
CONSTRUCTION DRAWINGS OF THE FRANKLIN FALLS DAM

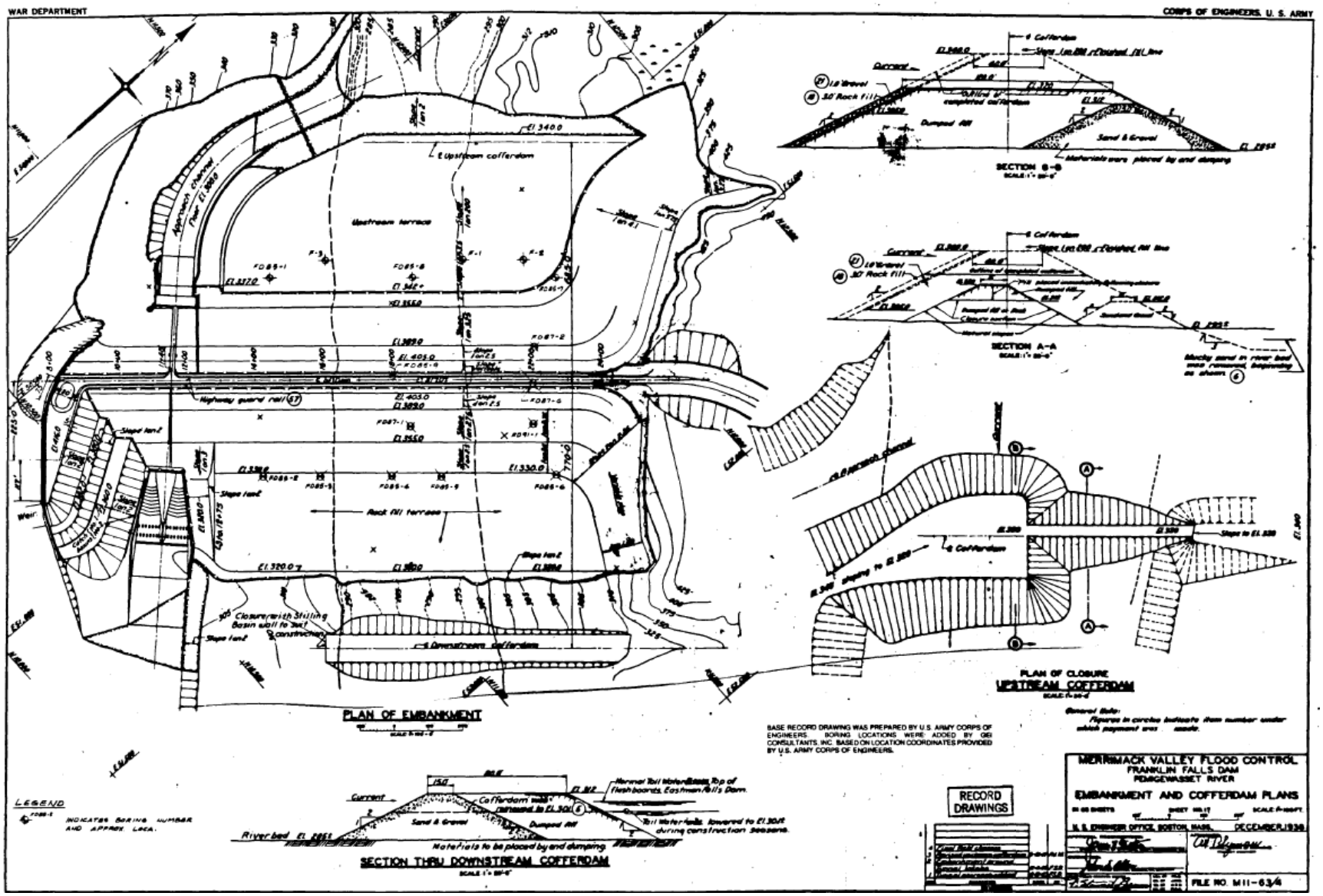

Figure A-1: Embankment and cofferdam plans

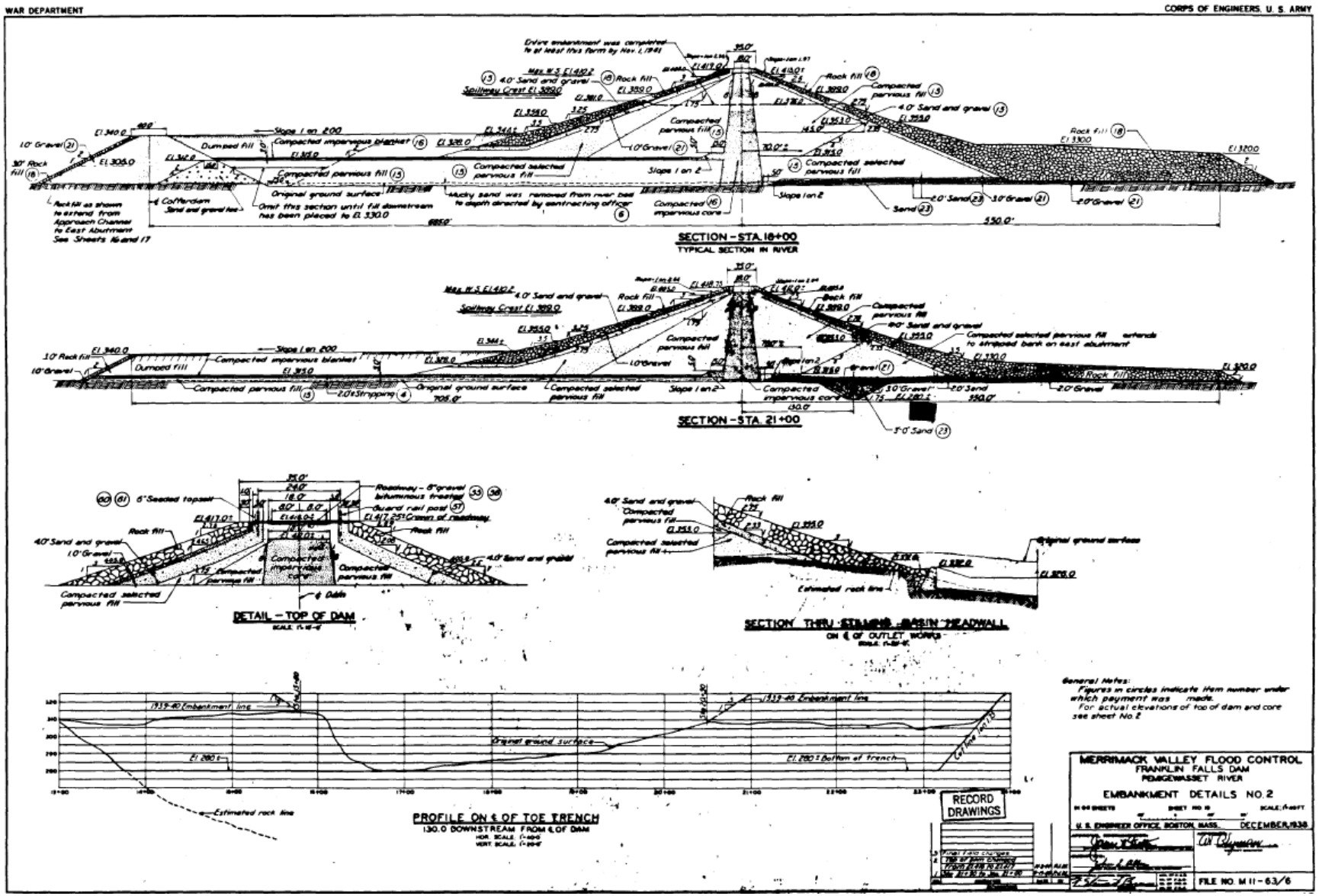

Figure A-2: Embankment details No.2

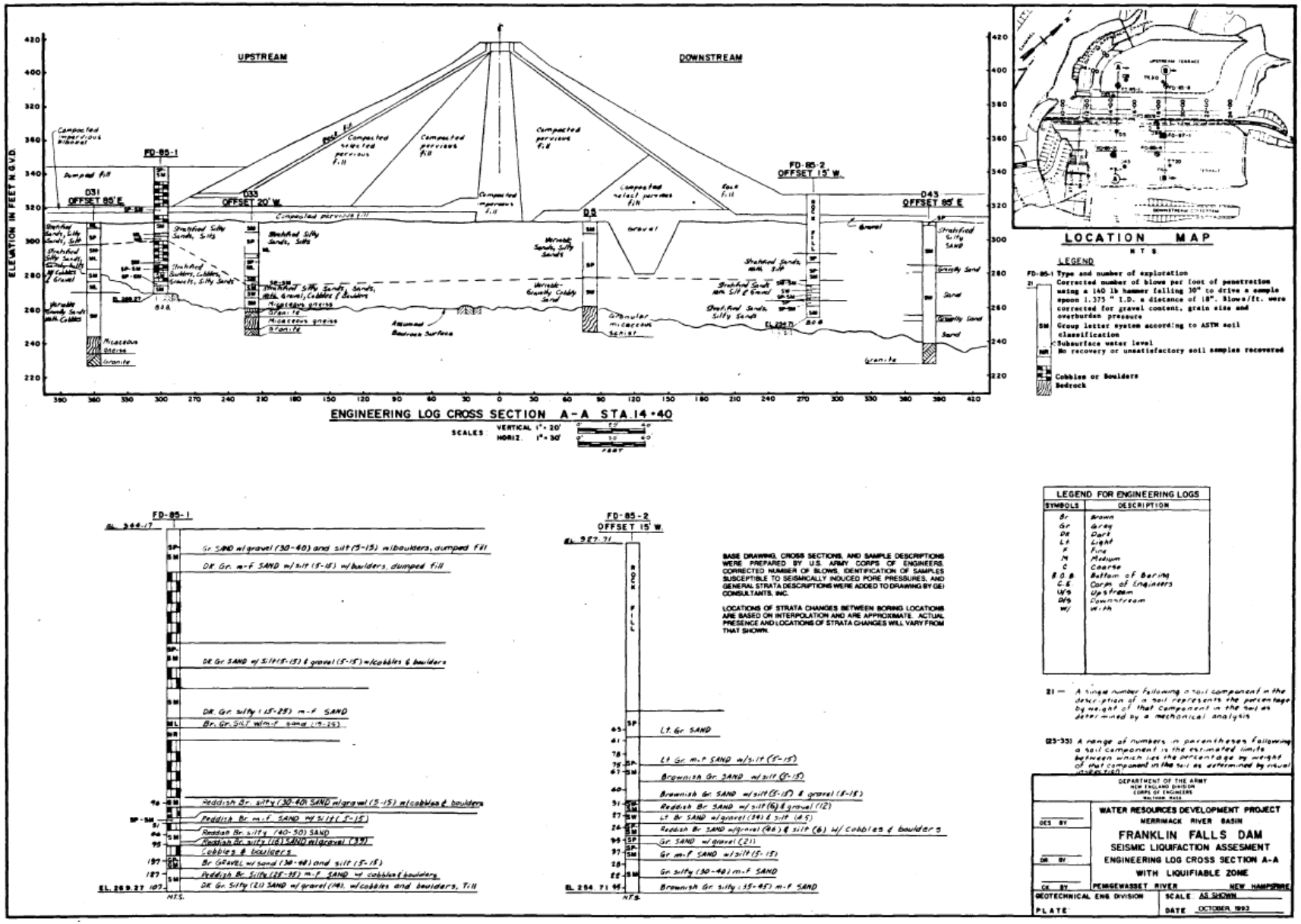

Figure A-3: Engineering log cross section A-A

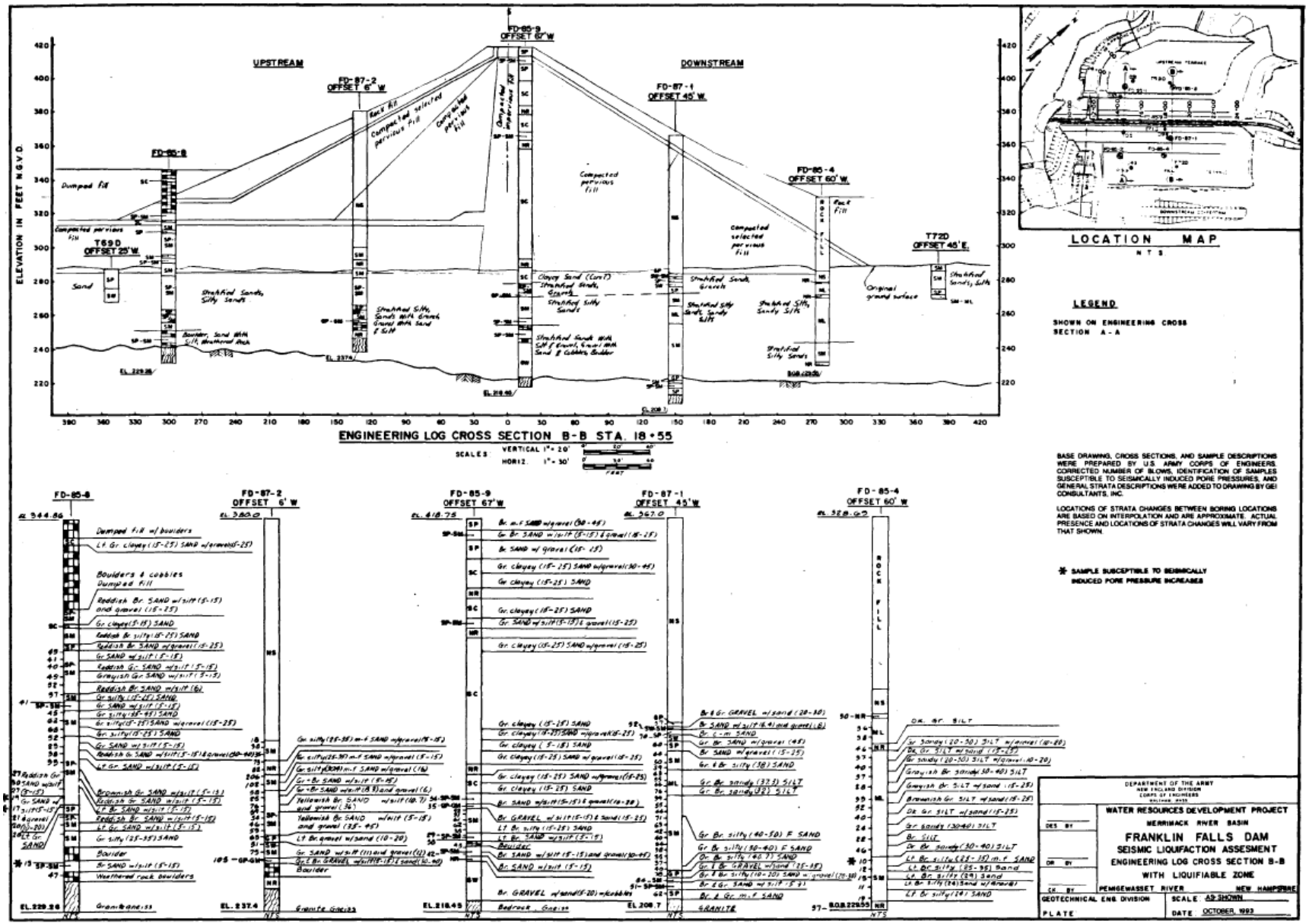

Figure A-4: Engineering log cross section B-B

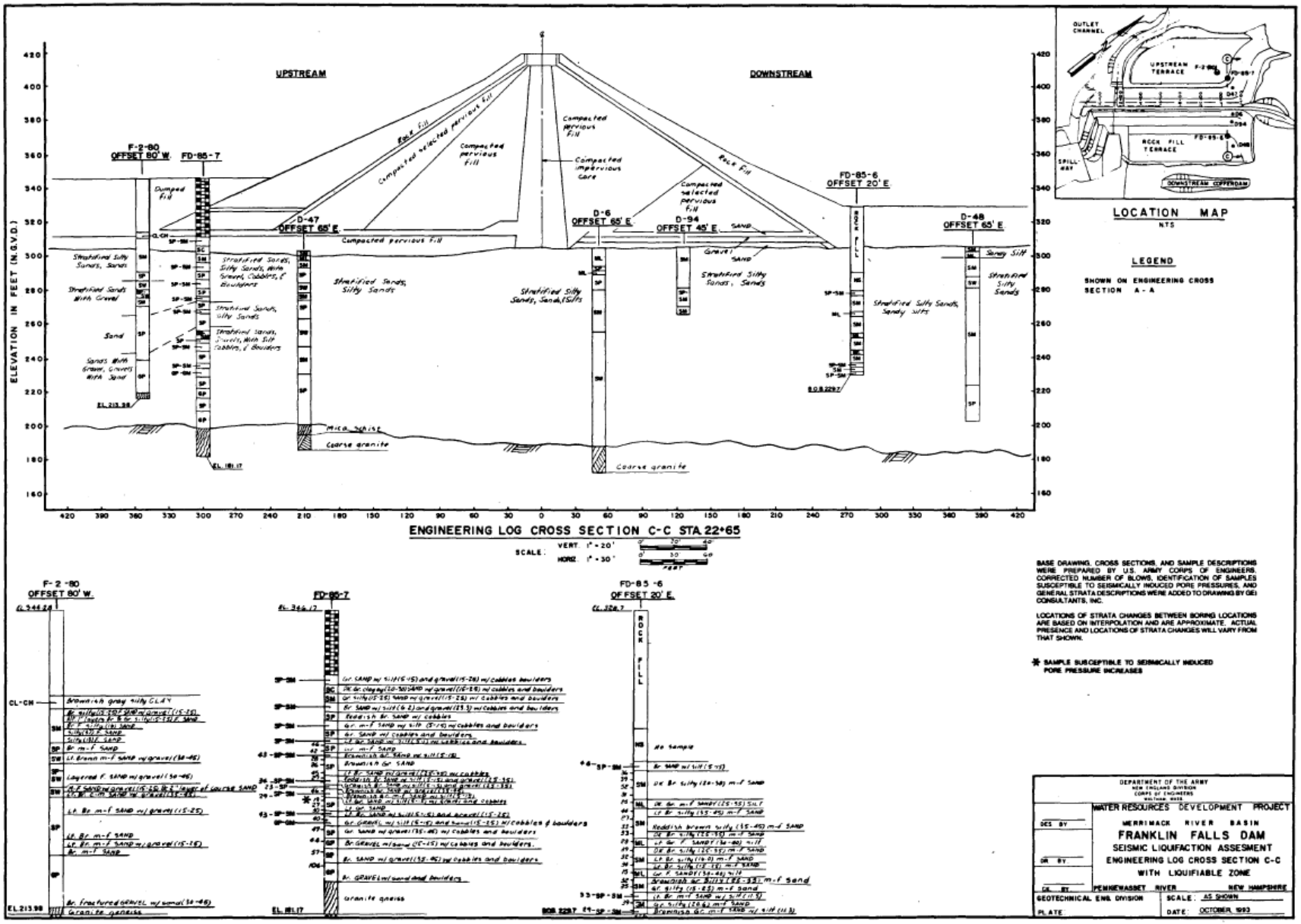

Figure A-5: Engineering log cross section C-C

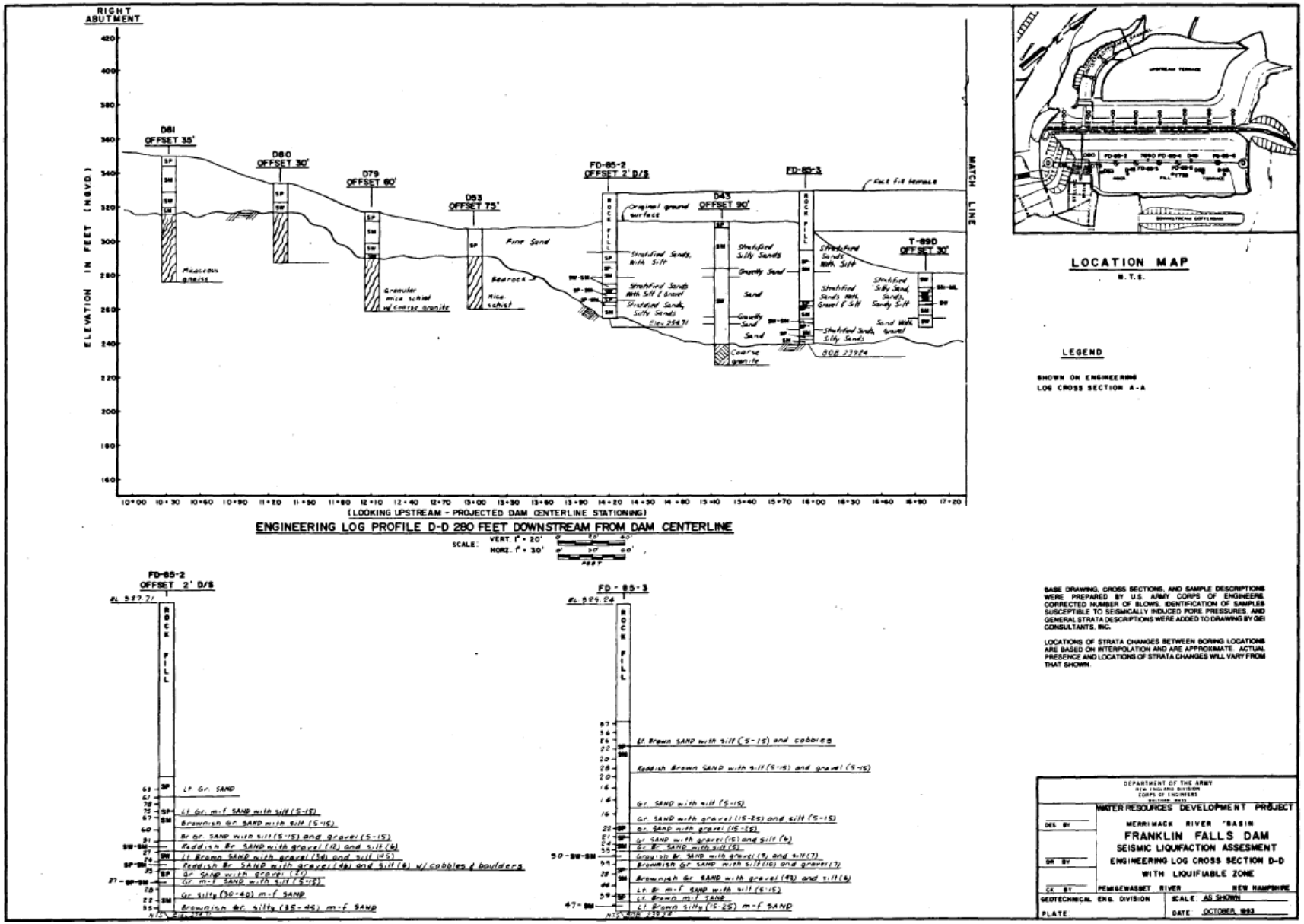

Figure A-6: Engineering log cross section D-D

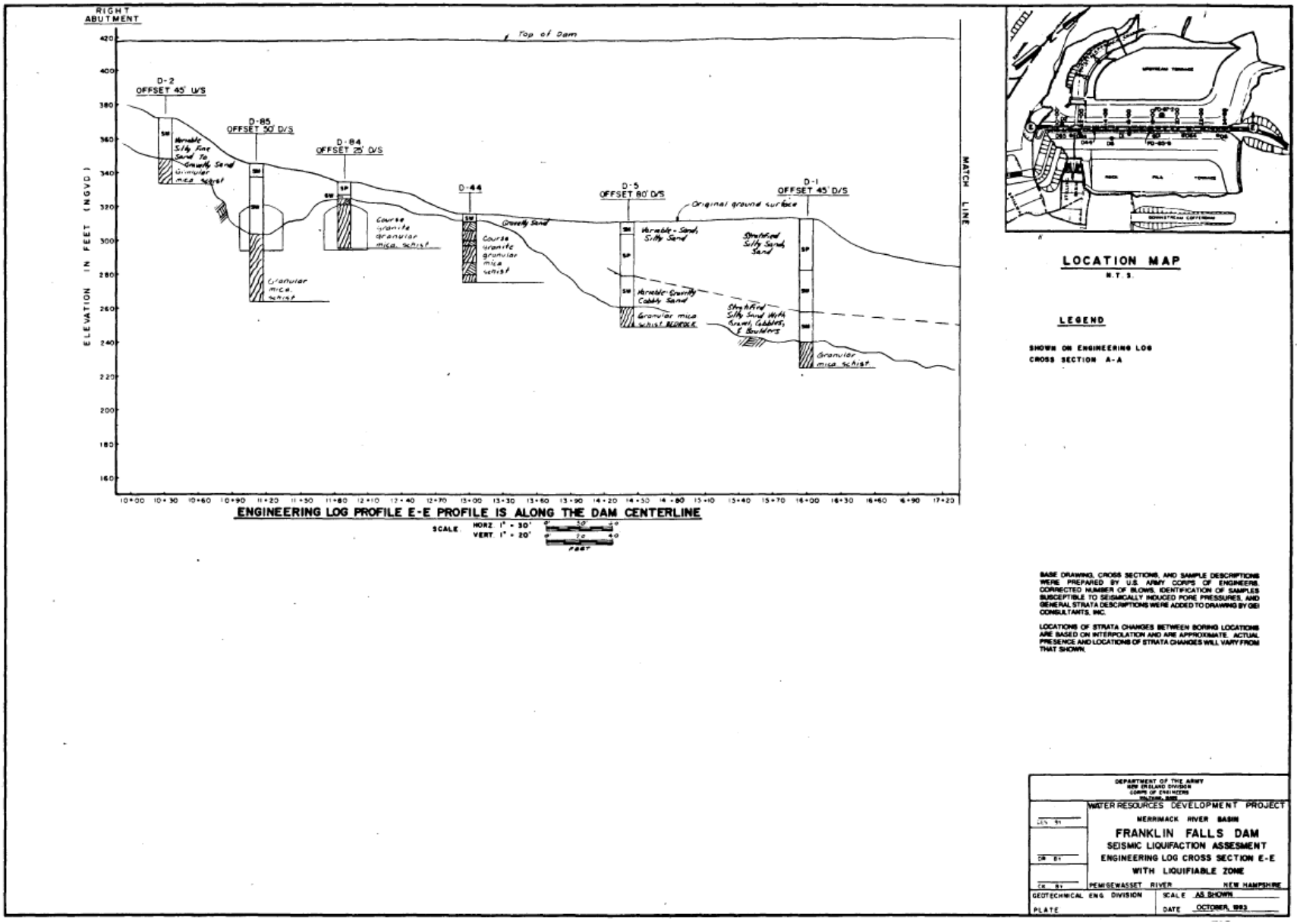

Figure A-7: Engineering log cross section E-E

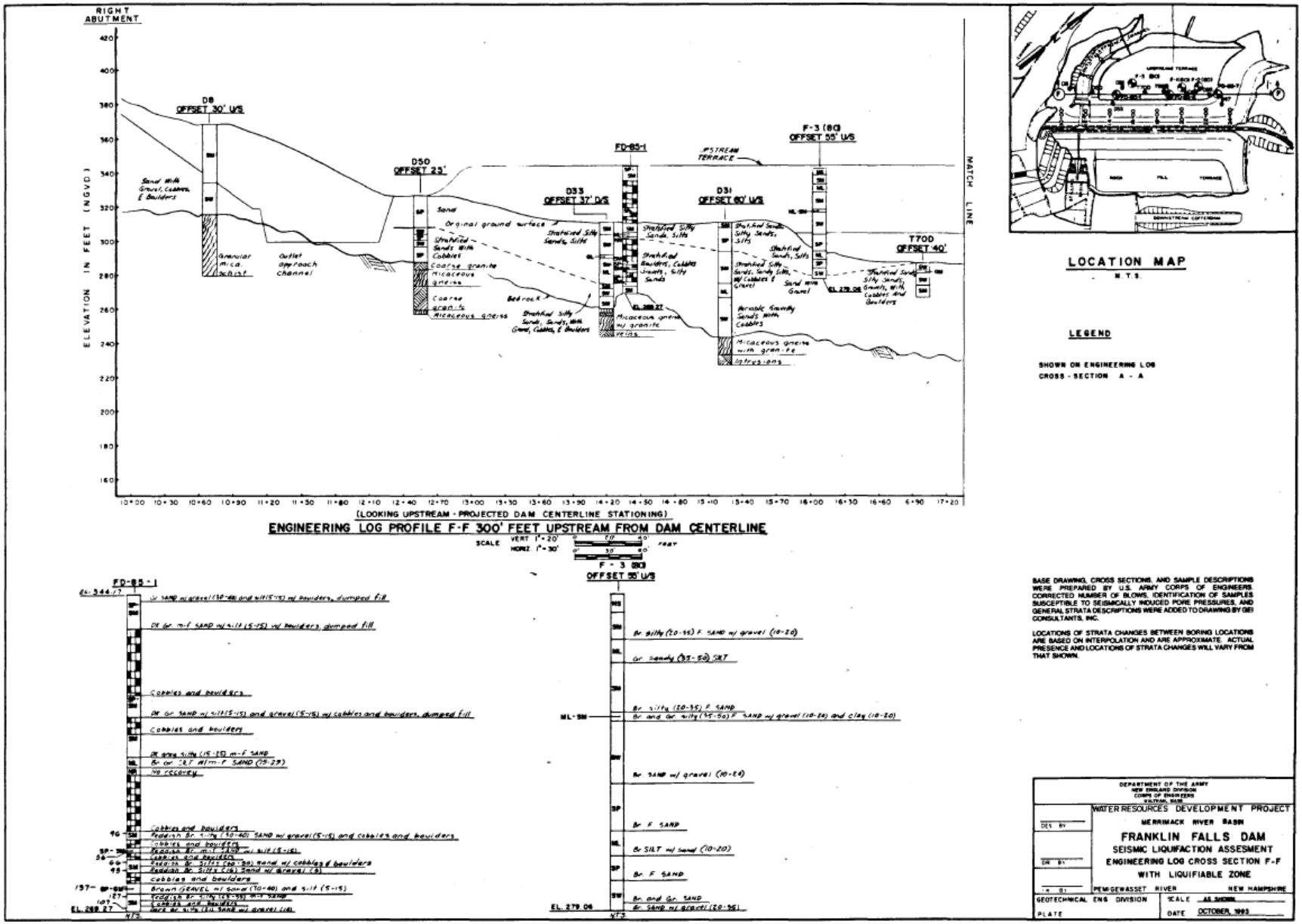

Figure A-8: Engineering log cross section F-F

APPENDIX B

BOREHOLE LOGS

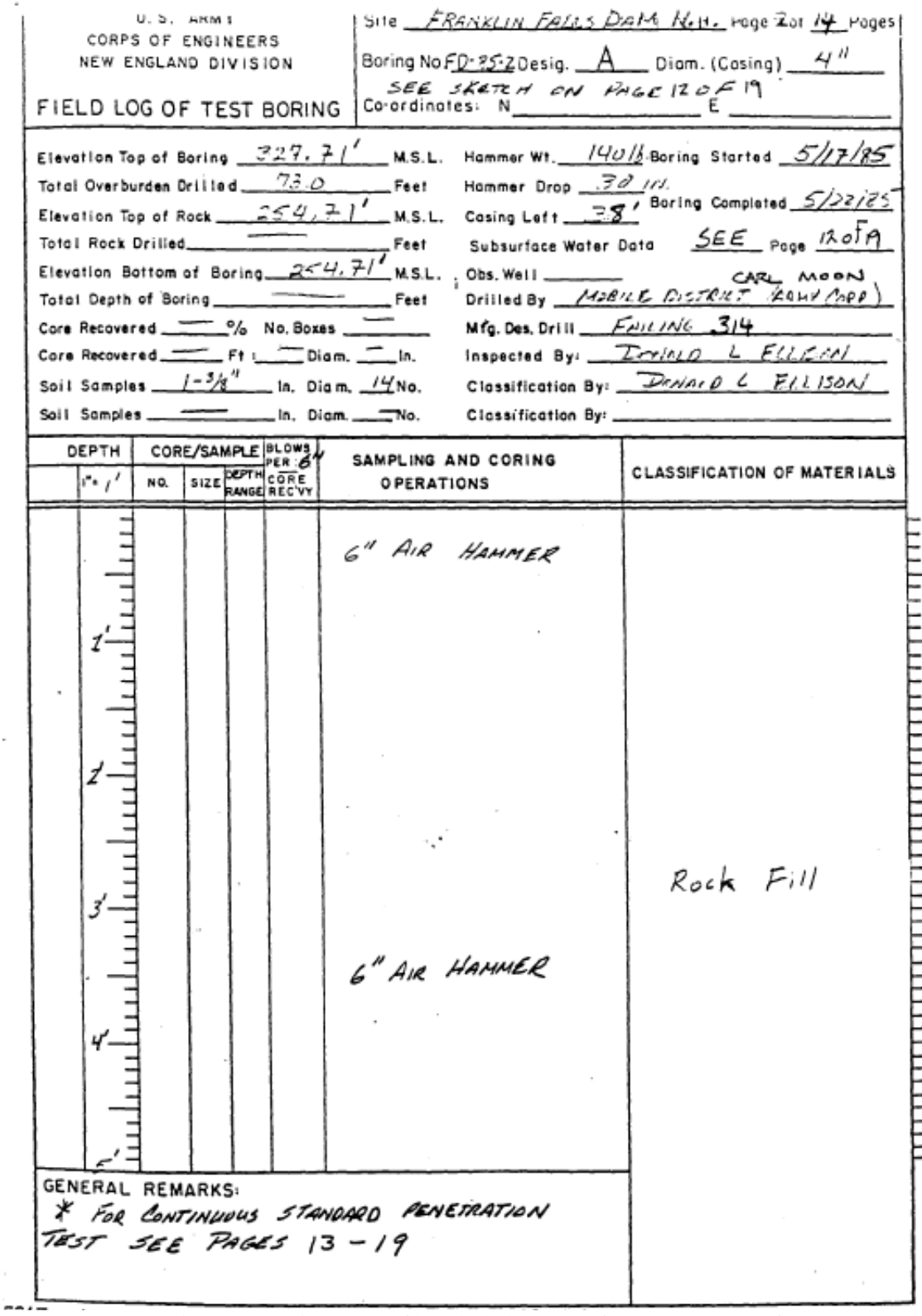

U. S. ARMY
CORPS OF ENGINEERS
NEW ENGLAND DIVISION

FIELD LOG OF TEST BORING

Site FRANKLIN FALLS DAM, N.H. Page 2 of 14 Pages

Boring No FD-85-2 Desig. A Diam. (Casing) 4"

SEE SKETCH ON PAGE 12 OF 19

Co-ordinates: N _____ E _____

Elevation Top of Boring 327.71' M.S.L.
Total Overburden Drilled 73.0 Feet
Elevation Top of Rock 254.71' M.S.L.
Total Rock Drilled _____ Feet
Elevation Bottom of Boring 254.71' M.S.L.
Total Depth of Boring _____ Feet
Core Recovered ___ % No. Boxes ___
Core Recovered ___ Ft ___ Diam. ___ In.
Soil Samples 1-3/8" In. Diam. 14 No.
Soil Samples ___ In. Diam. ___ No.

Hammer Wt. 140 lb. Boring Started 5/17/85
Hammer Drop 30 in. Boring Completed 5/22/85
Casing Left 38'
Subsurface Water Data SEE Page 12 of 19
Obs. Well _____
Drilled By MOBILE DISTRICT (ARMY CORPS) CARL MOON
Mfg. Des. Drill FAILING 314
Inspected By: DONALD L ELLISON
Classification By: DONALD L ELLISON
Classification By: _____

DEPTH	CORE/SAMPLE NO.	SIZE	DEPTH RANGE	BLOWS PER 6" CORE REC'VY	SAMPLING AND CORING OPERATIONS	CLASSIFICATION OF MATERIALS
0'					6" AIR HAMMER	
1'						
2'						
3'						Rock Fill
					6" AIR HAMMER	
4'						
5'						

GENERAL REMARKS:
* FOR CONTINUOUS STANDARD PENETRATION TEST SEE PAGES 13 - 19

Figure B-1: First page of borehole log FD-85-2 (USACE, 1986).

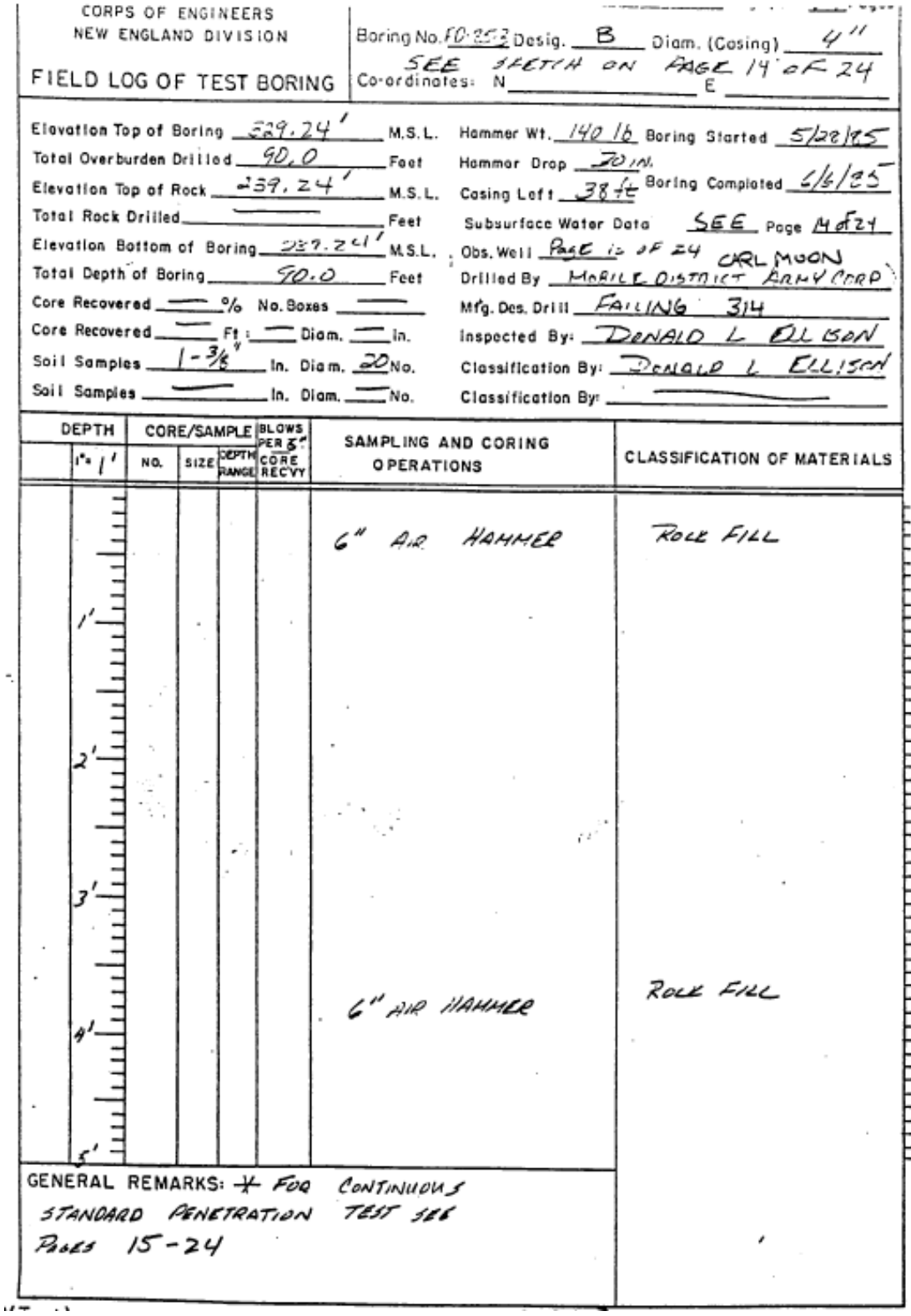

CORPS OF ENGINEERS
NEW ENGLAND DIVISION

FIELD LOG OF TEST BORING

Boring No. FD-85-3 Desig. B Diam. (Casing) 4"
Co-ordinates: N SEE SKETCH ON PAGE 14 OF 24 E

Elevation Top of Boring 239.24' M.S.L.
Total Overburden Drilled 90.0 Feet
Elevation Top of Rock 239.24' M.S.L.
Total Rock Drilled — Feet
Elevation Bottom of Boring 239.24' M.S.L.
Total Depth of Boring 90.0 Feet
Core Recovered — % No. Boxes —
Core Recovered — Ft. — Diam. — In.
Soil Samples 1-3/8" In. Diam. 20 No.
Soil Samples — In. Diam. — No.

Hammer Wt. 140 lb Boring Started 5/28/85
Hammer Drop 30 IN.
Casing Left 38 ft Boring Completed 6/6/85
Subsurface Water Data SEE Page 14 of 24
Obs. Well PAGE 15 OF 24 CARL MOON
Drilled By MOBILE DISTRICT ARMY CORP
Mfg. Des. Drill FALLING 314
Inspected By: DONALD L ELLISON
Classification By: DONALD L ELLISON
Classification By: —

DEPTH 1" = 1'	CORE/SAMPLE NO.	SIZE	DEPTH RANGE	BLOWS PER 6" CORE RECVY	SAMPLING AND CORING OPERATIONS	CLASSIFICATION OF MATERIALS
0					6" AIR HAMMER	ROCK FILL
1'						
2'						
3'						
4'					6" AIR HAMMER	ROCK FILL
5'						

GENERAL REMARKS: # FOR CONTINUOUS STANDARD PENETRATION TEST SEE PAGES 15-24

Figure B-2: First page of borehole log FD-85-3 (USACE, 1986).

Franklin Falls Dam N.H. 2 of 25 Pages

CORPS OF ENGINEERS
NEW ENGLAND DIVISION

FIELD LOG OF TEST BORING

Boring No. FD-85-4 Desig. D Diam. (Casing) 4"
SEE SKETCH ON PAGE 15 OF 25
Co-ordinates: N _____ E _____

Elevation Top of Boring 328.65' M.S.L.
Total Overburden Drilled 99.1' Feet
Elevation Top of Rock ——— M.S.L.
Total Rock Drilled ——— Feet
Elevation Bottom of Boring 229.55' M.S.L.
Total Depth of Boring 99.1' Feet
Core Recovered ——— % No. Boxes ———
Core Recovered ——— Ft : ——— Diam. ——— In.
Soil Samples 1-3" In. Diam. 20 No.
Soil Samples ——— In. Diam. ——— No.

Hammer Wt. 140lb Boring Started 6/10/85
Hammer Drop 30 in. Boring Completed 6/14/85
Casing Left 53
Subsurface Water Data SEE Page 15 of 25
Obs. Well P. 14 CARL MOON
Drilled By MOBILE DISTRICT ARMY CORP
Mfg. Des. Drill FAILING 314
Inspected By: DON ELLISON
Classification By: DON ELLISON
Classification By: _____

DEPTH 1" = 1'	CORE/SAMPLE NO.	SIZE	DEPTH RANGE	BLOWS PER FT. CORE RECVY	SAMPLING AND CORING OPERATIONS	CLASSIFICATION OF MATERIALS
1'					6" AIR HAMMER	ROCK FILL
2'						
3'					6" AIR HAMMER	ROCK FILL
4'						
5'						

GENERAL REMARKS: FOR CONTINUOUS STANDARD PENETRATION TEST SEE PAGES 16 THRU 25

Figure B-3: First page of borehole log FD-85-4 (USACE, 1986).

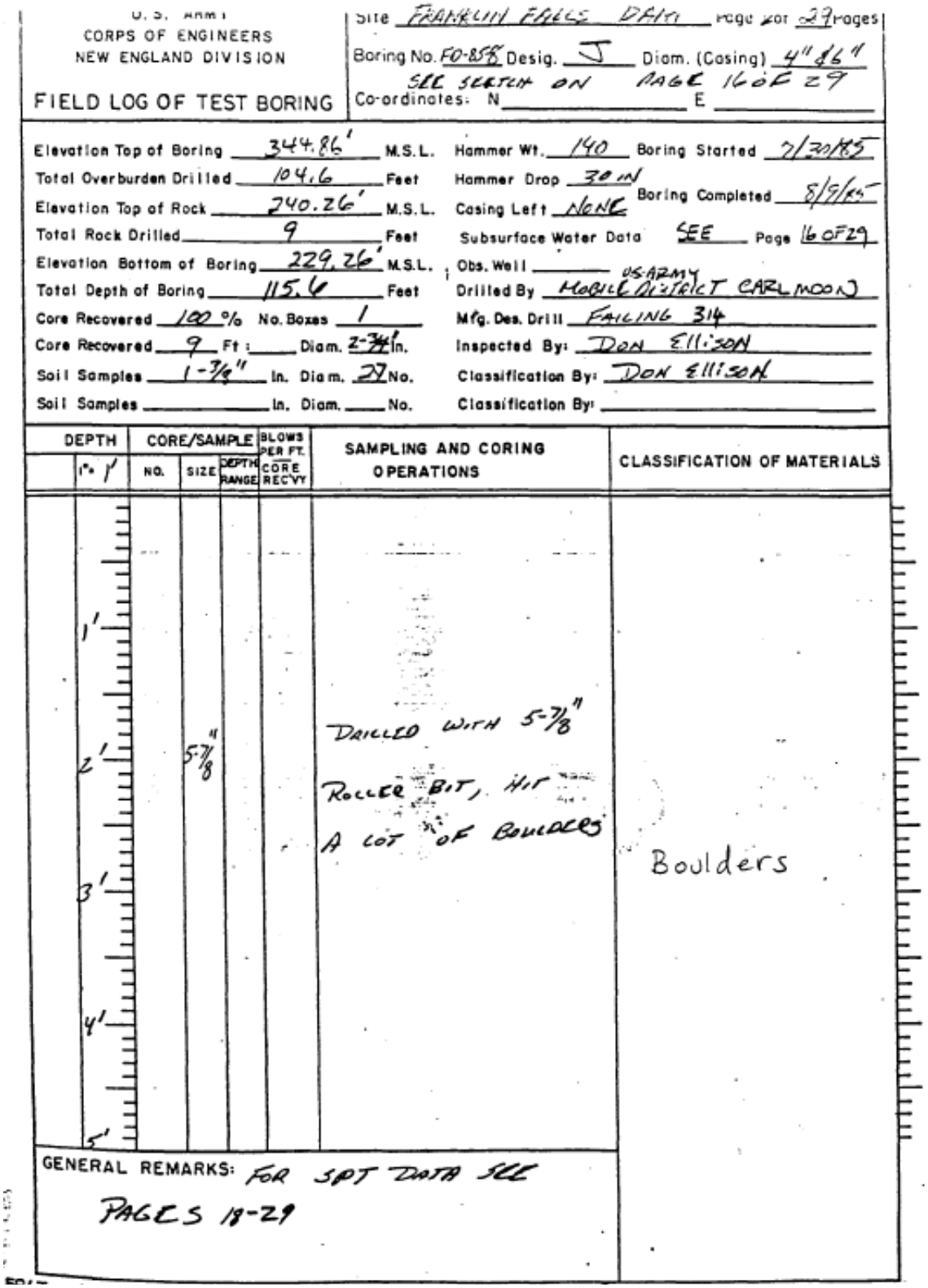

U.S. ARMY
CORPS OF ENGINEERS
NEW ENGLAND DIVISION

FIELD LOG OF TEST BORING

Site FRANKLIN FALLS DAM Page 1 of 29 Pages

Boring No. FD-85-8 Desig. J Diam. (Casing) 4" & 6"

SEE SKETCH ON PAGE 16 OF 29

Co-ordinates: N _____ E _____

Elevation Top of Boring 344.86' M.S.L.
Total Overburden Drilled 104.6 Feet
Elevation Top of Rock 240.26' M.S.L.
Total Rock Drilled 9 Feet
Elevation Bottom of Boring 229.26' M.S.L.
Total Depth of Boring 115.6 Feet
Core Recovered 100 % No. Boxes 1
Core Recovered 9 Ft. Diam. 2-3/4 In.
Soil Samples 1-3/8" In. Diam. 2" No.
Soil Samples _____ In. Diam. ____ No.

Hammer Wt. 140 Boring Started 7/30/85
Hammer Drop 30 IN Boring Completed 8/9/85
Casing Left NONE
Subsurface Water Data SEE Page 16 OF 29
Obs. Well _____
Drilled By US ARMY MOBILE DISTRICT CARL MOON
Mfg. Des. Drill FAILING 314
Inspected By: DON ELLISON
Classification By: DON ELLISON
Classification By: _____

DEPTH (ft)	CORE/SAMPLE NO.	CORE/SAMPLE SIZE	CORE/SAMPLE DEPTH RANGE	BLOWS PER FT. CORE RECVY	SAMPLING AND CORING OPERATIONS	CLASSIFICATION OF MATERIALS
1'					DRILLED WITH 5-7/8" ROLLER BIT, HIT A LOT OF BOULDERS	Boulders
2'		5-7/8"				
3'						
4'						
5'						

GENERAL REMARKS: FOR SPT DATA SEE PAGES 18-29

Figure B-4: First page of borehole log FD-85-8 (USACE, 1986).

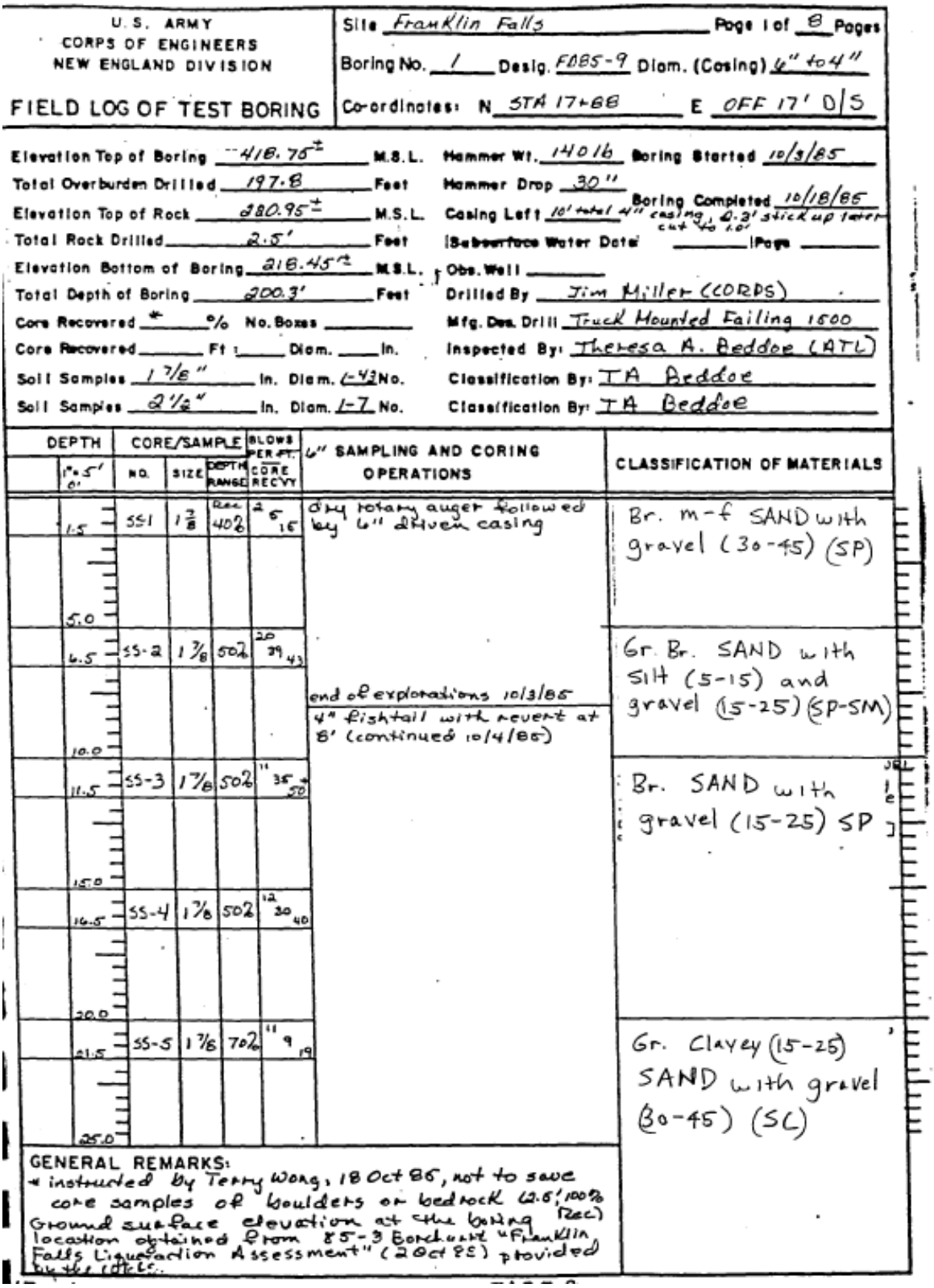

U.S. ARMY
CORPS OF ENGINEERS
NEW ENGLAND DIVISION

FIELD LOG OF TEST BORING

Site Franklin Falls — Page 1 of 8 Pages
Boring No. 1 — Desig. FDBS-9 — Diam. (Casing) 6" to 4"
Coordinates: N STA 17+68 — E OFF 17' O/S

Elevation Top of Boring ~418.75± M.S.L. — Hammer Wt. 140 lb — Boring Started 10/3/85
Total Overburden Drilled 197.8 Feet — Hammer Drop 30" — Boring Completed 10/18/85
Elevation Top of Rock 220.95± M.S.L. — Casing Left 10' total 4" casing, 0.3' stick up later cut to 1.0'
Total Rock Drilled 2.5' Feet — Subsurface Water Data — Page
Elevation Bottom of Boring 218.45± M.S.L. — Obs. Well
Total Depth of Boring 200.3' Feet — Drilled By Jim Miller (CORPS)
Core Recovered * % — No. Boxes — Mfg. Des. Drill Truck Mounted Failing 1500
Core Recovered Ft — Diam. In. — Inspected By: Theresa A. Beddoe (ATL)
Soil Samples 1 7/8" In. Diam. C-43 No. — Classification By: TA Beddoe
Soil Samples 2 1/2" In. Diam. I-7 No. — Classification By: TA Beddoe

DEPTH (ft)	CORE/SAMPLE NO.	SIZE	DEPTH RANGE	BLOWS PER FT. / CORE RECVY	6" SAMPLING AND CORING OPERATIONS	CLASSIFICATION OF MATERIALS
0' – 1.5	SS-1	1 3/8	Rec 40%	2 5 15	dry rotary auger followed by 6" driven casing	Br. m-f SAND with gravel (30-45) (SP)
5.0 – 6.5	SS-2	1 3/8	50%	20 39 43		Gr Br. SAND with silt (5-15) and gravel (15-25) (SP-SM)
10.0					end of explorations 10/3/85	
10.0 – 11.5	SS-3	1 3/8	50%	11 35+ 50	4" fishtail with revert at 8' (continued 10/4/85)	Br. SAND with gravel (15-25) SP
15.0 – 16.5	SS-4	1 3/8	50%	12 30 40		
20.0 – 21.5	SS-5	1 3/8	70%	11 9 19		Gr. Clayey (15-25) SAND with gravel (30-45) (SC)
25.0						

GENERAL REMARKS:
* instructed by Terry Wong, 18 Oct 85, not to save core samples of boulders or bedrock (2.5', 100% Rec)
Ground surface elevation at the boring location obtained from 85-3 Borehole "Franklin Falls Liquefaction Assessment" (20 Oct 85) provided by the COE.

Figure B-5: First page of borehole log FD-85-9 (USACE, 1986).

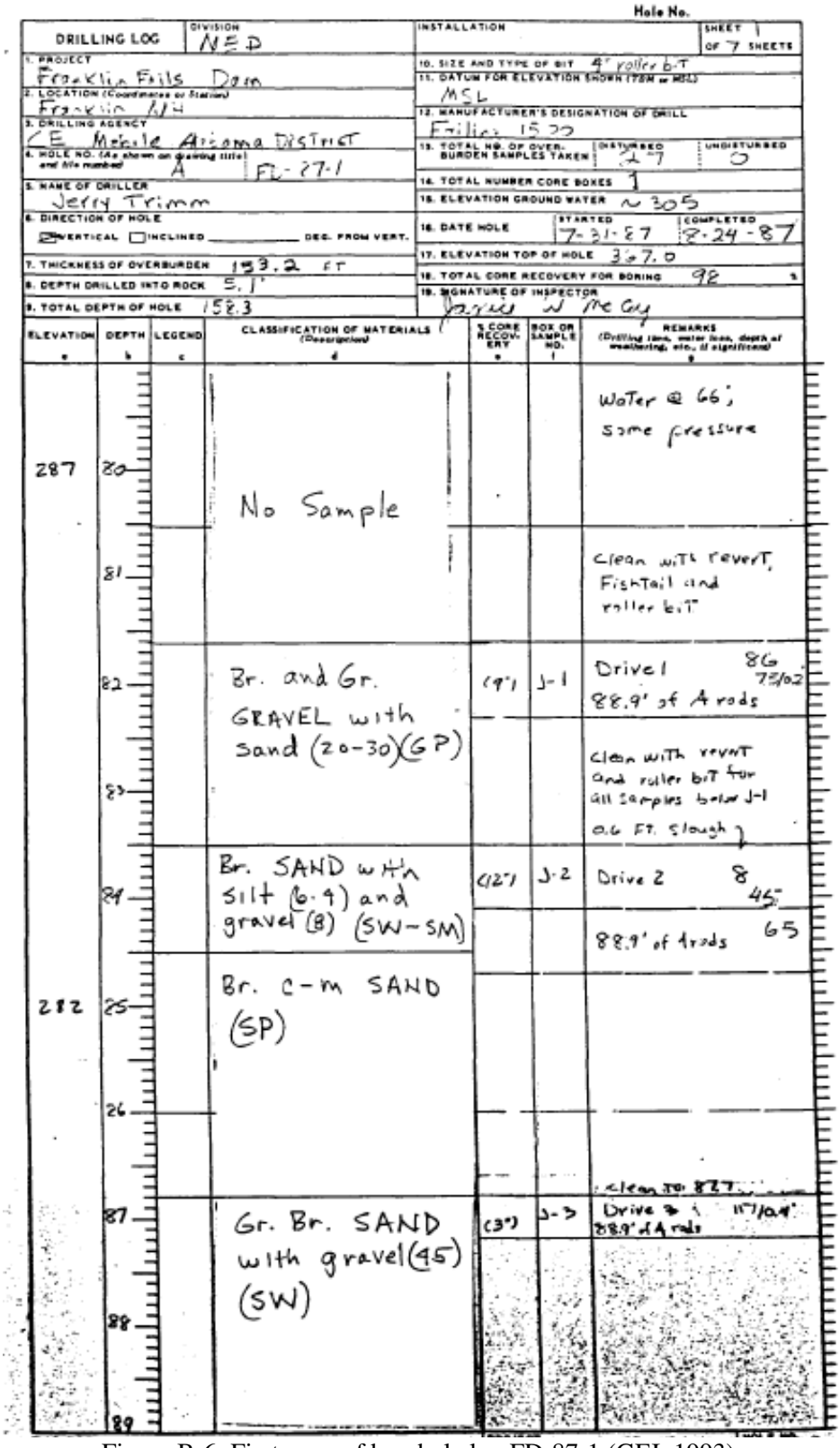

DRILLING LOG — DIVISION: NED — INSTALLATION — Hole No. — SHEET 1 OF 7 SHEETS

1. PROJECT: Franklin Falls Dam
2. LOCATION (Coordinates or Station): Franklin NH
3. DRILLING AGENCY: CE Mobile Alabama District
4. HOLE NO. (As shown on drawing title and file number): A — FL-87-1
5. NAME OF DRILLER: Jerry Trimm
6. DIRECTION OF HOLE: ☒ VERTICAL ☐ INCLINED ____ DEG. FROM VERT.
7. THICKNESS OF OVERBURDEN: 153.2 FT
8. DEPTH DRILLED INTO ROCK: 5.1'
9. TOTAL DEPTH OF HOLE: 158.3
10. SIZE AND TYPE OF BIT: 4" roller b.T
11. DATUM FOR ELEVATION SHOWN (TBM or MSL): MSL
12. MANUFACTURER'S DESIGNATION OF DRILL: Failing 1500
13. TOTAL NO. OF OVER-BURDEN SAMPLES TAKEN: DISTURBED 17; UNDISTURBED 0
14. TOTAL NUMBER CORE BOXES: 1
15. ELEVATION GROUND WATER: ~305
16. DATE HOLE: STARTED 7-31-87; COMPLETED 8-24-87
17. ELEVATION TOP OF HOLE: 307.0
18. TOTAL CORE RECOVERY FOR BORING: 98 %
19. SIGNATURE OF INSPECTOR: James W McCoy

ELEVATION a	DEPTH b	LEGEND c	CLASSIFICATION OF MATERIALS (Description) d	% CORE RECOVERY e	BOX OR SAMPLE NO. f	REMARKS (Drilling time, water loss, depth of weathering, etc., if significant) g
287	80		No Sample			Water @ 66'; some pressure
	81					clean with revert, Fishtail and roller bit
	82		Br. and Gr. GRAVEL with sand (20-30)(GP)	(9")	J-1	Drive 1 86 7/12 88.9' of A rods
	83					clean with revert and roller bit for all samples below J-1 0.6 FT. Slough
	84		Br. SAND with silt (6-9) and gravel (8) (SW-SM)	(12")	J-2	Drive 2 8 45" 88.9' of A rods 65
282	25		Br. c-m SAND (SP)			
	26					clean to 827
	87		Gr. Br. SAND with gravel (45) (SW)	(3")	J-3	Drive 3 11"/10" 88.9' of A rods
	88					
	89					

Figure B-6: First page of borehole log FD-87-1 (GEI, 1993).

U. S. ARMY
CORPS OF ENGINEERS
NEW ENGLAND DIVISION

FIELD LOG OF TEST BORING

Site Franklin Falls Dam N.H. Page 1 of 9 Pag
Boring No. FP-87-2 Desig. _____ Diam. (Casing) 4"
Co-ordinates: N _____ E _____

Elevation Top of Boring 380.0 NGVD M.S.L.
Total Overburden Drilled 134.2 Feet
Elevation Top of Rock 246.2 NGVD M.S.L.
Total Rock Drilled 9.5 Feet
Elevation Bottom of Boring 237.4 NGVD M.S.L.
Total Depth of Boring 142.6 Feet
Core Recovered 97 % No. Boxes 2
Core Recovered 9.2 Ft. HQ Diam. ____ In.
Soil Samples _____ In. Diam. ____ No.
Soil Samples _____ In. Diam. ____ No.

Hammer Wt. 140 LBS. Boring Started 27 Aug 87
Hammer Drop 30" Boring Completed 11 Sep 87
Casing Left _____
Subsurface Water Data _____ Page 1 of
Obs. Well _____
Drilled By CE SAM DISTRICT.
Mfg. Des. Drill Failing-314, J. Trimm
Inspected By: B. Bryant & A. Fricano
Classification By: B. Bryant & A. Fricano
Classification By: _____

DEPTH	CORE/SAMPLE NO.	SIZE	DEPTH RANGE	BLOWS PER FT. CORE RECVY	SAMPLING AND CORING OPERATIONS	CLASSIFICATION OF MATERIALS
0' 1.5'					ODEX Air Hammer. No Samples Taken.	* water Enc. @ d - 53.0' Static W.L. @ d - 75.0'
10.0						

GENERAL REMARKS:

Figure B-7: First page of borehole log FD-87-2 (GEI, 1993).

APPENDIX C
RAW GROUND MOTIONS AT THE ABUTMENT, DOWNSTREAM AND CREST ACCELEROGRAPHS

```
FFD0A
     1982  01  19    0014 New Hampshire
Moment Mag=          Ms=          Ml=      4.7
station = Franklin Falls Dam, Rt Abut    component= 045
epicentral dist =      8.0       pk acc =    279.1
inst type=           data source = USACE
*
*
*
    -32768      1982        19         0        14        42    -32768    -32768
    -32768    -32768    -32768    -32768        90        45    -32768         4
      3448    -32768    -32768    -32768    -32768    -32768    -32768    -32768
    -32768    -32768    -32768    -32768    -32768    -32768    -32768    -32768
    -32768    -32768    -32768    -32768    -32768    -32768    -32768    -32768
    -32768    -32768    -32768    -32768    -32768    -32768    -32768    -32768
  0.1700000E+39  0.2000000E+03  0.4350000E+02 -0.7160000E+02  0.1700000E+39
  0.1700000E+39  0.1700000E+39  0.4700000E+01  0.1700000E+39  0.1700000E+39
  0.4344700E+02 -0.7166000E+02  0.1700000E+39  0.1700000E+39  0.1700000E+39
  0.1700000E+39  0.8000000E+01  0.1700000E+39  0.1000000E+05  0.1700000E+39
  0.1700000E+39  0.1700000E+39  0.1700000E+39  0.1800000E+01  0.1700000E+39
  0.1700000E+39  0.1700000E+39  0.1700000E+39  0.1185000E+01  0.2791287E+03
  0.1240000E+01 -0.2175907E+03  0.1700000E+39  0.1700000E+39  0.1700000E+39
  0.1700000E+39  0.1700000E+39  0.1700000E+39  0.1700000E+39  0.1700000E+39
  0.1700000E+39  0.1700000E+39  0.1700000E+39  0.1700000E+39  0.1700000E+39
  0.1700000E+39  0.1700000E+39  0.1700000E+39  0.1700000E+39  0.1700000E+39
|
|ref - Chang, Frank K. (1987) Response Spectral Analysis of Franklin Falls Dam,
|New Hampshire;  U.S. Army Corps of Engineers Miscellaneous Paper GL-87-1.
|
-2.5564E+0-4.5484E+0-1.3136E+0 4.8766E+0 4.2721E+0 1.5196E+0-7.0623E-1-1.9487E+0
-1.9564E+0 2.1002E-1 9.4486E-1 5.1236E-1 2.4390E-1 3.2785E-1 1.0934E+0 3.6658E-1
-2.0426E-1 6.9082E-2 1.8685E+0 2.2111E+0-1.5207E+0-9.9096E+0-1.3769E+1-1.2401E+1
-8.4828E-1 6.8825E+0 1.4699E+1 1.7832E+1 1.2404E+1 3.4313E+0-1.9122E+0-6.0039E+0
-1.2986E+1-1.7198E+1-1.3586E+1-1.1543E+0 3.9181E+0 8.2190E+0 1.1168E+1 1.2928E+1
 1.1297E+1 6.8610E+0-5.5321E+0-1.0851E+1-8.9455E+0-6.8099E-1 2.5270E+0 5.1597E+0
 9.0096E+0 1.1167E+1 9.9388E+0 3.5462E+0-2.0728E+0-5.6437E+0-8.8523E+0-1.3298E+1
-1.5154E+1-1.2513E+1-1.2515E+0 5.3853E+0 8.6088E+0 8.3295E+0 8.1520E+0 1.0088E+1
 1.1099E+1 6.6067E+0-1.1847E+0-4.7975E+0-6.8562E+0-8.2990E+0-7.7635E+0-2.8318E+0
 3.3339E-1 2.1751E-1-2.0327E-1 3.6000E+0 8.6883E+0 7.2550E+0 2.2448E+0-1.0924E+0
-2.3457E+0-2.3620E+0-3.4337E+0-4.8377E+0-4.3142E+0 3.3356E+0 1.1052E+1 1.2360E+1
 4.1637E+0-1.2883E+0-4.0978E+0-9.2615E+0-1.2912E+1-1.2963E+1-3.1840E+0 4.4778E+0
 1.3583E+1 2.0483E+1 1.8275E+1 1.0426E+1-8.5966E+0-1.9215E+1-2.5097E+1-2.3784E+1
-1.1289E+1 9.5430E+0 2.4681E+1 2.7931E+1 1.9968E+1 1.1337E+1 1.8570E+0-5.9960E+0
-9.2564E+0-9.1175E+0-7.4927E+0-8.1501E+0-1.2246E+1-1.4317E+1-7.3268E+0 9.8153E+0
 1.9362E+1 2.2813E+1 2.0919E+1 8.9513E+0-8.4529E+0-1.8102E+1-1.9542E+1-1.0845E+1
-9.4353E-2 8.0723E+0 1.2023E+1 8.8173E+0-4.9359E+0-1.9506E+1-2.2069E+1-1.1609E+1
-1.1371E+0 2.5842E+0-1.0222E+0-1.2154E+1-1.8378E+1-1.5957E+1-1.6537E+0 1.6862E+1
 2.8326E+1 1.4851E+1 6.0896E-1-1.4676E+1-3.0374E+1-1.5322E+1-3.0050E+0 7.3740E+0
 2.3046E+1 3.2875E+1 2.0717E+1 4.7978E+0-1.2373E+1-2.5741E+1-3.2417E+1-1.6002E+1
 1.1221E+1 3.3858E+1 4.6176E+1 2.7577E+1-1.5548E+0-2.3647E+1-3.5088E+1-3.1601E+1
-1.7780E+1-5.5446E-1 2.1444E+1 3.2048E+1 3.9682E+1 3.7180E+1 2.2477E+1 2.0207E+0
-2.4190E+1-4.2593E+1-5.5402E+1-4.1988E+1-2.0160E+1 1.0616E+1 4.0969E+1 5.6935E+1
 3.8589E+1 1.9651E+1-7.9756E+0-2.6330E+1-3.5891E+1-2.7841E+1-1.5564E+1-1.0330E+1
-1.9497E+0 6.2737E+0 1.3393E+1 1.4965E+1 1.0542E+1 4.9625E+0-2.4157E-1-3.3133E+0
-3.5087E+0-2.6712E+0-3.5085E+0-6.4834E+0-1.0744E+1-1.5213E+1-2.2416E+1-2.0733E+1
 2.8228E+1 5.3433E+1 6.5826E+1 4.3212E+1 3.5546E+0-2.4164E+1-4.7037E+1-5.2244E+1
-1.7858E+1 4.6807E+0-7.2759E+0-2.6501E+1-4.7683E+1-2.2889E+1 1.2836E+1 5.2789E+1
 7.6843E+1 8.9008E+1 7.0511E+1 4.8151E+1 2.0576E+1-9.4170E+0-4.5665E+1-7.2441E+1
-9.4503E+1-1.3002E+2-1.4481E+2-1.2034E+2-2.6967E+1 2.7913E+2 2.6977E+2 2.2302E+2
 1.6146E+2 9.6820E+1 3.2182E+1-3.2456E+1-8.2797E+1-1.2228E+2-1.5331E+2-1.9692E+2
-2.1759E+2-2.0732E+2-6.4832E+1 2.0018E+2 2.3354E+2 2.1511E+2 1.7860E+2 1.2844E+2
```

Figure C-1: First page of ground motion at abutment, longitudinal direction (Chang, 1987).

```
FFDOC
     1982  01  19    0014 New Hampshire
Moment Mag=           Ms=           Ml=      4.7
station = Franklin Falls Dam, Rt Abut    component= 315
epicentral dist =      8.0       pk acc =    -556.0
inst type=            data source = USACE
*
*
*
    -32768      1982        19         0        14        42    -32768    -32768
    -32768    -32768    -32768    -32768        90       315    -32768         4
      3442    -32768    -32768    -32768    -32768    -32768    -32768    -32768
    -32768    -32768    -32768    -32768    -32768    -32768    -32768    -32768
    -32768    -32768    -32768    -32768    -32768    -32768    -32768    -32768
    -32768    -32768    -32768    -32768    -32768    -32768    -32768    -32768
  0.1700000E+39  0.2000000E+03  0.4350000E+02 -0.7160000E+02  0.1700000E+39
  0.1700000E+39  0.1700000E+39  0.4700000E+01  0.1700000E+39  0.1700000E+39
  0.4344700E+02 -0.7166000E+02  0.1700000E+39  0.1700000E+39  0.1700000E+39
  0.1700000E+39  0.8000000E+01  0.1700000E+39  0.1000000E+05  0.1700000E+39
  0.1700000E+39  0.1700000E+39  0.1700000E+39  0.1800000E+01  0.1700000E+39
  0.1700000E+39  0.1700000E+39  0.1700000E+39  0.1160000E+01  0.5235679E+03
  0.1225000E+01 -0.5560040E+03  0.1700000E+39  0.1700000E+39  0.1700000E+39
  0.1700000E+39  0.1700000E+39  0.1700000E+39  0.1700000E+39  0.1700000E+39
  0.1700000E+39  0.1700000E+39  0.1700000E+39  0.1700000E+39  0.1700000E+39
  0.1700000E+39  0.1700000E+39  0.1700000E+39  0.1700000E+39  0.1700000E+39
|
|ref - Chang, Frank K. (1987) Response Spectral Analysis of Franklin Falls Dam,
|New Hampshire;  U.S. Army Corps of Engineers Miscellaneous Paper GL-87-1.
|
-1.3046E+1-1.9187E+1-2.0807E+1-1.2416E+1-2.3006E+0 9.4688E+0 1.3037E+1 1.3310E+1
 1.2177E+1 8.6676E+0 7.9828E-1-8.5058E+0-1.4351E+1-3.3418E+0 7.8702E+0 1.5308E+1
 1.2017E+1 3.8535E+0-3.7055E+0-9.8936E+0-1.5905E+1-1.0387E+1-1.0141E+0 1.1356E+1
 1.8179E+1 1.6727E+1 1.0334E+1-4.7867E-1-9.8717E+0-1.7757E+1-1.8114E+1-1.3369E+1
-1.0354E+1-3.7017E+0 9.8584E+0 1.9725E+1 2.0232E+1 1.1365E+1-3.2759E+0-1.3078E+1
-1.4933E+1-9.6801E+0-6.5776E+0-3.1778E+0 2.0195E+0 6.2030E+0 4.6320E+0 7.4584E-1
-6.1132E+0-4.7496E+0 1.7231E-2 2.4305E+0 3.0096E+0 3.4561E+0 4.0696E+0 3.1791E+0
 1.5396E-1-4.9465E+0-4.0716E+0 4.8901E-1 2.3952E+0-3.0013E+0-9.2139E+0-7.4817E+0
 4.0638E+0 6.5177E+0 2.9852E+0-2.1780E+0-3.8479E+0-2.6614E+0-1.1261E+0-1.4086E+0
-2.7667E+0-2.6777E+0 1.1798E+0 5.8502E+0 7.2468E+0 6.4579E+0 3.8435E+0-1.0788E+1
-1.6613E+1-1.0163E+1 2.2941E+0 5.5951E+0 3.4605E+0 1.4215E+0 2.4130E+0 4.0118E+0
 4.4679E+0 3.7536E+0 1.9984E+0-4.7379E+0-1.0362E+1-1.1270E+1-9.6250E+0-9.5019E+0
-1.4664E+1-2.0533E+1-6.5440E-1 1.9987E+1 3.7231E+1 4.8620E+1 4.1049E+1 2.4467E+1
 4.9024E+0-2.0264E+1-5.6606E+1-7.7503E+1-5.8066E+1-2.0721E+1 1.9281E+1 4.6751E+1
 5.4804E+1 5.1967E+1 4.1198E+1 2.5633E+1 7.1490E+0-2.9286E+1-4.1151E+1-5.1154E+1
-4.5312E+1-3.4483E+1-1.9837E+1 2.9847E+1 5.2038E+1 6.8975E+1 6.0336E+1 4.3167E+1
-2.0020E+0-3.3803E+1-5.9838E+1-5.5485E+1-3.9748E+1-3.0919E+1-2.6284E+1-2.6256E+1
-2.0817E+1 7.0407E+0 1.7535E+1 2.5632E+1 2.0410E+1 1.0352E+1-1.5006E+0-1.5571E+1
-2.3818E+1-1.2187E+1-6.0312E-1 1.0916E+1 1.8737E+1 2.3929E+1 1.5593E+1-4.3512E+0
-1.4884E+1-2.2086E+1-1.0448E+1 1.3699E+1 3.8474E+1 5.3703E+1 4.1716E+1 2.1235E+1
-8.3863E+0-2.9068E+1-3.6631E+1-2.0862E+1-4.7092E+0 8.6909E+0 1.7367E+1 3.4231E+1
 5.7612E+1 6.6557E+1 5.2942E+1 2.9943E+1 2.8429E+0-4.8199E+1-7.5599E+1-9.2052E+1
-7.1965E+1-8.0551E+0 2.3085E+1 4.4268E+1 4.8526E+1 3.5196E+1 2.4222E+1 1.4040E+1
 6.0274E+0 2.2494E+0-7.9904E+0-1.9219E+1-3.3076E+1-4.3534E+1-4.3421E+1-3.1502E+1
-1.3069E+1 8.9550E+0 2.3528E+1 2.3774E+1 1.3164E+1-3.3161E+0-2.0037E+1-3.2507E+1
-4.0530E+1-4.0272E+1-2.3518E+1-4.5110E+0 4.3651E+1 7.4367E+1 7.0184E+1 4.4161E+1
 9.3824E+0-4.0633E+1-6.1463E+1-7.3365E+1-6.3414E+1-3.8999E+1-9.1013E+0-1.1384E+1
-1.4635E+1 3.9571E+1 1.3179E+2 2.2401E+2 2.4134E+2 2.0352E+2 1.3230E+2 6.1084E+1
-1.0134E+1-8.1352E+1-1.5257E+2-2.2379E+2-2.9501E+2-3.6622E+2-4.3685E+2-2.6590E+2
 5.2357E+2 4.9266E+2 4.0404E+2 3.1542E+2 2.2679E+2 1.3817E+2 4.9549E+1-3.9074E+1
-1.2770E+2-2.1632E+2-3.0494E+2-3.9356E+2-4.8219E+2-5.5600E+2 1.2700E+2 2.9279E+2
 2.8498E+2 2.6705E+2 2.4802E+2 2.2068E+2 1.9639E+2 1.7192E+2 9.8676E+1 2.5427E+1
```

Figure C-2: First page of ground motion at abutment, transverse direction (Chang, 1987).

```
FFD0B
     1982  01  19    0014 New Hampshire
Moment Mag=          Ms=          Ml=      4.7
station = Franklin Falls Dam, Rt Abut    component= up
epicentral dist =      8.0       pk acc =    171.2
inst type=           data source = USACE
*
*
*
    -32768      1982        19         0        14        42    -32768    -32768
    -32768    -32768    -32768    -32768         0    -32768    -32768         4
      3447    -32768    -32768    -32768    -32768    -32768    -32768    -32768
    -32768    -32768    -32768    -32768    -32768    -32768    -32768    -32768
    -32768    -32768    -32768    -32768    -32768    -32768    -32768    -32768
    -32768    -32768    -32768    -32768    -32768    -32768    -32768    -32768
  0.1700000E+39  0.2000000E+03  0.4350000E+02 -0.7160000E+02  0.1700000E+39
  0.1700000E+39  0.1700000E+39  0.4700000E+01  0.1700000E+39  0.1700000E+39
  0.4344700E+02 -0.7166000E+02  0.1700000E+39  0.1700000E+39  0.1700000E+39
  0.1700000E+39  0.8000000E+01  0.1700000E+39  0.1000000E+05  0.1700000E+39
  0.1700000E+39  0.1700000E+39  0.1700000E+39  0.1800000E+01  0.1700000E+39
  0.1700000E+39  0.1700000E+39  0.1700000E+39  0.1190000E+01  0.1711854E+03
  0.1255000E+01 -0.1487067E+03  0.1700000E+39  0.1700000E+39  0.1700000E+39
  0.1700000E+39  0.1700000E+39  0.1700000E+39  0.1700000E+39  0.1700000E+39
  0.1700000E+39  0.1700000E+39  0.1700000E+39  0.1700000E+39  0.1700000E+39
  0.1700000E+39  0.1700000E+39  0.1700000E+39  0.1700000E+39  0.1700000E+39
|
|ref - Chang, Frank K. (1987) Response Spectral Analysis of Franklin Falls Dam,
|New Hampshire;  U.S. Army Corps of Engineers Miscellaneous Paper GL-87-1.
|
 2.7148E+0 6.3008E+0 5.9671E+0 2.3831E+0-2.4777E+0-6.6128E+0-3.3702E+0 6.1008E+0
 1.0595E+1 4.1010E+0-2.2618E+0-3.0104E+0 2.6765E-1 3.6285E+0 5.4103E+0 3.7794E+0
 3.1682E+0 6.6386E+0 7.8611E+0 4.5455E+0-1.5760E+0-1.0185E+0 3.6165E+0 4.6944E+0
-6.6401E-1 1.8765E+0 6.9643E+0 6.5761E+0 7.2368E+0 1.0201E+1 1.2725E+1 5.6278E+0
-4.4103E+0-3.6471E+0 7.4063E+0 9.5221E+0 3.5160E+0-2.4892E+0-1.1482E+0 5.7867E+0
 6.5237E+0-1.0786E+0-3.8275E+0 3.7214E+0 9.4526E+0 3.9179E+0-5.2354E+0-6.2048E+0
 1.1499E+0 3.3232E+0 8.6797E-1 2.8389E+0 8.9022E+0 1.0974E+1 4.9271E+0-7.9119E+0
-8.6175E+0 4.0705E+0 8.9602E+0 5.0337E+0-7.8415E+0-8.8364E+0-1.8695E+0 5.4079E+0
 4.9058E+0 1.0408E+0 4.2672E+0 1.0002E+1 9.0021E+0 4.8856E+0 4.0242E+0 4.8129E+0
 1.1864E+0-2.5538E+0 2.0407E+0 1.0413E+1 1.1180E+1 5.8148E+0-3.0695E-1-2.3053E+0
-1.6028E+0 1.7527E+0 2.0515E+0-2.4061E-1 2.3395E-1 1.5662E+0 4.0892E-1 1.7079E+0
 1.2143E+1 1.4904E+1 8.5061E+0 3.3228E+0 6.9353E+0 1.2697E+1 7.1889E+0-3.6610E+0
-1.3858E+1-8.8207E+0-3.0918E+0 9.5346E-1-5.2846E+0-2.5024E+0 7.8316E+0 1.8859E+1
 2.2023E+0-1.6288E+1-2.2929E+1-7.8734E+0 2.5261E+0 4.6540E-1-8.9386E+0-1.7332E+1
-1.0241E+1 4.4397E+0 1.5853E+1 1.0239E+1 2.5154E+0 4.4536E+0 1.2134E+1 3.3619E+0
-3.0997E+0-8.0338E+0-8.2144E+0-1.1743E+0 1.0006E+1 1.8860E+1 1.8238E+1 1.5063E+0
-1.0689E+1 2.0581E+0 2.0956E+1 2.8819E+1 1.6158E+1 1.0343E+0-9.2362E+0-4.9476E+0
 5.4569E+0 1.6433E+1 2.1669E+1 1.0759E+1-3.3147E+0-1.7398E+1-2.4826E+1-1.1906E+1
-5.3120E-1 6.2321E+0 5.4222E+0 3.3148E+0 1.9373E+0 4.3518E-1-8.6956E+0-2.3652E+1
-3.0289E+1-2.7015E+1-1.8743E+1-5.9984E+0 8.3257E+0 5.6149E+0-1.1111E+1-3.5281E+1
-5.5211E+1-3.9388E+1-3.8239E+0 1.2599E+1 1.4383E+1 1.3219E+1 1.2806E+1 1.2626E+1
 1.2793E+1 1.3981E+1 1.6194E+1 1.4281E+1 8.1164E+0 7.8424E+0 1.7189E+1 2.3181E+1
 2.3863E+1 2.4196E+1 2.4319E+1 2.4233E+1 1.5378E+1 2.9913E+0-1.0340E+1-1.1607E+0
 6.9256E+0 1.0156E+1 9.8888E+0 7.9789E+0 6.4804E+0 5.7425E+0 3.6855E+0 2.2028E+0
 5.0885E+0 1.0133E+1 1.1297E+1 1.0417E+1 1.2283E+1 1.5096E+1 5.4578E+0-6.8203E+0
-2.0720E+1-3.1879E+1-1.6824E+1-7.8592E-1 7.5830E+0 7.4721E+0-2.8650E+0-1.2430E+1
-2.5439E+1-3.6850E+1-2.3729E+1-4.1792E+0 1.5334E+1-9.4978E+0-3.6981E+1-6.0575E+1
-6.5934E+1-5.1863E+1-3.8444E+1-3.5495E+1-3.9376E+1-3.5326E+1-1.4689E+1 3.9691E+1
 7.1204E+1 7.1203E+1 3.8666E+1-2.4697E+0-5.7186E+1-6.9008E+1-4.1980E+1-3.5551E+1
-3.3361E+1-3.2497E+1-3.2862E+1-3.8127E+1-2.3501E+1 7.5520E+1 1.7119E+2 1.4996E+2
 8.5335E+1 1.5203E+1-5.4929E+1-1.0514E+2-8.3258E+1 2.5556E+1 3.0473E+1 1.5535E+1
-2.4142E+1-6.4868E+1-1.0559E+2-1.4871E+2-9.5092E+1 1.9820E+1 8.5933E+1 1.0050E+2
```

Figure C-3: First page of ground motion at abutment, vertical direction (Chang, 1987).

```
FFDOF
     1982  01  19    0014 New Hampshire
Moment Mag=          Ms=          Ml=      4.7
station = Franklin Falls Dam, Downstream component= 135
epicentral dist =      8.0       pk acc =    255.4
inst type=           data source = USACE
*
*
*
    -32768      1982        19         0        14        42    -32768    -32768
    -32768    -32768    -32768    -32768        90       135    -32768         4
      3857    -32768    -32768    -32768    -32768    -32768    -32768    -32768
    -32768    -32768    -32768    -32768    -32768    -32768    -32768    -32768
    -32768    -32768    -32768    -32768    -32768    -32768    -32768    -32768
    -32768    -32768    -32768    -32768    -32768    -32768    -32768    -32768
  0.1700000E+39  0.2000000E+03  0.4350000E+02 -0.7160000E+02  0.1700000E+39
  0.1700000E+39  0.1700000E+39  0.4700000E+01  0.1700000E+39  0.1700000E+39
  0.4344700E+02 -0.7166000E+02  0.1700000E+39  0.1700000E+39  0.1700000E+39
  0.1700000E+39  0.8000000E+01  0.1700000E+39  0.1000000E+05  0.1700000E+39
  0.1700000E+39  0.1700000E+39  0.1700000E+39  0.1850000E+01  0.1700000E+39
  0.1700000E+39  0.1700000E+39  0.1700000E+39  0.1545000E+01  0.2554439E+03
  0.1575000E+01 -0.1949465E+03  0.1700000E+39  0.1700000E+39  0.1700000E+39
  0.1700000E+39  0.1700000E+39  0.1700000E+39  0.1700000E+39  0.1700000E+39
  0.1700000E+39  0.1700000E+39  0.1700000E+39  0.1700000E+39  0.1700000E+39
  0.1700000E+39  0.1700000E+39  0.1700000E+39  0.1700000E+39  0.1700000E+39
|
|ref - Chang, Frank K. (1987) Response Spectral Analysis of Franklin Falls Dam,
|New Hampshire;  U.S. Army Corps of Engineers Miscellaneous Paper GL-87-1.
|
-2.4246E-1 1.6319E+0 2.6941E+0 1.9121E+0-8.4792E-1-3.7864E+0-2.9788E+0 2.4013E+0
 6.6303E+0 4.6436E+0-1.5684E+0-6.2085E+0-4.8072E+0 2.9068E+0 6.1424E+0 2.6581E+0
-9.2858E+0-1.0884E+1-7.1308E+0 1.1941E+0 6.3782E+0 5.2169E+0 6.3525E-1-2.8641E+0
-1.2154E+0 3.8952E+0 7.4913E+0 5.6970E+0-1.6203E+0-8.7760E+0-7.7027E+0-1.0819E+0
 4.7171E+0 5.5244E+0 2.7187E+0-1.2663E+0-2.7296E+0-4.5929E+0-6.1176E+0-3.4080E+0
 1.8103E+0 6.8736E+0 6.7030E+0 3.8891E+0 3.2703E+0 3.2818E+0 1.2095E+0-1.7781E+0
-4.9847E+0-5.9092E+0-6.9079E+0-6.1312E+0-9.3627E-1 5.1389E+0 7.6617E+0 5.8310E+0
 3.4602E+0 6.1805E-1-1.0152E-1-1.0285E+0-1.8539E+0-2.8768E+0-3.5541E+0-4.1641E+0
-3.0137E+0-2.3262E+0-2.9979E+0-5.4574E+0-3.8361E+0 5.8586E+0 1.5482E+1 2.1107E+1
 2.1694E+1 1.6913E+1 8.1736E+0 1.7934E+0-4.3433E+0-1.4046E+1-1.8761E+1-1.7413E+1
-9.2555E+0 1.3756E+0 5.7310E+0 8.1552E+0 9.2125E+0 8.0472E+0 3.9792E+0-2.7742E+0
-7.4564E+0-8.0004E+0-9.8107E+0-1.1418E+1-8.7853E+0-3.9012E+0-1.5548E+0-1.3335E+0
-5.6064E-1 3.4226E+0 7.6779E+0 8.2528E+0 4.8509E+0-8.4375E-1-4.0732E+0-7.1177E+0
-8.1097E+0-5.0913E+0 3.2877E+0 1.0473E+1 1.2360E+1 1.1046E+1 7.7447E+0 3.1903E+0
-1.1692E+0-1.3764E+1-1.1313E+1 3.8925E-1 6.3598E+0 5.2738E+0 1.8422E+0 1.3383E+0
 3.3885E+0 2.3136E+0-2.5487E+0-1.2100E+1-1.4560E+1-1.3745E+1-1.1707E+1-8.9030E+0
-5.7407E+0-4.4162E+0-5.8830E+0-8.5744E+0-4.9818E+0 7.1742E+0 1.6106E+1 1.8032E+1
 1.5487E+1 1.3523E+1 1.3778E+1 1.2577E+1 6.8245E+0-3.1109E+0-2.6515E+0 2.4801E+0
 8.7493E+0 9.2187E+0 8.7588E+0 1.0222E+1 1.1005E+1 8.5106E+0 3.9103E+0-3.2991E+0
-7.5369E+0-1.0004E+1-7.5572E+0 8.7654E-1 1.0150E+1 1.5869E+1 1.7725E+1 1.6853E+1
 1.4473E+1 9.3127E+0-3.2628E+0-2.1890E+1-3.4047E+1-3.5581E+1-3.0268E+1-2.6940E+1
-2.3664E+1-2.0184E+1-1.4743E+1-5.1018E+0 9.3041E+0 3.0749E+1 4.3657E+1 4.4084E+1
 2.6157E+1 7.5467E+0-1.4076E+1-2.6461E+1-4.2888E+1-4.8908E+1-4.4200E+1 2.3156E+0
 3.5115E+1 4.8176E+1 4.4005E+1 2.4728E+1 9.0394E+0-1.0253E+1-1.7215E+1-2.2598E+1
-2.3063E+1-2.0367E+1-1.9496E+1-1.8038E+1-1.1160E+1 6.6092E+0 3.5459E+1 5.8498E+1
 6.3107E+1 5.7060E+1 4.8458E+1 3.7914E+1 3.2275E+1 1.9394E+1 3.2395E+0-1.3539E+1
-2.0657E+1-2.7179E+1-3.4213E+1-3.9431E+1-3.7774E+1-2.0927E+1 4.2315E+0 1.9638E+1
 2.5959E+1 2.5891E+1 2.0549E+1 4.6739E+0-1.8212E+1-2.7135E+1-2.5949E+1-2.1951E+1
-2.2753E+1-3.5378E+1-5.5272E+1-5.8485E+1-5.3986E+1-2.6300E+1 1.8719E+1 3.9320E+1
 2.9314E+1 1.3189E+1-2.5152E+1-5.3874E+1-6.9305E+1-7.5559E+1-6.7634E+1-4.9034E+1
-2.2771E+1 2.1494E+1 4.6847E+1 6.2447E+1 6.6490E+1 6.6983E+1 5.1927E+1 2.7491E+1
 1.3867E+0-1.6764E+1-2.6433E+1-2.8425E+1-2.2780E+1-1.5916E+1-3.1438E+0 1.6872E+0
```

Figure C-4: First page of ground motion at downstream, transverse direction (Chang, 1987).

```
FFDOD
     1982  01  19    0014 New Hampshire
Moment Mag=          Ms=          Ml=      4.7
station = Franklin Falls Dam, Downstream component= 225
epicentral dist =      8.0       pk acc =   -110.0
inst type=           data source = USACE
*
*
*
    -32768      1982        19         0        14        42    -32768    -32768
    -32768    -32768    -32768    -32768        90       225    -32768         4
      3858    -32768    -32768    -32768    -32768    -32768    -32768    -32768
    -32768    -32768    -32768    -32768    -32768    -32768    -32768    -32768
    -32768    -32768    -32768    -32768    -32768    -32768    -32768    -32768
    -32768    -32768    -32768    -32768    -32768    -32768    -32768    -32768
  0.1700000E+39  0.2000000E+03  0.4350000E+02 -0.7160000E+02  0.1700000E+39
  0.1700000E+39  0.1700000E+39  0.4700000E+01  0.1700000E+39  0.1700000E+39
  0.4344700E+02 -0.7166000E+02  0.1700000E+39  0.1700000E+39  0.1700000E+39
  0.1700000E+39  0.8000000E+01  0.1700000E+39  0.1000000E+05  0.1700000E+39
  0.1700000E+39  0.1700000E+39  0.1700000E+39  0.1910000E+01  0.1700000E+39
  0.1700000E+39  0.1700000E+39  0.1700000E+39  0.1530000E+01  0.8690212E+02
  0.1605000E+01 -0.1099578E+03  0.1700000E+39  0.1700000E+39  0.1700000E+39
  0.1700000E+39  0.1700000E+39  0.1700000E+39  0.1700000E+39  0.1700000E+39
  0.1700000E+39  0.1700000E+39  0.1700000E+39  0.1700000E+39  0.1700000E+39
  0.1700000E+39  0.1700000E+39  0.1700000E+39  0.1700000E+39  0.1700000E+39
|
|ref - Chang, Frank K. (1987) Response Spectral Analysis of Franklin Falls Dam,
|New Hampshire;  U.S. Army Corps of Engineers Miscellaneous Paper GL-87-1.
|
-2.9625E+0-6.2272E+0-5.8742E+0-3.5099E+0-1.8502E+0-1.7736E-1-8.1274E-2-1.0188E+0
 3.1300E-1 3.4759E+0 7.6004E+0 7.6530E+0 4.8316E+0-4.7983E-1-1.8206E+0-3.8102E-1
 1.9783E+0 3.2181E-1-4.1527E+0-1.5595E+1-1.9420E+1-1.6600E+1-1.1455E+1-6.7055E+0
-2.0302E+0 2.7206E+0 1.0440E+1 1.8278E+1 1.3129E+1 3.1031E+0-1.1822E+1-1.6506E+1
-1.3704E+1-7.0448E+0-2.8640E-1 8.5303E+0 1.7209E+1 2.4552E+1 2.7568E+1 2.5405E+1
 1.4253E+1 2.2659E+0-9.0287E+0-8.6048E+0 2.0261E+0 1.4737E+1 1.6134E+1 9.1665E+0
 2.9203E+0-5.3310E+0-5.4570E+0 2.6714E-1 5.1945E+0 6.1552E+0 6.4733E+0 7.2453E+0
 9.7217E+0 6.6434E+0-2.4241E+0-1.4611E+1-2.1449E+1-2.3133E+1-1.8270E+1-1.0658E+1
-5.7131E+0-3.7026E+0-3.1398E+0-3.0616E+0-3.0623E+0-3.7009E+0-2.6293E+0 1.7223E-1
 2.0569E+0 4.5551E+0 7.4818E+0 1.1583E+1 1.5038E+1 1.3118E+1 7.2259E+0-3.7102E+0
-1.1442E+1-1.5348E+1-1.6402E+1-1.1117E+1 9.1914E-1 1.0780E+1 1.7106E+1 1.6704E+1
 9.1024E+0-7.5284E+0-1.4041E+1-2.1009E+1-2.1495E+1-2.0307E+1-1.8670E+1-1.4298E+1
-9.2994E+0-3.9860E+0 6.5093E-1 5.9327E+0 9.4847E+0 1.0235E+1 6.6794E+0 1.5782E+0
-4.7728E+0-6.7265E+0-6.3182E+0-3.7737E+0 3.1683E-2 3.5383E+0 8.5554E+0 1.2627E+1
 1.6483E+1 1.8089E+1 1.9720E+1 2.0758E+1 1.8363E+1 1.4352E+1 5.6891E+0-2.1685E+0
-3.6401E+0-3.1187E+0-2.2022E+0-2.9743E+0-8.5092E-1 1.2945E+0 4.0804E+0 3.6560E+0
 1.7399E+0 6.1740E-1 1.1410E-1-1.7975E+0-8.4728E+0-1.4229E+1-1.5469E+1-1.5387E+1
-1.4780E+1-1.3718E+1-8.2954E+0 2.8399E+0 1.4122E+1 1.9449E+1 1.8811E+1 1.3879E+1
 5.3314E+0-2.2634E+0-6.8039E+0-4.9638E+0 1.6226E+0 7.5271E+0 1.1294E+1 1.5030E+1
 1.7375E+1 1.6938E+1 3.3185E+0-8.5227E+0-2.0860E+1-2.4151E+1-2.1393E+1-1.8832E+1
-1.5663E+1-1.2663E+1-5.2873E+0 2.0921E+0 8.4458E+0 8.9760E+0 2.4124E+0-6.4763E+0
-1.9153E+1-2.2997E+1-1.9818E+1-8.5222E+0 2.4194E+0 1.1956E+1 1.6612E+1 1.6646E+1
 1.0951E+1-4.9436E+0-1.7746E+1-1.8669E+1-6.0694E+0 8.1518E+0 1.4758E+1 1.1182E+1
 1.6294E+0-6.6719E+0-9.8161E+0-7.7294E+0 3.9940E+0 2.3246E+1 3.3716E+1 2.8509E+1
 2.0963E+1 8.7847E+0 1.1494E+0-6.4522E+0-1.0989E+1-1.6636E+1-1.7373E+1-1.7218E+1
-1.7801E+1-1.9499E+1-1.8793E+1-6.8539E+0 2.2530E+1 4.1851E+1 4.5090E+1 2.8044E+1
 1.1381E+1-4.4831E-1-5.4208E+0 1.2722E+0 1.2885E+1 2.8693E+1 3.7230E+1 3.6506E+1
 3.0868E+1 2.3848E+1 2.0746E+1 1.8199E+1 1.6927E+1 1.8355E+1 2.2190E+1 2.3792E+1
 1.2764E+1-2.1986E+1-3.9404E+1-3.2036E+1-1.8514E+1-5.5011E+0 5.1353E+0 8.6472E+0
 7.9618E+0 1.4940E+0-1.8246E+1-2.5399E+1-2.4967E+1-2.2296E+1-2.0327E+1-2.2654E+1
-3.0306E+1-3.3564E+1-3.3526E+1-2.9766E+1-2.4775E+1-1.7974E+1-1.2131E+1-9.2887E+0
-1.0462E+1-1.2580E+1-1.2725E+1-8.3385E+0-3.7717E-1 6.1086E+0 7.3428E+0 4.6595E+0
```

Figure C-5: First page of ground motion at downstream, longitudinal direction (Chang, 1987).

```
FFD0E
     1982  01  19    0014 New Hampshire
Moment Mag=          Ms=          Ml=     4.7
station = Franklin Falls Dam, Downstream component= up
epicentral dist =      8.0       pk acc =    206.7
inst type=           data source = USACE
*
*
*
    -32768      1982        19         0        14        42    -32768    -32768
    -32768    -32768    -32768    -32768         0    -32768    -32768         4
      3855    -32768    -32768    -32768    -32768    -32768    -32768    -32768
    -32768    -32768    -32768    -32768    -32768    -32768    -32768    -32768
    -32768    -32768    -32768    -32768    -32768    -32768    -32768    -32768
    -32768    -32768    -32768    -32768    -32768    -32768    -32768    -32768
  0.1700000E+39  0.2000000E+03  0.4350000E+02 -0.7160000E+02  0.1700000E+39
  0.1700000E+39  0.1700000E+39  0.4700000E+01  0.1700000E+39  0.1700000E+39
  0.4344700E+02 -0.7166000E+02  0.1700000E+39  0.1700000E+39  0.1700000E+39
  0.1700000E+39  0.8000000E+01  0.1700000E+39  0.1000000E+05  0.1700000E+39
  0.1700000E+39  0.1700000E+39  0.1700000E+39  0.1800000E+01  0.1700000E+39
  0.1700000E+39  0.1700000E+39  0.1700000E+39  0.1425000E+01  0.2067427E+03
  0.1755000E+01 -0.9842130E+02  0.1700000E+39  0.1700000E+39  0.1700000E+39
  0.1700000E+39  0.1700000E+39  0.1700000E+39  0.1700000E+39  0.1700000E+39
  0.1700000E+39  0.1700000E+39  0.1700000E+39  0.1700000E+39  0.1700000E+39
  0.1700000E+39  0.1700000E+39  0.1700000E+39  0.1700000E+39  0.1700000E+39
|
|ref - Chang, Frank K. (1987) Response Spectral Analysis of Franklin Falls Dam,
|New Hampshire;  U.S. Army Corps of Engineers Miscellaneous Paper GL-87-1.
|
 2.2112E+1 2.4386E+1 2.0466E+1 1.6430E+1 1.7710E+1 2.3103E+1 1.7796E+1-7.6184E+0
-3.9172E+1-5.2757E+1-3.7366E+1-2.1480E+1-6.8932E+0 8.6164E+0 3.8388E+1 7.8917E+1
 7.0822E+1 2.7679E+1-2.0043E+1-5.8680E+1-8.0474E+1-7.7671E+1-5.7524E+1-1.0113E+1
 3.6341E+1 7.6497E+1 8.5195E+1 6.3944E+1 3.6070E+1 3.4933E+0-3.1888E+1-6.4734E+1
-6.0702E+1-4.5928E+1-1.3676E+1 3.0880E+1 3.7365E+1 2.3532E+1 1.1806E+1-1.9120E+1
-3.1697E+1-3.3998E+1-2.4877E+1-3.9494E+0 1.6083E+1 3.8365E+1 4.3177E+1 3.1188E+1
-4.1256E+0-2.3696E+1-3.4408E+1-2.8674E+1-2.8098E+1-1.1519E+1 9.3411E+0 4.2601E+1
 4.5375E+1 1.5062E+1-9.8139E+0-2.0017E+1-2.2546E+1-3.1605E+1-3.0443E+1-1.9850E+1
 6.2644E+0 2.0565E+1 2.4041E+1 2.2630E+1 1.8713E+1 1.8019E+1 1.3530E+1-3.9718E+0
-1.5480E+1-1.7111E+1-1.6130E+1-1.5429E+1-1.2608E+1-9.5765E+0-2.1833E+0 4.2963E+0
 1.0112E+1 1.4086E+1 1.3280E+1 1.1278E+1 8.1137E+0-4.4054E-1-3.4305E+0-3.3394E+0
-9.2052E+0-1.4616E+1 1.2911E+0 3.9940E+0-1.1518E+1-2.2655E+1-9.7948E+0 1.9455E+0
 3.5731E+0-7.8054E+0-5.6423E+0 7.5056E+0 1.9298E+1 1.4696E+1 1.0430E+1 1.8388E+1
 3.2755E+1 1.4231E+1-1.1037E+1-2.6946E+1-1.3796E+1-1.5676E+1-3.1181E+1-3.4178E+1
-1.0131E+1 1.6365E+1 2.2266E+1 9.7082E+0 8.7929E+0 1.9148E+1 3.0205E+1 1.1447E+1
-2.8319E+0-1.1106E+1-8.8397E+0-5.8354E+0-4.8189E+0-2.6511E+0-6.5472E-1-1.3045E-1
-2.5924E+0-3.7347E-1 8.2831E+0 1.1834E+1 5.1326E+0-6.9001E+0-1.3428E+1-1.6171E+1
-4.3913E+0 1.5346E+1 2.0997E+1 1.9567E+1 1.2482E+1 8.5552E+0 7.0054E+0 1.5518E+0
-2.6657E+1-3.5845E+1-2.8132E+1 2.2038E+0 1.9649E+1 2.8848E+1 2.3278E+1 8.4424E+0
-2.7604E+0-9.0434E+0-1.4479E+1-2.5427E+1-4.3259E+1-4.2721E+1-1.0283E+1 1.9239E+1
 3.5248E+1 2.7414E+1 2.6081E+1 3.1574E+1 2.8193E+1-2.9570E+0-1.9450E+1-1.2605E+1
 1.7162E+0-2.0046E+0-1.5887E+1-1.6137E+1-1.6989E+0 5.5279E+0 1.3156E+1 1.2226E+1
 1.3106E+1 2.3033E+1 3.7913E+1 2.0918E+1-1.7453E+0-1.0189E+1-5.2249E-1 9.7889E+0
 1.0466E+1-8.4649E+0-2.1289E+1-9.0249E+0-9.6431E-1-1.6079E+1-3.1649E+1-3.9195E+1
-1.6754E+1 9.2176E+0 3.1969E+1 3.2584E+1 1.9930E+1 6.5609E+0-2.2428E+1-4.9716E+1
-5.3234E+1-1.9408E+1 1.6419E+1 1.9145E+1 4.1214E+0-5.5932E+0 3.9086E-1-4.0493E+0
-1.5821E+1-2.5388E+1-2.6679E+1 6.3652E+0 3.6571E+1 5.1764E+1 6.0814E+1 7.0147E+1
 7.7235E+1 2.5633E+1-3.0927E+1-7.5019E+1-6.1433E+1-3.3333E+1-3.8404E+0 2.8023E+1
 4.9246E+1 7.8387E+1 5.3270E+1 2.3450E+1-2.4302E+1-4.6875E+1-6.0779E+1-7.9326E+1
-7.4650E+1-5.2835E+1-1.6671E+1 2.9523E+1 5.7408E+1 6.6934E+1 6.4871E+1 3.5647E+1
 6.8343E+0-2.3518E+0-7.9475E-1 4.0695E+0 4.6243E+0-5.1190E+0-1.7447E+1-2.9509E+1
-2.8521E+1-7.0275E+0 6.3132E+1 9.8720E+1 7.0052E+1 4.3202E-1-5.4835E+1-6.9293E+1
```

Figure C-6: First page of ground motion at downstream, vertical direction (Chang, 1987).

```
FRANKLIN FALLS DAM, NEW HAMPSHIRE: CREST
45 DEGREES
EARTHQUAKE OF JANUARY 19, 1982, 0014:42UTC
BUTTERWORTH AT .330 HZ, N=4
YEAR=1982 JULIAN DAY= 19 HOUR= 0 MINUTE=14 SECOND=42 COMPONENT=  45
SAMPLES/SEC=200 FILTER TYPE=BUTTERWORTH  CORNER= 0.33 ORDER=4 DATA TYPE=AC
NO OF POINTS=  3765, UNITS=CM/SEC**2, CM/SEC, AND CM
 -23.72  -10.02    6.63   -1.59   -0.83   -2.38  -17.20  -17.26  -11.01  -11.64
  11.18   24.79    4.30    4.68    9.75    0.95   -2.55   -2.48   -0.17   -3.98
   8.28   31.36   27.73   25.26   30.55   21.14   -9.30   -8.98   -8.57  -25.33
  -5.17   14.66   17.93   22.62   25.12   13.50   -1.50   -8.29   -9.32  -14.66
 -11.91   -5.45   -2.97   -6.04  -11.97  -11.42  -10.60  -11.69  -17.68  -19.39
 -12.93   -8.16   -8.14  -11.99  -11.08   -6.38   -6.00    0.09    8.87    7.31
   3.27    0.55   -6.23  -12.64  -14.63  -11.19   -4.23    0.56    5.06    0.50
  -7.62   -2.48    2.39    6.21   11.66    7.59    3.49   -1.16   -2.53    5.26
   2.41   -5.71   -2.46    4.53    3.66   -5.45  -16.15  -14.02    0.40    7.27
  -0.74   -4.05    8.03   14.39    8.00    2.75    5.61    8.82    9.37    6.27
  -0.53   -4.16  -15.64  -29.31  -23.78    6.19   27.47   23.67   19.92   19.44
   2.70  -17.89   -6.18   10.90   28.58   26.65    1.66   -0.24   -6.18  -22.93
 -19.18   -9.25  -10.48   -9.98   -8.13  -14.82  -20.43  -16.33   -3.15   14.85
  14.91    5.94    1.10   -1.55    3.12    2.09   -0.87    3.66    3.02   -5.68
 -12.78  -12.78   -4.20    2.05   -5.45  -18.14  -31.83  -38.20  -33.97  -30.08
 -26.92  -14.82    7.05   15.67   12.97    3.57  -25.94  -47.56  -45.51  -52.45
 -33.15    8.17    1.39    4.10   -5.30  -46.20  -40.43  -45.87  -50.33   -8.24
  14.04   29.41   34.67   22.79   37.15   41.88   44.55   58.11   52.63   44.95
  39.74   38.00   44.00   45.77   48.85   51.34   49.47   30.72   -5.52    0.88
  -6.48  -43.08  -16.05   -7.94  -27.20   -2.00   29.37   22.59    8.01   11.93
  -1.37   -8.46   -6.11   -3.16    3.94    7.17  -17.01  -64.09  -57.72  -44.59
 -48.43  -22.54   26.28   58.32   42.78   16.16   -9.95  -41.63  -61.02   15.79
  86.91   41.45   29.87   24.97  -60.65 -117.65 -123.96  -38.90   49.99    2.91
 -19.63   23.07   28.80   10.20   21.91   24.73  -17.03  -85.96 -107.19  -73.26
 -93.62  -73.81  -25.27  -17.27   26.16   48.10   74.65   97.50   69.44   60.46
  47.53   21.41   33.38   32.73   -2.27  -10.80  -11.29  -17.85  -11.93    1.74
  10.17    2.71    3.71   22.15   35.59   24.91   14.34   11.88    7.59   -2.58
 -26.19  -28.23  -24.17  -27.54  -23.44   -5.71   19.10   26.08   30.11   29.02
  35.35   45.58   38.69   32.71    2.77  -30.15  -26.69  -21.78  -18.82  -16.82
  -7.52    5.42   -1.83   -2.03    2.28    0.57    6.05    2.81   -5.72  -23.26
 -39.83  -25.36  -15.74  -18.67  -20.79  -26.81  -32.95  -35.70  -30.17  -32.73
 -40.38  -40.94  -24.02   -4.05   12.80   28.29   29.62   26.60   20.52   16.92
   2.42    0.03   10.46   17.15   26.42   36.22   61.67   67.25   42.17   21.72
   5.86  -18.59    2.63   23.55   -1.47   -5.29   -1.57   -6.14   -7.86    1.97
   6.96   -0.11   -1.41   -1.47   -5.43   -8.99   -9.26  -10.68  -11.36   -4.57
   2.88    3.91    4.06    3.81    2.39    0.70   -4.11   -7.25   -6.35   -2.39
  -3.56   -8.35   -7.44    7.50   29.80   25.88   13.71   -3.93  -28.78  -27.09
 -17.10  -10.52   -6.55   -8.72  -16.63  -21.14  -21.49  -23.11  -25.82  -30.69
 -28.05   -7.76   16.14   21.36   22.98   16.75   15.20   13.35  -10.28  -12.43
  -3.89   -3.18   13.25   30.91   34.77   33.39   30.69   27.35   26.23   25.31
  18.62   -1.49   -9.80   -0.74   -2.52  -11.42  -15.52  -10.59   -2.22    3.77
   7.24    3.82   -3.06   -4.66  -13.70  -29.93  -26.25  -13.49    6.43   34.92
  17.57   -4.56    2.45   -9.99  -16.30   -6.95   -3.75   -1.07    4.76    9.18
   9.82    9.67    1.86   -8.90   -7.73   -2.15   -2.00   -0.89    7.71   16.07
  12.11    6.43    3.51  -11.32  -20.40  -14.71  -12.77  -12.61  -14.30  -15.01
 -11.01   -4.55    7.37   10.26    4.18    1.93   -6.20  -12.27   -6.23    0.30
  11.88   15.10    4.13   -1.62   -2.54   -7.15  -21.78  -22.97   -7.94   -2.69
   0.75   23.33   32.72   35.15   26.50   -2.06    0.98    5.95   10.12   19.57
  23.66   23.47   17.84   17.18   11.73    4.22    2.67   -2.66  -10.08   -6.77
   1.34   17.36   25.58   25.06   23.71   15.78   15.33   -3.61  -18.10   -3.80
  -2.59   -3.43   -0.95   -1.76   -0.99   -4.88   -5.15   -3.83   -5.34   -9.92
 -21.44  -25.45  -18.42  -14.62  -10.26   -8.04  -12.71  -13.28  -14.40  -20.74
 -24.07  -21.19  -15.78   -7.93   -0.03    4.34    1.04   -3.74   -4.48   -6.69
  -6.30   -3.56    1.20    1.39   -3.16   -5.71   -9.20   -5.36   -0.80   -1.29
  -1.48   -5.53   -8.01   -6.48   -4.01    1.95    4.26    4.34    9.96    7.44
   5.79    2.76   -7.98   -2.50    4.03    2.21    2.52    3.53    2.37    2.75
```

Figure C-7: First page of ground motion at crest, longitudinal direction (Chang, 1987).

```
FRANKLIN FALLS DAM, NEW HAMPSHIRE: CREST
315 DEGREES
EARTHQUAKE OF JANUARY 19, 1982, 0014:42UTC
BUTTERWORTH AT .330 HZ, N=4
YEAR=1982 JULIAN DAY= 19 HOUR= 0 MINUTE=14 SECOND=42 COMPONENT= 315
SAMPLES/SEC=200 FILTER TYPE=BUTTERWORTH  CORNER= 0.33 ORDER=4 DATA TYPE=AC
NO OF POINTS=  3789, UNITS=CM/SEC**2, CM/SEC, AND CM
  18.56   11.87    7.02    7.06    2.43    0.21   -1.40   -5.31   -7.97   -8.08
  -8.79  -10.97   -7.07   -5.00   -8.17   -3.63    1.40    9.12    5.77   -5.98
 -13.56  -18.67   -8.15   -1.22   -3.19   -1.26    4.55    9.88   11.11   12.62
  10.88    3.04    1.32    2.06   -1.65   -5.38   -8.85   -5.70    2.00    7.26
   3.77   -3.51   -5.43   -2.89   -3.63    1.53   13.78    9.07   -1.12   -2.53
   0.65    0.06   -7.58   -9.31   -3.25   -0.84   -3.60   -7.81   -7.54   -4.71
  -2.94   -0.99    0.38    2.95    0.43   -3.57   -3.64   -1.77    3.24    3.46
  -7.50  -16.65  -11.54   -6.78   -5.64   -8.27   -8.77    4.50    4.09   -5.27
  -7.20   -8.76   -6.98   -5.02   -5.43   -7.43   -2.44   12.27   15.31    2.56
  -4.04   -8.01  -15.04  -11.91   -8.38  -14.12   -0.18   19.31    9.50   -1.63
  -0.29   -9.40  -34.10  -21.04   14.53   13.59   11.11   21.41   23.85   30.80
  15.30  -32.54  -32.48  -14.75  -21.00  -11.39   -0.41   -2.38    3.18    9.84
   4.13    4.08    7.75    6.14    2.86   -0.50   -6.49   -5.49   -5.09   -9.58
 -10.44   -1.91   16.58   14.23    6.57    6.01   -7.19  -15.53  -11.78  -18.41
 -28.22  -31.91  -38.38  -41.97  -45.83  -55.62  -40.84  -11.74  -13.71  -14.18
  -2.84    9.75   18.89   13.12   14.17    7.67   -5.01   -8.38  -12.84  -21.72
 -16.14   19.35   25.15   30.28   49.54   55.62   51.94    6.39  -16.34  -12.73
 -34.34  -21.35   32.16   41.69   71.63   86.72   51.88   42.44   24.45   14.22
 -11.77  -37.26  -17.80    0.95   -1.00   -2.67    7.02   10.24   10.39   18.53
  17.82   21.85   17.91  -38.34  -44.69   -9.92  -26.01  -13.64    1.84    1.11
   3.61  -22.52  -35.34  -30.87  -39.75  -41.48  -35.31  -36.32  -36.68  -43.56
 -54.20  -56.48  -63.52  -48.21  -28.57  -36.00  -23.20  -14.40  -26.24  -25.55
 -18.77  -17.98  -34.48  -41.39  -54.79  -13.94   81.82   87.09   98.74  146.22
 180.43  226.27  212.39  148.73   -5.08 -123.87 -124.53 -247.99 -306.83  -85.42
  35.01  -18.52   34.84  117.33  191.97  239.08  189.05   80.59  -41.78  -56.15
-109.78 -224.18  -81.51   51.61  -18.52    7.31   58.43   12.05  -28.10  -23.38
   1.06   35.59   43.46   36.67   32.21    0.97  -23.29  -27.51  -13.43    9.97
  11.95    5.27    3.72   -4.81    5.14   57.27   75.48   53.92   73.68   78.43
  45.24   40.36   41.80    8.68  -13.77   -1.54   -9.33  -28.68  -26.48  -32.08
 -43.11  -49.20  -26.59   -1.65   -9.18   15.56   42.53   38.63   47.30   22.74
 -30.38  -39.79  -63.10 -100.23  -92.09 -110.03  -81.46  -26.87  -46.86  -23.84
  29.91   12.33  -28.05  -17.93  -10.00  -21.72  -21.32  -22.28  -15.43    3.20
   1.27   -8.53   -9.88  -14.00  -26.73  -33.54  -20.22   -6.54   10.28   26.43
  47.93   57.69   59.05   75.46   45.18   13.01    4.03   -1.01   -5.66  -21.97
  11.93   27.40   23.68   38.06   38.81   49.90   50.67   46.71   45.56   26.78
   9.25   13.59    9.48   -7.29  -12.90   -5.52   -0.06   -4.90    4.54   12.92
  11.95   23.52   24.69   12.77   12.47    3.13  -10.13   -5.30  -10.25  -13.91
 -14.50  -22.34  -28.29  -34.12  -41.85  -43.69  -33.20  -18.26   -6.36  -15.02
 -24.23  -19.78  -15.10  -14.94  -18.91  -21.69  -23.01  -22.36  -26.59  -31.61
 -30.04  -21.49  -13.13   -5.68    3.11    0.89    3.17   13.96   17.99   20.90
  15.96    6.62    1.34   -2.75   -9.54  -15.55  -11.84   -3.25    6.03    8.43
   3.81    2.75    0.40   -2.60   -2.63    6.91   24.93   23.81   30.47   47.74
  39.55   29.85   25.97   15.14    2.04   -4.84    6.93   11.36    7.17   16.29
  25.09   27.44   23.21   13.29    8.85   -1.25  -34.00  -32.14   -9.14  -18.24
 -23.25  -24.43  -26.99  -19.60  -13.12   -5.18   -5.89  -10.47   -5.24   -4.82
  -8.03   -2.36    2.13   -2.60   -3.77   -2.86   -4.99   -3.12    1.00   14.85
  24.72   15.60   10.71   12.75   17.30   22.13   19.07   15.48    9.03    5.47
   8.20   -6.91  -13.38   -2.12   -3.80   -3.41    2.52   10.98   21.68   15.75
  10.54   12.94    5.22   -2.73   -6.40   -9.96   -7.49   -2.22   -3.92   -8.46
  -5.55   -1.78   -7.11  -10.51  -10.40  -14.21  -15.87  -23.69  -34.06  -33.41
 -20.15   -6.33   -9.53  -10.36   -4.63   -3.25   -7.87  -14.14  -15.79  -16.48
 -15.88  -14.96  -18.06  -10.01   -3.13   -8.54    7.83   22.33   17.66   21.75
  19.89   14.82   16.13    8.92    4.84    7.50   15.11   28.08   36.15   37.98
  33.41   30.38   24.93   12.83    5.06    5.20    7.39    3.89   -0.61    0.76
   3.94    1.48    1.77    4.53   -0.27   -5.54   -5.30   -9.42  -17.46  -20.70
 -19.63  -12.82   -9.85   -7.66   -3.06   -6.08   -1.24    3.38    2.14    2.25
```

Figure C-8: First page of ground motion at crest, transverse direction (Chang, 1987).

```
 FRANKLIN FALLS DAM, NEW HAMPSHIRE: CREST
 UP
 EARTHQUAKE OF JANUARY 19, 1982, 0014:42UTC
 BUTTERWORTH AT .330 HZ, N=4
 YEAR=1982 JULIAN DAY= 19 HOUR= 0 MINUTE=14 SECOND=42 COMPONENT=  UP
SAMPLES/SEC=200 FILTER TYPE=BUTTERWORTH  CORNER= 0.33 ORDER=4 DATA TYPE=AC
NO OF POINTS=  3790, UNITS=CM/SEC**2, CM/SEC, AND CM
   16.92   22.08   23.74   34.28    8.67  -14.35   -6.58  -29.38  -25.45   18.09
   16.20    9.88   24.32   41.34   33.85   -4.98   -3.85    7.67   -4.96   -8.13
  -12.77   -3.13   16.96   15.93   10.82    0.07   -0.89    5.71   -3.82   -6.70
   -1.66   -0.08   -4.46   -5.11   -4.81  -16.01  -18.81  -13.07  -24.95  -31.39
  -15.67  -11.19  -14.51   -8.96   -6.13   -4.64   -2.69   -2.83   -0.17   10.18
   11.84    3.23    1.53    0.61    0.00   -0.67   -5.65   -4.91    4.60   12.22
    5.45   -6.48   15.25   32.16   23.61   23.35   -0.45  -15.77   -4.57  -14.36
   -9.40   13.27    7.88   11.94   18.22   -1.42   -5.13    4.27    8.00   -0.74
  -13.65   -9.80   -3.41    5.09   -0.71  -26.54  -24.16  -13.52  -27.12  -31.91
  -20.21   -6.56   -6.59   -0.54   19.28   20.40   -3.55  -20.07  -14.61  -24.51
   -0.22   17.99  -41.39  -12.03   54.26   18.42   24.67   30.60  -11.01   -5.75
   -5.37   -9.50    1.70    3.95    0.80   -6.86   -9.27   -4.15    4.86   18.71
   33.93   36.42   48.50   57.93    9.60   -9.38   18.02   10.40    4.64    0.58
  -19.30  -23.96  -19.15  -28.57  -12.21   12.79    6.60   16.56   -0.51  -34.87
  -35.50  -47.11  -62.22  -69.04  -58.18  -27.40  -21.05  -36.68  -45.82  -44.03
  -38.11  -29.52  -14.40   -9.63  -11.72   -7.58   -9.29  -14.43  -10.03   16.36
   38.73   28.58   19.49   34.25   38.33   18.96   25.08   59.28   69.75   66.00
   88.86   81.61   18.47    7.41   15.66  -12.12  -26.93  -27.26   10.98   32.56
   15.00   28.79    8.73  -19.53   27.83   25.87  -24.33  -26.07  -25.91  -33.98
  -44.87  -32.30  -13.17  -16.99   -8.01    3.67  -11.31  -37.63  -48.93  -46.03
   -3.74   13.36   17.41   30.11  -27.09  -50.11  -59.58 -113.23 -114.31  -96.28
  -41.73   -2.05  -24.93   -9.62   11.32   42.80   97.12   82.63   77.01   83.48
   16.90    6.30  -27.18 -103.26  -83.14  -24.49   21.62   35.32   66.70   78.06
   62.94   50.01   45.55   64.09   70.25   77.19   29.41  -10.98   26.54   57.08
   29.65  -24.55  -52.93  -63.11  -49.42    4.15    7.60    1.90  -29.69  -84.85
  -45.79  -14.92   -1.44   20.24   22.27   -1.89  -46.32  -68.96  -59.90  -50.15
  -74.66  -46.28   -1.19    1.93   42.49   63.80   54.54   47.68   20.34    8.52
   -1.80  -14.90    9.45   26.76   15.50   14.80   24.33   20.87   17.10   15.25
   12.62   19.04   30.49   31.65   29.79   42.97   27.13  -10.67   -6.66   -5.38
  -22.59  -29.23  -37.81  -39.26  -41.92  -56.08  -34.46  -12.14  -19.70   28.98
   34.55   10.20   31.53   -5.26  -25.36  -19.04  -34.21  -36.82  -38.05  -31.66
  -11.91   -3.84   -0.83   14.02   26.93   40.08   54.45   27.74  -18.69  -28.87
  -19.72  -30.95  -37.64    6.05   19.79    7.99   25.48   38.41   50.63   45.18
   12.22    7.78   16.03    3.73   10.28   21.40   13.50   14.24   20.95   18.17
   10.51   -2.80   -7.46   -2.01   -0.78    1.13   -2.28  -10.77  -10.25   -9.46
  -16.12  -19.27  -17.45  -16.09  -23.04  -30.59  -28.07  -24.88  -20.03  -16.18
  -21.27  -23.34  -19.97  -19.17  -16.99   -6.51   -2.57  -12.45  -11.11   -4.83
   -4.53   -0.09   10.82   26.34   38.94   35.63   17.15   13.57   23.76   22.22
   18.25   16.55   14.28   20.93   27.71   22.54   17.18   20.46   20.95   15.13
   15.03   16.55   14.49   14.21   10.27    3.78    3.52    5.16  -31.80  -52.26
  -23.90  -26.74  -25.64  -14.44  -22.68  -21.21  -21.28  -31.95  -37.68  -35.97
  -32.56  -16.45   -2.21   -9.01   -3.71    6.60   18.32   31.51   13.50    4.84
   13.82   13.33   12.33    8.34    4.30    3.09    4.99   13.34   13.73    0.74
   -8.95   -6.67    5.62   21.73   21.19   16.42   27.47   32.33   27.93   27.45
   20.74   -1.34   -3.39    6.12    4.81   12.23    9.98    1.13    1.76    0.33
   -4.91  -13.96  -16.12  -14.37  -18.33  -17.73  -17.04  -19.60  -19.72  -19.70
  -17.52  -13.55  -14.96  -19.03  -20.47  -16.62   -5.10    3.74    5.18   -0.72
   -1.43    8.96    8.53    4.81    3.21    6.65   19.57   22.51   16.97   13.21
   10.10    8.03    3.43    2.53   12.53   14.54    9.82   10.41    9.72    7.50
    4.74    6.23   12.28    9.90   -0.89   -6.02   -1.17    0.17   -3.38   -5.52
  -11.61  -16.89  -16.90  -18.64  -20.84  -18.84  -17.34  -16.14  -11.43   -4.63
    0.44    2.31    1.00    9.01   20.69   15.02    7.16    5.19   -9.66  -16.99
   -7.10   -8.93   -3.59   12.18    6.48   -2.76    3.13    9.46    7.64    4.23
    4.85    3.91    2.62    3.22    4.43    5.73    3.23   -1.72   -1.91    3.74
    6.27    2.70   -7.43  -12.24   -4.93   -5.22   -7.22   -0.04    5.05   -0.39
   -6.84   -9.01  -10.57   -7.83   -7.54  -11.46  -13.58  -10.05    0.67   12.41
```

Figure C-9: First page of ground motion at crest, vertical direction (Chang, 1987).

APPENDIX D
ROCK GROUND MOTION OBTAINED BY THE PRELIMINARY DECONVOLUTION ANALYSIS

FFD Estimated DS GM at Bedrock (T) (30 April 2015).txt
Franklin Falls Dam - New Hampshire
Estimated horizontal accelerations on bedrock from the 1982 Gaza Earthquake mb=4.4
These accelerations are based on deconvolution analysis of the transverse component
of the downstream accelerometer (C)
M. James and A. Abraiza (30 April 2015)
Time interval = 0.005 [sec] Acceleration [g]

4.67E-03	1.15E-03	-6.95E-03	-5.13E-03	-3.62E-03	2.93E-03	4.21E-03	2.86E-03
-1.44E-03	-3.02E-03	-8.60E-04	3.22E-03	4.76E-03	2.67E-03	-2.90E-03	-5.64E-03
-2.58E-03	1.88E-03	3.51E-03	1.83E-03	-4.00E-04	-1.44E-03	2.50E-04	-1.15E-03
-2.96E-03	-2.55E-03	6.00E-05	4.01E-03	4.02E-03	2.13E-03	-1.30E-04	-1.86E-03
-2.32E-03	-1.39E-03	-7.00E-04	-5.20E-04	-3.15E-03	-3.46E-03	5.00E-05	4.48E-03
5.53E-03	3.76E-03	1.15E-03	-2.18E-03	-2.15E-03	-1.57E-03	1.10E-04	1.70E-04
-4.00E-04	-1.98E-03	-1.43E-03	-1.93E-03	-2.75E-03	-5.11E-03	-2.07E-03	5.20E-03
9.98E-03	1.14E-02	1.06E-02	7.18E-03	2.05E-03	2.20E-04	-2.93E-03	-8.69E-03
-9.78E-03	-9.19E-03	-2.52E-03	3.88E-03	5.62E-03	6.24E-03	5.33E-03	3.87E-03
1.48E-03	-1.95E-03	-3.41E-03	-3.52E-03	-5.57E-03	-6.19E-03	-3.45E-03	-6.80E-04
-1.05E-03	-2.13E-03	-1.63E-03	3.33E-03	7.50E-03	9.12E-03	7.15E-03	3.57E-03
5.60E-04	-3.25E-03	-5.25E-03	-5.31E-03	-2.05E-03	3.20E-04	1.33E-03	3.65E-03
3.21E-03	3.03E-03	1.09E-03	-7.81E-03	-1.96E-03	2.32E-03	2.70E-03	-6.70E-04
-2.52E-03	-2.69E-03	-9.70E-04	-2.10E-04	-1.36E-03	-6.98E-03	-5.71E-03	-5.91E-03
-2.51E-03	-8.40E-04	1.13E-03	-1.73E-03	-4.42E-03	-7.78E-03	-4.14E-03	3.34E-03
7.91E-03	8.75E-03	8.18E-03	7.76E-03	7.80E-03	6.22E-03	1.49E-03	-6.76E-03
-4.18E-03	1.00E-04	6.50E-03	4.87E-03	5.37E-03	4.65E-03	5.67E-03	3.99E-03
2.34E-03	-4.34E-03	-6.56E-03	-9.65E-03	-5.49E-03	-2.00E-05	6.32E-03	7.06E-03
7.77E-03	5.85E-03	7.11E-03	6.96E-03	3.54E-03	-6.24E-03	-9.16E-03	-9.54E-03
-4.64E-03	-6.23E-03	-4.46E-03	-8.78E-03	-6.06E-03	-3.41E-03	8.05E-03	1.83E-02
2.44E-02	2.03E-02	1.07E-02	1.67E-03	-7.83E-03	-1.34E-02	-2.30E-02	-2.63E-02
-2.40E-02	1.12E-02	1.91E-02	2.83E-02	2.00E-02	1.12E-02	2.22E-03	-7.02E-03
-6.99E-03	-1.46E-02	-1.76E-02	-1.97E-02	-1.95E-02	-1.71E-02	-1.28E-02	-2.22E-03
1.39E-02	2.60E-02	2.84E-02	3.00E-02	2.90E-02	2.52E-02	2.31E-02	1.27E-02
1.16E-03	-1.22E-02	-1.61E-02	-2.35E-02	-2.38E-02	-1.90E-02	-6.80E-03	7.43E-03
2.23E-02	2.20E-02	2.01E-02	1.15E-02	6.68E-03	-6.53E-03	-1.55E-02	-1.57E-02
-1.18E-02	-1.06E-02	-8.14E-03	-1.45E-02	-1.72E-02	-1.12E-02	-7.66E-03	9.42E-03
3.42E-02	3.16E-02	2.02E-02	7.47E-03	-2.01E-02	-3.32E-02	-4.04E-02	-4.36E-02
-3.98E-02	-3.53E-02	-2.24E-02	3.31E-03	1.44E-02	2.63E-02	2.71E-02	3.13E-02
1.93E-02	6.69E-03	-1.19E-02	-2.04E-02	-2.62E-02	-2.25E-02	-1.83E-02	-1.64E-02
-1.45E-02	-1.84E-02	-1.86E-02	-8.41E-03	1.16E-02	2.44E-02	2.58E-02	1.86E-02
1.01E-02	-5.17E-03	-1.28E-02	-1.67E-02	-1.27E-02	-5.46E-03	4.23E-03	1.30E-02
1.99E-02	2.45E-02	3.19E-02	3.89E-02	3.54E-02	1.58E-02	7.00E-05	6.71E-03
1.85E-02	2.98E-02	2.49E-02	1.60E-02	-6.93E-03	-4.00E-02	-5.73E-02	-5.05E-02
-4.05E-02	-4.26E-02	-3.91E-02	-4.46E-02	-1.54E-02	1.21E-02	4.88E-02	7.11E-02
7.33E-02	6.95E-02	4.79E-02	-2.25E-03	1.83E-02	-4.79E-03	1.30E-02	-1.20E-02
-1.96E-02	-7.82E-02	-8.96E-02	-5.12E-02	-6.10E-03	1.41E-02	5.81E-02	1.57E-01
8.92E-02	7.01E-02	-1.41E-02	-6.14E-02	-1.33E-01	-1.24E-01	-1.00E-01	-5.63E-02
-1.92E-02	-5.10E-03	-3.40E-03	7.03E-03	1.26E-02	3.82E-02	4.97E-02	5.66E-02
3.67E-02	2.56E-02	1.73E-02	-6.67E-03	-1.78E-02	-5.59E-02	-8.48E-02	-9.00E-02

Figure D-1: First page of ground motion on rock, transverse direction (James and Arbaiza, 2015).